

# **BATCH AQUEOUS-PHASE REFORMING OF LIGNOCELLULOSIC BIOMASS FOR HYDROGEN PRODUCTION**

A Thesis  
Presented to  
The Academic Faculty

by

**Mariefel Bayta Valenzuela**

In Partial Fulfillment  
of the Requirements for the Degree  
Master of Science in Paper Science and Engineering in the  
School of Chemical & Biomolecular Engineering

Georgia Institute of Technology  
August 2006

# **BATCH AQUEOUS-PHASE REFORMING OF LIGNOCELLULOSIC BIOMASS FOR HYDROGEN PRODUCTION**

Approved by:

Dr. Pradeep K. Agrawal, Co-advisor  
School of Chemical & Biomolecular  
Engineering  
*Georgia Institute of Technology*

Dr. Christopher W. Jones, Co-advisor  
School of Chemical & Biomolecular  
Engineering  
*Georgia Institute of Technology*

Dr. Sujit Banerjee  
School of Chemical & Biomolecular  
Engineering  
*Georgia Institute of Technology*

Dr. Howard “Jeff” Empie  
School of Chemical & Biomolecular  
Engineering  
*Georgia Institute of Technology*

Date Approved: July 5, 2006

To *la familia* Bayta-Valenzuela,  
my family,  
through thick and thin

## ACKNOWLEDGEMENTS

Coming to Georgia Tech was a dream come true. I knew it will be different – even difficult at times, but all I could, would think of, was that it would be worth it. Despite the tears, of missing home, I know I have been blessed with experiences, friendships and lessons that will stay with me for life. Life is, will be, always beautiful. And I would like to thank those who have made it meaningful and worthwhile as well during my stay here. Without them, this achievement would have been impossible.

To Dr. Chris Jones, who has been a mentor from the beginning to the uncertain girl who first came here. Your kindness, encouraging words and unwavering belief have helped me tremendously throughout my stay here. I have learned a lot during the time I have worked with you and the group. Thank you for being an inspiration for excellence and dedication.

To Dr. Pradeep Agrawal, who has been a great adviser and teacher. I thank you for your generosity of spirit, your patience and your insightful comments on matters relating from research to history and politics. Our discussions have always afforded me to analyze things, relax and learn at the same time.

To my committee members, Dr. Sujit Banerjee and Dr. Jeff Empie, for their insights and comments regarding my research. I would like to thank IPST, too, for funding my studies.

To the Jones group, for all the help, discussions and advice. It has been a great experience working with a bunch of dedicated individuals who are serious about their science and enthusiastic about their research. Being a part of this team gives added motivation to work harder.

To the Meredith group, who have “adopted” me to their fold. From my hardworking midnight buddies – Pedro and Dr. Pratyay; to Reginald, who always has time to be disturbed by a question or a comment; to Gracy and Keith, who are ready to discuss research and are very free with their encouragement; and to Charlene and Jing – all you guys have made my “solitary lab existence” far from being lonely.

Special thanks go to Ms. Erin Maris and Dr. Robert Davis of UVa, Dr. Hanno Leisen, Mr. Ashwini Sinha and Mr. William Sommer for their invaluable help during the characterization of my materials. Thanks also to Dr. David Bush and Dr. Aryn Teja.

I would also like to extend my heartfelt thanks to these people whose friendships I have come to value so highly. To Yeny, whose kindness, thoughtfulness and enthusiasm I am very grateful for. Thanks! To my hardworking previous roommate, Vidhya, who introduced me to a 7-day work schedule – truly an inspiration. To my roommates, Nivi and Radhika, without whose company and diverting conversations I know I would have suffered a burn-out earlier on. It has been wonderful sharing a lot of memories with you.

My gratitude to my parents and all my siblings, whose nurturing love, understanding and unstinting support have cheered me up when I am down and kept me going. My grandmothers, who are my inspiration of courage, each unique in her own way. And to Ryan, my fiancé, whose love and patience make me remember what the important things in life are. Thank you so much.

Lastly, to God, He who has always been there and always will be. To You be the glory. And to all friends and acquaintances who I have not mentioned but were a part of this endeavor, thank you very much.

# TABLE OF CONTENTS

	Page
<b>ACKNOWLEDGEMENTS</b>	iv
<b>LIST OF TABLES</b>	x
<b>LIST OF FIGURES</b>	xi
<b>LIST OF ABBREVIATIONS</b>	xiv
<b>SUMMARY</b>	xvii
<b><u>CHAPTER</u></b>	
<b>1 INTRODUCTION</b>	1
<b>2 REVIEW OF RELATED LITERATURE</b>	5
2.1 CURRENT STATUS OF WORLD ENERGY	5
2.1.1 Supply and Demand of Oil	5
2.1.2 The Issue of Non-Sustainability: Declining Oil Reserves	7
2.1.3 Coal	12
2.1.4 Natural Gas	17
2.1.5 Nuclear Energy	19
2.1.6 Renewable Sources	21
2.1.6.1 Solar Energy	21
2.1.6.2 Hydroelectric Energy	23
2.1.6.3 Geothermal, Wind and Biomass Energy	25
2.2 BIOMASS	26
2.2.1 Chemical Composition of Biomass	27
2.2.1.1 Cellulose	27

2.2.1.2 Hemicellulose	30
2.2.1.3 Lignin	32
2.2.1.4 Extractives	35
2.2.1.5 Ash	36
2.2.2 Biomass as a Renewable Resource	37
2.2.2.1 Biochemical Conversions	41
2.2.2.2 Thermochemical Conversions	45
2.2.2.2.1 Pyrolysis	45
2.2.2.2.2 Gasification	48
2.3 AQUEOUS-PHASE REFORMING	51
<b>3 OBJECTIVES OF THE STUDY</b>	<b>57</b>
<b>4 EXPERIMENTAL METHODS</b>	<b>59</b>
4.1 RAW MATERIAL PREPARATION AND CHARACTERIZATION	59
4.2 REACTION METHOD	60
4.2.1 Reactor	60
4.2.2 Process Description	63
4.2.2.1 Acid Hydrolysis	63
4.2.2.2 Pt-catalyzed Reforming	64
4.3 GAS PHASE ANALYSIS	65
4.3.1 Thermal Conductivity Detector: Brief Background	65
4.3.2 GC Calibration	68
4.4 SOLID BIOMASS RESIDUE ANALYSIS	71
4.4.1 Proximate Analysis	74

4.5 SPENT CATALYST CHARACTERIZATION	75
4.5.1 Elemental Analysis	75
4.5.2 Hydrogen Chemisorption	75
4.5.3 Nitrogen Physisorption	76
4.5.4 X-ray Photoelectron Spectroscopy (XPS)	76
<b>5 RESULTS AND DISCUSSION</b>	<b>77</b>
5.1 BIOMASS CHARACTERIZATION	77
5.1.1 Elemental Analysis	77
5.1.2 Proximate Analysis	78
5.2 BATCH REACTION	82
5.2.1 Batch Reaction with Intermittent Sampling	82
5.2.2 Acid Hydrolysis	83
5.2.2.1 Cellulose and Hemicelluloses	85
5.2.2.2 Lignin	88
5.2.3. Addition of Reforming Catalyst: Aqueous-phase Reforming (APR)	89
5.2.3.1 H <sub>2</sub> Production	89
5.2.3.2 Characterization of Spent Catalyst	91
5.2.4 APR of Different Substrates	98
5.2.4.1 Batch APR of Model Feed Compounds	101
5.2.5 Baseline Reactions	103
5.2.6 Comments on Batch and Continuous Mode	105
<b>6 CONCLUSIONS AND RECOMMENDATIONS</b>	<b>109</b>



<b>APPENDIX A: Sample Calculations</b>	112
<b>APPENDIX B: Temperature and Pressure Profile Sample Data</b>	117
<b>APPENDIX C: Hydrogen Chemisorption Isotherm Plots</b>	118
<b>APPENDIX D: ICP-OES Analysis of a Liquid Sample</b>	121
<b>APPENDIX E: CP-TOSS MAS <math>^{13}\text{C}</math> NMR of Biomass APR Residue</b>	122
<b>APPENDIX F: Aqueous-phase Reforming of Formic Acid (Single Run Experiments)</b>	126
<b>REFERENCES</b>	129

## LIST OF TABLES

	Page
<b>Table 2.1:</b> Solar intensity values (on horizontal surface).	22
<b>Table 2.2:</b> Summary of lignosulfonate major applications.	35
<b>Table 2.3:</b> Problems of biotechnological processes and possible solutions.	44
<b>Table 4.1:</b> Quantities used for run with different acid concentrations.	63
<b>Table 4.2:</b> Thermal conductivities of the different gas species in the study.	67
<b>Table 5.1:</b> Elemental analysis of Southern pine sawdust used in the study.	78
<b>Table 5.2:</b> Chemical composition of Southern pine sawdust used in the study.	80
<b>Table 5.3:</b> Constituent monosaccharides of softwood hemicelluloses.	80
<b>Table 5.4:</b> Proximate analysis of pine sawdust solid by-products due to hydrolysis (5% H <sub>2</sub> SO <sub>4</sub> ) and APR (5% H <sub>2</sub> SO <sub>4</sub> + 10% Pt/Al <sub>2</sub> O <sub>3</sub> ).	84
<b>Table 5.5:</b> Platinum, aluminum and sulfur content of fresh and spent Pt/Al <sub>2</sub> O <sub>3</sub> catalyst.	91
<b>Table 5.6:</b> Summary of physisorption tests of several catalyst pellets.	97
<b>Table 5.7:</b> H <sub>2</sub> turnover frequency (TOF) of APR of different substrates.	106
 <b>Table A.1:</b> Summary of GC analysis results	 113
<b>Table A.2:</b> Sample raw gas composition based on each GC	115
<b>Table A.3:</b> Run 70 gas phase volumetric composition	115
<b>Table B.1:</b> T-P data of Run 70	117
<b>Table D.1:</b> Summary of liquid sample ICP-OES analysis of Run 117 (formic acid, Pt/Al <sub>2</sub> O <sub>3</sub> , water)	121

## LIST OF FIGURES

	Page
<b>Figure 2.1:</b> 2003 World primary energy production by source.	6
<b>Figure 2.2:</b> Energy flow in the US in 2004.	7
<b>Figure 2.3:</b> M.K. Hubbert's prediction of peaking of US crude oil supply.	9
<b>Figure 2.4:</b> Actual US crude oil production from 1949 to 2004.	10
<b>Figure 2.5:</b> Coal resource in the US by area.	13
<b>Figure 2.6:</b> Total net generation of electricity by energy source in the US.	16
<b>Figure 2.7:</b> Projected incremental increase in natural gas consumption by region and country group (light blue = mature economies; lavender = transition economies; maroon = emerging economies).	18
<b>Figure 2.8:</b> Growth of world nuclear power.	20
<b>Figure 2.9:</b> Hydroelectricity consumption from 1979 to 2004.	24
<b>Figure 2.10:</b> Structure representation of cellulose.	28
<b>Figure 2.11:</b> Interaction between chains in native cellulose I.	29
<b>Figure 2.12:</b> Cellulose ultra-structure in plants. (a) organization from micelles to cell wall; (b) illustration of crystalline and amorphous regions in microfibrils.	29
<b>Figure 2.13:</b> Hemicelluloses. (a) Galactoglucomannan; (b) Arabinoglucuronoxylans; (1) $\beta$ -D-glucopyranose; (2) $\alpha$ -D-galactopyranose; (3) $\beta$ -D-mannopyranose; (4) $\beta$ -D-xylopyranose; (5) $\alpha$ -L-arabinofuranose.	31
<b>Figure 2.14:</b> Proposed structural segment of lignin.	33
<b>Figure 2.15:</b> Lignin precursor units. (a) coniferyl alcohol; (b) p-coumaryl alcohol; (c) syringyl alcohol.	33
<b>Figure 2.16:</b> Examples of wood extractives. (a) abietic acid (oleoresin); (b) catechin (flavonoid); (c) palmitic acid (fatty acid).	36

<b>Figure 2.17:</b> General schematic of a lignocellulosic refinery.	39
<b>Figure 2.18:</b> Schematic of the two-platform biorefinery system.	40
<b>Figure 2.19:</b> Chemical structure of starch. (a) amylose; (b) 3-D structure representation; (c) amylopectin.	42
<b>Figure 2.20:</b> Thermodynamics of alkane and oxygenate reforming.	53
<b>Figure 2.21:</b> Possible pathways of competing bond breaking on Pt. (a) C-C bond breakage leading to formation of H <sub>2</sub> and CO. (b) C-O bond breakage leading to formation of alkane/dehydrated molecule through reaction of intermediate with hydrogen.	54
<b>Figure 4.1:</b> Parr reactor assembly. (a) Top assembly (valve for liquid sampling not included); (b) bottom bomb; (c) picture of set-up.	61
<b>Figure 4.2:</b> Wheatstone bridge circuit for a TCD.	67
<b>Figure 4.3:</b> BS-GC calibration curve of air.	69
<b>Figure 4.4:</b> BS-GC calibration curve of carbon monoxide.	70
<b>Figure 4.5:</b> BS-GC calibration curve of methane.	70
<b>Figure 4.6:</b> BS-GC calibration curve of carbon dioxide.	71
<b>Figure 4.7:</b> BS-GC calibration curve of ethane.	71
<b>Figure 4.8:</b> BS-GC calibration curve of carbon dioxide at higher concentrations.	72
<b>Figure 4.9:</b> HP-GC calibration curve of helium.	72
<b>Figure 4.10:</b> HP-GC calibration curve of hydrogen.	73
<b>Figure 4.11:</b> HP-GC calibration curve of air.	73
<b>Figure 4.12:</b> HP-GC calibration curve of carbon dioxide.	74
<b>Figure 5.1:</b> HPLC-PAD chromatogram of wood monosaccharides from pine sawdust.	81
<b>Figure 5.2:</b> Gas production due to acid hydrolysis of biomass in the absence of reforming catalyst.	87
<b>Figure 5.3:</b> Comparison of gas production in the absence and presence of platinum using woody biomass as feed.	90

<b>Figure 5.4:</b> S2p <sub>3/2</sub> spectra of calcined, spent and acidified Pt/Al <sub>2</sub> O <sub>3</sub> catalyst pellets. Insert: Tabulated expected line shift for sulfur species based on compound.	96
<b>Figure 5.5:</b> Comparison of APR gas production using different feed sources in the presence of both acid and reforming catalysts.	99
<b>Figure 5.6:</b> Mutarotation of β-D-glucopyranose.	102
<b>Figure 5.7:</b> Increase in system pressure due to evolution of gases. Pressure profiles: water-He baseline (◆); water-He-Pt (▲); water-He-Pt-acid (×); biomass with both 5% acid and Pt/Al <sub>2</sub> O <sub>3</sub> (○).	104
<b>Figure C.1:</b> Isotherm plot of fresh Pt/Al <sub>2</sub> O <sub>3</sub> catalyst pellets.	118
<b>Figure C.2:</b> Isotherm plot of spent Pt/Al <sub>2</sub> O <sub>3</sub> catalyst pellets.	119
<b>Figure C.3:</b> Isotherm plot of calcined spent Pt/Al <sub>2</sub> O <sub>3</sub> catalyst pellets.	120
<b>Figure E.1:</b> CP MAS <sup>13</sup> C NMR spectra of natural lignin from Douglas fir.	122
<b>Figure E.2:</b> Structural units expected from lignin.	123
<b>Figure E.3:</b> CP MAS <sup>13</sup> C NMR spectra of natural lignin from oak.	123
<b>Figure E.4:</b> CP-TOSS MAS <sup>13</sup> C NMR spectra of residue from biomass APR.	124
<b>Figure F.1:</b> Gas composition of different formic acid experiments.	127
<b>Scheme 1:</b> Proposed pathway of degradation of D-glucopyranose in the presence of acid.	86

## LIST OF ABBREVIATIONS

B	Billion
Btu	British thermal unit
ORNL	Oak Ridge National Laboratory
APR	Aqueous-phase reforming
WGS	Water-gas shift
OPEC	Organization of Petroleum Exporting Countries
OECD	Organization for Economic Cooperation and Development
DOE	Department of Energy
CE	Common Era
GPa	Gigapascals
EIA	Energy Information Administration
USGS	United States Geological Survey
USSR	Union Soviet Socialist Republic
MJ	Megajoules
IFP	French Oil Institute (Intstitut français du pétrole)
LNG	Liquefied natural gas
CNG	Compressed natural gas
kWh	kilowatt-hr
DP	Degree of polymerization
PNNL	Pacific Northwest National Laboratory
NREL	National Renewable Energy Laboratory
LCF	Lignocellulosic fibers

BCO	Bio-crude oil
HPLC-PAD	High performance liquid chromatography/chromatograph – pulsed amperometric determination
GC	Gas chromatography/chromatograph
SCWG	Supercritical water gasification
$\Delta G_{\text{rxn}}$	Gibb's free energy of reaction
TOF	Turn-over frequency
TGA	Thermogravimetric analysis
DCM	Dichloromethane
PID	Proportional-Integral-Derivative
dI	de-ionized
L/W	liquid-to-water
EERE	Energy Efficiency and Renewable Energy
TCD	Thermal conductivity detector
WX	Tungsten-rhenium alloy
BS	Buck Scientific
HP	Hewlett-Packard
XPS	X-ray photoelectron spectroscopy
ESCA	Electron Spectroscopy for Chemical Analysis
BET	Brunauer-Emmett-Teller
ICP-OES	Inductively Coupled Plasma – Optical Emission Spectrometer
HMF	5-hydroxymethyl-2-furaldehyde
TPO	Temperature-programmed oxidation
EDX	Energy Dispersive X-ray spectroscopy
TPG	Temperature-programmed gasification
GCC	Ground calcium carbonate

PCC	Precipitated calcium carbonate
RR	Reforming ratio
DC	Direct current
KE	Kinetic energy
$h$	Planck's constant
$v$	speed of light
BE	Binding energy
$\phi_s$	Spectrophotometer work function
eV	Electron volt
ppm	parts per million



## SUMMARY

Aqueous-phase reforming (APR) is a relatively recent technology for producing hydrogen from biomass-derived substrates. Amidst the worldwide concerns about increasing petroleum prices and declining supplies, this process has the potential to address the need for a readily-available source of energy that is renewable and environment-friendly. APR uses temperatures much lower than those used in existing thermochemical methods for biomass: ~500K as opposed to about 600K to 1100K for pyrolysis and gasification. The reaction occurs in aqueous phase in the presence of a reforming metal catalyst that can catalyze both reforming and water-gas shift reactions. To date, known APR studies dealt only with applying this technology to oxygenated compounds that were used to mimic biomass. However, it is considered that application of APR to real biomass is needed to gauge whether this technology can be considered a viable approach for hydrogen production.

This study deals with the first known application of APR for the production of H<sub>2</sub> from actual biomass. Milled sawdust of Southern pine was used. The experiments were carried out in batch using a 100mL Parr microreactor heated to 225°C. In this one-pot, two-step process, acid hydrolysis was considered to break down the polymeric constituents of biomass to smaller soluble molecules. These simple compounds were then reformed using a Pt/Al<sub>2</sub>O<sub>3</sub> catalyst. The gas-phase products were typically H<sub>2</sub>, CO<sub>2</sub> and CO. In some instances, methane was detected but was too small to be quantified. Two gas chromatographs with thermal conductivity detectors (TCD) were used in order to quantify the gas phase.

The results of the experiments showed that increasing sulfuric acid concentration from 1% to 5% (by weight) caused more than a twelve-fold increase in H<sub>2</sub> concentration. Hydrogen was a minor product, accounting for about 18% of the non-condensable gas phase, while CO<sub>2</sub> was the major product. In the presence of the Pt/Al<sub>2</sub>O<sub>3</sub> reforming catalyst, both the selectivity and yield of hydrogen in the gas phase increased. Hydrogen percentage averaged at about 33% of the gas phase. This was accompanied by a noticeable decrease in carbon monoxide production, which is attributed to the activation of the water-gas shift reaction catalyzed by platinum.

APR was applied also to other substrates such as glucose, wastepaper and ethylene glycol. Comparison of their respective hydrogen yields showed that the amount of hydrogen produced from biomass was of a comparable magnitude per gram of feed. However, biomass yielded the most hydrogen per gram of carbohydrate among the substrates. On the other hand, ethylene glycol exhibited the highest hydrogen selectivity. Among the previously mentioned feed, it was the only one that did not produce any solid residue. Both ethylene glycol and glucose formed homogeneous solutions with water at the beginning of the reaction.

Baseline experiments with only the catalysts charged to the reactor, in the absence of any biomass, showed no increase in the reactor system pressure when only water and helium were present. This indicated that the observed hydrogen production was sourced from the biomass itself.

Characterization of the spent catalysts showed loss of hydrogen chemisorption activity for the platinum. Further calcination of the spent catalysts to remove possible

coke formation on the catalyst surface did not improve chemisorption. The presence of sulfur species on the catalyst, as revealed by elemental analysis and confirmed through X-ray photoelectron spectroscopy (XPS), was considered the cause of this loss in chemisorption activity. XPS further characterized the sulfur species as sulfates. However, the presence of these possible hydrogen chemisorption poisons on the catalyst surface does not preclude activity of the catalyst for APR reactions. Addition of sulfuric acid to ethylene glycol batch APR resulted in about 22% reduction in hydrogen yield – a change not as drastic as would be expected based on the complete loss of hydrogen chemisorption activity of the catalyst.

# CHAPTER 1

## INTRODUCTION

According to anthropologists, human civilization thrived with the discovery of the fire. From then on, human ancestors, the *Homo erectus*, could protect themselves from the cold and keep wild beasts away better during the night. With fire, living in colder places – away from Africa – became possible [1]. They learned how to cook. And because they needed to contain whatever food they hunted or produced, cooking implements were invented as well as other tools. Charcoal, a by-product of their wood burning, became a tool by which they have learnt to express themselves. Witness the arts on the walls of the caves in Lascaux, France. From survival to invention and aesthetic concerns.

Throughout history, energy has been a driver in humankind's progress. Its utilization brought comfort, sustenance and an increasing standard of living throughout the years. Together with its growing utilization, the sources from which energy could be harvested or generated had evolved as well. From burning of wood to the burning of coal, from harnessing the inherent power of sunlight to generating energy from the fission of uranium, these are testaments to the ingenuity as well as the need of the human race to feed what has been sustaining them. Among these, fossil fuel became the most important source for nearly the past two centuries.

Over the years, concerns about the steady decline of the available petroleum in the face of ever-increasing demand for this valuable commodity have fueled researchers to look for possible alternative energy sources as well as chemical feedstock. Coupled with

unrest in most nations where the majority of crude oil is sourced, the fear of losing a steady supply of fuel gave impetus to renewed efforts in countries to being self-reliant. Recently, most governments all over the world have turned their policies towards improving renewable and sustainable energy sources that are accessible in their own backyard. One such resource is biomass.

Biomass is considered by most to be a renewable, CO<sub>2</sub>-neutral and readily available source of energy. In the United States, Oak Ridge National Laboratory (ORNL) estimated that about 512 million dry tons of biomass per year could be initially available at less than \$50/dry ton delivered [2]. This amount is equivalent to 8.09 Quads<sup>a</sup> of primary energy. Currently, only 72 million dry tons (1.2 Quads) of these are utilized as fuel. This leaves quite a margin which can still be exploited for energy production. Putting this into perspective, 6.89 Quads is about 1.2 B barrels of oil – equivalent to about 27% of the US net import of crude oil in 2004 [3].

Hydrogen has been identified as a very attractive energy carrier [4]. The hydrogen economy has been considered by many to be the answer to solving the problems currently faced by the world regarding energy [5]. In fuel cells, hydrogen, together with oxygen, is transformed into water. This process generates electricity [6]. Unfortunately, many technologies still rely on fossil fuel as the hydrogen source, most notable of which is coal gasification. Considering the concerns about the future supply of petroleum as well as environmental concerns regarding the use of coal, extensive research on alternative hydrogen generation technologies is currently underway.

---

<sup>a</sup> 1 Quad =  $1 \times 10^{15}$  Btu  $\approx$  172 Million barrels of oil

Several processes have been explored to produce hydrogen from biomass. One of the existing approaches involves the pyrolysis of biomass, followed by subsequent reforming of the bio-oil produced [7-9]. Another technology is biomass gasification. However, these processes require very high temperatures (673 K–1100 K) even in the presence of catalysts and different gasification agents [4, 7, 10-12]. Dalai et al. reported a yield of about 26 and 32 mmol/g sawdust in the gasification of aspen and cedar wood, respectively, at 2.4 wt% impregnation with CaO [10]. They reported that the presence of CaO caused a decrease in the temperature from ~850°C to ~675°C at which the hydrogen production rate was at a maximum.

In 2002, Dumesic et al. first reported the aqueous-phase reforming (APR) of oxygenated compounds that were chosen as model biomass mimics [13]. They demonstrated the capacity to produce hydrogen at temperatures (~500K) much lower than those required for either pyrolysis or gasification. In this process, feed molecules such as glucose are mixed with water and fed to a fixed-bed type flow reactor with metal catalysts. Selectivity to production of hydrogen<sup>b</sup> could reach as high as 99% for molecules more reduced than sugars (methanol and ethylene glycol) [13-16]. Dumesic's group considered two reactions to be of major importance for hydrogen evolution: the reforming reaction (C-C cleavage),



<sup>b</sup> Dumesic et al. defined selectivity as (molecules H<sub>2</sub> produced)/(total C atoms in gas phase) x 100/RR. Reforming ratio (RR) refers to the ratio of theoretical moles of H<sub>2</sub> that can be produced per mole C in the feed molecule. (RR for ethylene glycol is 2.5 while for glucose, it is 2.0)

and the water-gas shift (WGS) reaction,



Hydrogen could also be consumed during the process due to side reactions such as methanation.

Currently, there has been no report of the application of APR to *actual biomass*. In order to address the sustainability issue of aqueous-phase reforming, application of this technology directly to biomass would be more attractive. Dumesic et al. reported that substrates with lower hydrogen to oxygen ratio are actually less favored for hydrogen production [13, 17, 18]. Since biomass is expected to have lower H/O ratio, it would be interesting to probe its performance in aqueous-phase reforming.

This thesis is a recounting as well as a discussion of the first known attempt made to use actual biomass (Southern pine sawdust) for aqueous phase reforming and the results and interpretation of these efforts. In Chapter 2, a review of literature pertinent to the study is presented. This includes a discussion on current energy demand and sourcing as well as consideration of existing technologies for energy and hydrogen production from biomass. Chapter 3 lists the goals that guided the completion of this study. Descriptions of reagents as well as experimental procedures used in the study are presented in Chapter 4. Analyses methods used are also briefly described. In Chapter 5, data gathered in the course of the study are reported. Discussion of the possible interpretations of the results and trends observed are given as well. Lastly, conclusions and some recommendations for further study are presented in Chapter 6.

## **CHAPTER 2**

### **REVIEW OF RELATED LITERATURE**

Energy drives our modern society. It is necessary in almost every aspect of our lives – at home, while traveling, in our offices, during leisure, in the operation of varied businesses and industries and in the production and transfer of goods and services. Energy supply and demand has a big impact on economic policies. Without energy, it would be impossible to maintain and further develop the level of advancement and way of life that is characteristic and more often than not, taken for granted, in modern-day living.

#### **2.1 CURRENT STATUS OF WORLD ENERGY**

##### ***2.1.1 Supply and demand of oil***

Energy can be derived from such sources as geothermal, hydrothermal, solar and other renewable resources as well as nuclear reactions. However, the bulk of energy is derived from nonrenewable fossil fuels, namely, coal, oil and natural gas. Figure 2.1 illustrates the world production of energy by source in 2003. As can be seen from the graph, of all the fossil fuels, crude oil is the major source of energy in the world – comprising about 35% of the sources [19, 20]. Petroleum (crude oil) is produced by countries belonging to the Organization of Petroleum Exporting Countries (OPEC) and Organization for Economic Cooperation and Development (OECD) as well as others including China and the Former Soviet Union. According to the US Department of



Energy (US DOE) [21], 85% of all the energy consumed in the United States is provided by fossil fuels. Figure 2.2 maps out the energy flow from sourcing to application in the United States. In 2004, bulk of the energy requirement was made by industries, followed closely by the transportation sector. Also in this figure, it was shown that about 32% of US primary energy source (mainly petroleum) was imported from other countries.

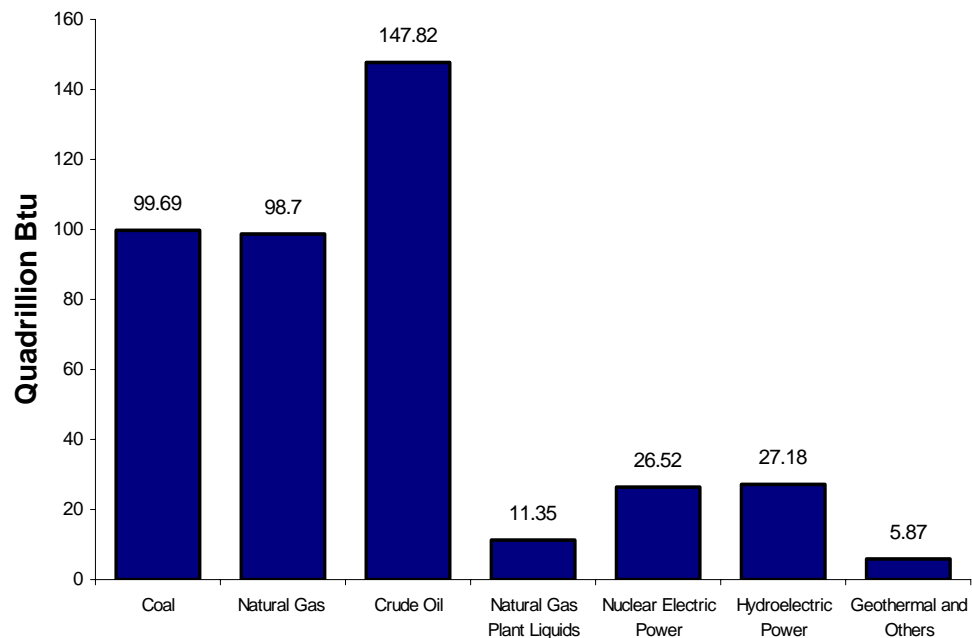


**Figure 2.1** 2003 World primary energy production by source [20]

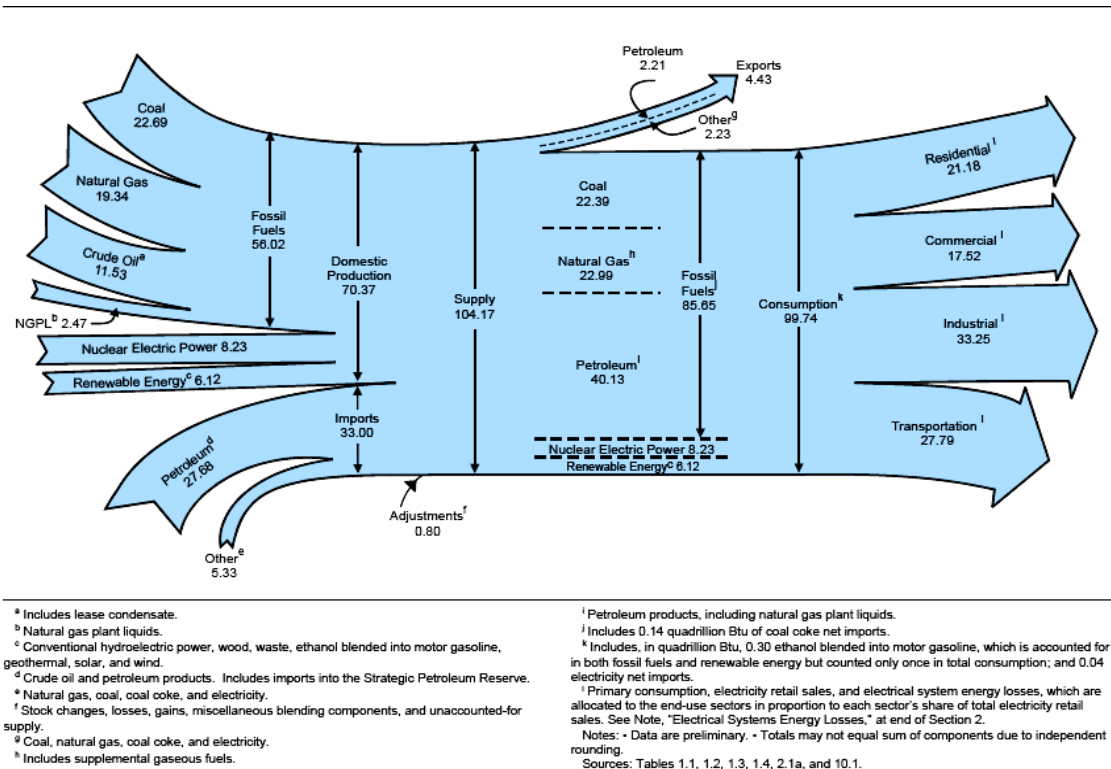


**Figure 2.2** Energy flow in the US in 2004 [20]

### 2.1.2 The Issue of Non-sustainability: Declining oil reserves

Fossil fuels are generally considered as non-renewable resources. They are carbon-containing materials (mainly hydrocarbons) that are largely derived from accumulated organic matter, such as plant or animal remains that have long been deeply buried. Due to extreme pressures and temperatures, these organic matters are converted from peat into coal, from kerogen to petroleum (crude oil) or into natural gas (also into natural-gas liquids) [22]. Their first utilization was attributed to northeast Englishmen in the 13<sup>th</sup> century who discovered that a kind of black rock found near the seashore would burn. They called these “sea coles”. This led to the first mining of coal, the beginning of

the systematic fossil fuel utilization [23, 24]. However, another source said coal has been the major source of fuel in China since the 4<sup>th</sup> century CE [25].

As noted before, petroleum (also known as crude oil or “black gold”) supplies about 35% of the world’s source of primary energy and fuels nearly all of the world’s transportation [19, 20]. This heavy dependence on petroleum makes the issue of its sustainability a very important one [26, 27]. A small group of scientists, mostly from Russia and Ukraine, contends that crude oil is not from biotic origins but are spontaneously generated and therefore should be unlimited [28]. Though some studies have shown that abiogenetic formation of hydrocarbon is possible through synthesis under hydrothermal conditions (150°C) [29] as well as conditions similar to the earth’s mantle ( $P = 5$  and  $11$  GPa;  $T = 500^{\circ}\text{C}$  to  $1,500^{\circ}\text{C}$ ) [30], the general consensus is that crude oil is derived from the decay of organic matter and is thus finite once this resource is depleted. The big question is when.

A chief consultant from Shell, M. King Hubbert, accurately predicted the US oil production peak around 1970. As early as 1949, he had put forward the concept that fossil fuels are finite resources and that he strongly expected their production to exhibit an exponential increase, passing through one or several maxima and then a decline asymptotically to zero [24]<sup>c</sup>. In a paper presented at a meeting of the American Petroleum

---

<sup>c</sup> In the same article, M. King Hubbert predicted that it would take 200 more years since then (1949) before the 9 billion mark in human population – which he considered as the maximum number of people the earth can hold – would be reached. He gave three scenarios that could happen: (a) maintain the population at peak, (b) slightly be lowered or, (c) approach the population of our agrarian ancestors. In this, he

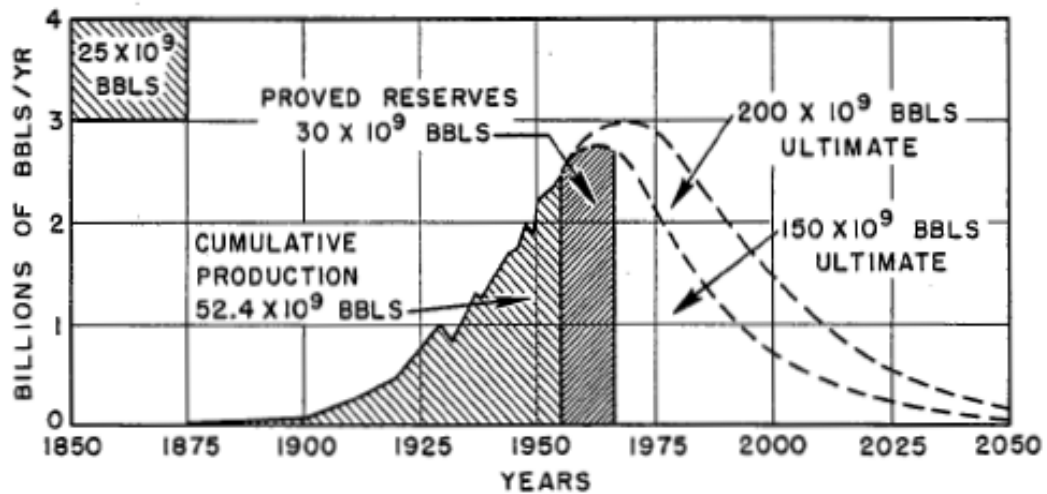


**Figure 2.3** M.K. Hubbert's prediction of US crude oil supply peaking [23]

Society in 1956 [23], Hubbert contended that US crude oil supply would peak at 1965 or 1970 when he incorporated an additional 50 billion barrels to the original assumption of 150 billion barrels of total US crude oil reserve. Figure 2.3 illustrates this prediction. On the other hand, Figure 2.4 shows actual US crude oil production as reported by the US Energy Information Administration (EIA) [20]. As can be seen, Hubbert's prediction came to pass.

---

considered energy supply availability, specifically from fossil fuels, to be a very significant factor in determining the fate of the human race.

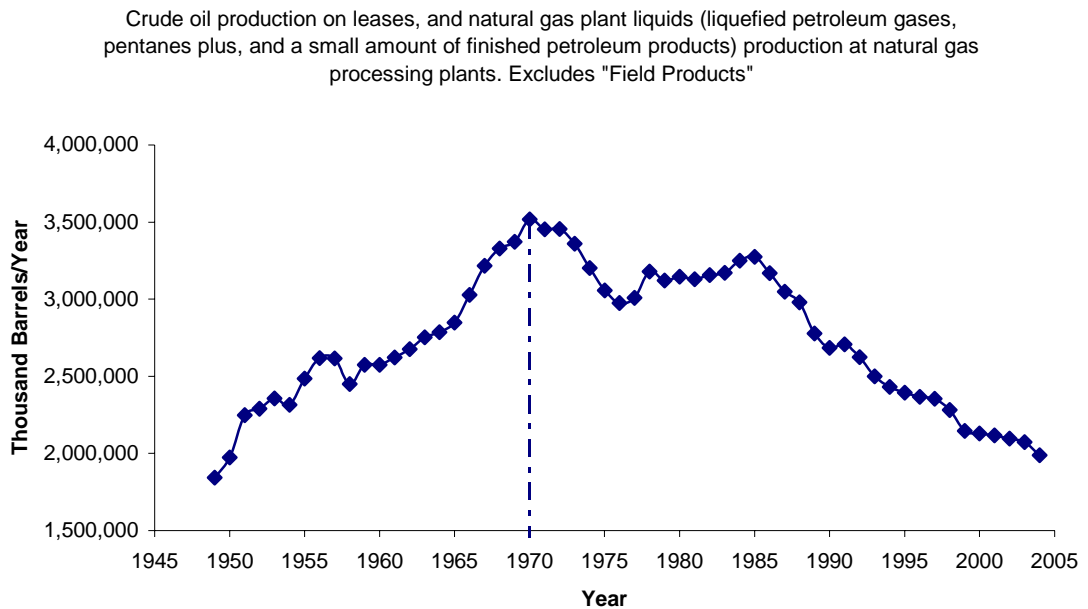


**Figure 2.4** Actual US crude oil production from 1949 to 2004 [20]

With respect to world crude oil production peaking, Hubbert stated [23] that he expected this to occur in 2000 – though he did qualify in all his predictions that a change in the then current rate of production could either retard or accelerate the culmination date. Actual data [31] showed that the amount of petroleum produced in the world had not yet peaked by 2003. In 2006, Greene et al. published a paper wherein they presented their estimate on when world conventional<sup>d</sup> oil peaking would occur based on two data sources: (1) the 2000 assessment of the US Geological Survey (USGS) of the world's conventional oil resources (produced, discovered and undiscovered estimate); and, (2) the

---

<sup>d</sup> Conventional oil refers to “liquid hydrocarbons of light and medium gravity and viscosity” that occurs in porous and permeable reservoirs. It includes natural gas liquids. On the other hand, unconventional oil consists of oil deposits “of greater density than water (heavy oil), viscosities in excess of 10,000 cP (oil sands) and occurrences in tight formations (oil shale)”. See Greene et al., 2006.

more conservative figures reported by Campbell in 2003 [32-35]. According to Greene et al., the peak year for world conventional oil is 2040 based on the first set of data (i.e. by USGS). This is a very optimistic prediction compared to Hubbert's assessment. The same could be said with the projected peak year (2016) when Campbell's data were used. However, if only the "rest-of-the-world" (ROW) (excluding the Middle East) [35] figures are considered, Greene et al. expected peaking to occur before 2030. Projections for ROW conventional oil peak year are 2023, based on USGS data and 2006, according to Campbell's figures. Unless the Middle Eastern oil producers step up their production to fill the gap due to ROW peaking, the authors concluded that tremendous pressure would be put upon unconventional oil to expand and intensify their processing and utilization [34, 35].

The price of crude oil has about doubled within the last two years [36]. Oil prices are expected to remain high due to three reasons: (1) world petroleum demand grew at a fast rate of 3.4% in 2004 (equivalent to 2.7 million barrels per day) in the face of very little spare upstream capacity; (2) oil prices are sensitive to any incremental tightening of supply during high periods of economic growth; and, (3) volatility of the oil market due to geopolitical issues in oil-producing countries [37]. The continued increase has an effect of dampening the world petroleum demand rate [26, 27, 36]. However, EIA reported that actual world consumption still rose by 3.8 million barrels per day (bbl/d) during the same time frame [36]. Emerging economies, especially in Asia, are seen to demand for more energy as progress drives them to require more transportation and build more infrastructure [37]. Together with North America, they are considered to account for most of the projected growth in world oil demand. Before 1973, when the first oil

crisis hit the world, developing countries capacity for oil production as well as their oil consumption did not garner much attention. However, since 1973, when every source mattered, contribution from developing countries was quoted to be around 30% of the world's primary energy [26]. They are also considered responsible for about one half of the world increase in primary consumption. For the year 2005, US EIA reported a total world demand for petroleum averaged at 83.7 million barrels/day while total world supply amounted to 84.0 million barrels/day [38] showing a very small margin of surplus which is mostly centered in Saudi Arabia [36].

In her paper, Dunkerley [26] considered one aspect of the increase in oil price that is “helpful”. According to her, as prices rise, it will encourage the development of the other forms of energy that were not considered as cost-competitive as petroleum. This state was seen also to encourage better conservation efforts. Indeed, this has been the case, as reflected by different government policies as well as the trends in research activities that are currently being undertaken [39, 40].

### ***2.1.3 Coal***

The world has more coal reserves than it has crude oil. According to the agency's latest data at hand, EIA reported an estimated ~1 trillion short tons of recoverable coal in 2003 – 27% of which was said to be located in the US, the largest reserve of any country [31]. The Eastern Europe bloc and the Former USSR were reported to have the ~28% of the total world reserves, quite comparable to that of North America.

Coal is touted by some as the closest alternative to crude oil that we have today [6, 41]. The World Coal Institute issued a document entitled “The Role of Coal as an

Energy Source” wherein they listed coal’s importance in the quest of world energy in the face of fears of fuel shortage. Paramount to their list is coal’s availability (being more widely distributed than crude oil), abundance and affordability as well as its relative ease of handling and storage [41]. It is approximated that the world coal reserve will last for 190 years at current consumption rate [37] . Figure 2.5 shows the distribution of this resource in the US. In 2004, there were a total of 1,379 mines existing and operational all over the US, which produced a total of 1,112 million short tons [42].

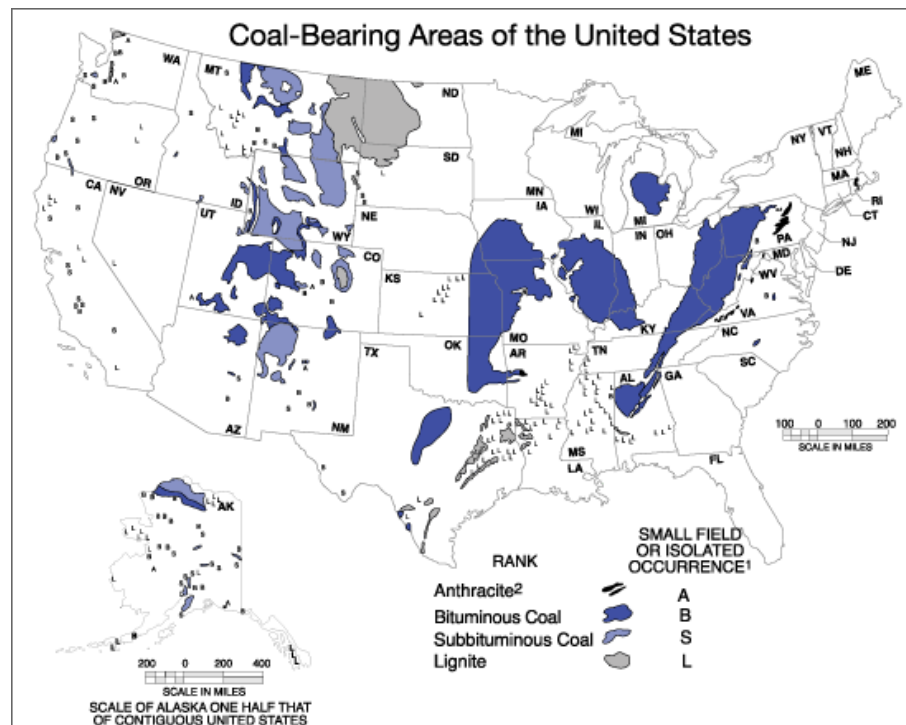


**Figure 2.5** Coal resource in the US by area [31]

Coal, like other fossil fuels, is derived from the remains of trees, ferns and other plants that were said to exist in tropical forests (especially during the Carboniferous



Period) some 400 million to 1 billion years ago. Through heat and pressure over a long period of time, these materials were transformed into the resource that is being mined today [25, 43]. Major coal beds of Europe and the Eastern United States are thought to be coastal swamps buried by sea-level changes caused by the southern hemisphere glaciation [6].

The quality of coal is based on (a) the organic content of the coalified plant remains; and, (b) the inorganic substance contributed by the plants, water seepage and surrounding geological matter [44]. The organic content is mostly made up of carbon with smaller amounts of nitrogen, hydrogen and oxygen. On the other hand, inorganics refer to sulfur as well as small but possibly toxic amounts of antimony, arsenic, beryllium, cadmium, mercury, lead, selenium, zinc, heavy radionuclides and asbestos [44]. Sulfur emission is one of the major drawbacks of using coal.

Coal is categorized into different grades. Ranking is based on calorific value as well as organic content. Anthracite is the cleanest- and slowest-burning coal. It has low volatility and high carbon content (95-98%). Anthracite is the oldest of all types and has the highest heating value (>32.5 MJ/kg). Bituminous coal comes in second, classified itself into three: low, medium and high volatile bituminous. Low volatile bituminous coal produces less ash than anthracite making it the best material for making coke<sup>e</sup>. From Figure 2.5, it can be seen that majority of the US coal reserves are bituminous. The next two types are sub-bituminous and lignite, respectively. Sub-bituminous coal is a dull black coal with a calorific value range of 19.3-26.7 MJ/kg. The lowest rank coal, lignite,

---

<sup>e</sup> Coke is a solid fuel that remains when coal is heated to a high temperature in the absence of air or during coal gasification.

has lower heating value than sub-bituminous coal. It is brownish-black in color and has generally both high moisture and ash content. [43, 44]

Coal powered the Industrial Revolution. From its discovery, mining of coal followed. This resource was then used for the smelting of metals which was instrumental in the development of the steam engine. From there came the locomotive, the steamship and the steam-electric power.[24] Due to Britain's large deposits of coal and its ability to exploit that resource ahead of the other countries, it led the world during the Industrial Revolution. Until about 1870, Britain alone supplied over 30% of the manufactured goods in the world [25]. In today's world, coal is the main source for electricity. It supplies energy for about 39% of the world's electricity production, according to the World Energy Outlook 2002 by the Paris-based International Energy Agency [41]. Shown in Figure 2.6 is the generation of electricity based on primary sources in the US from 1993 to 2004<sup>f</sup>. At 51% [45], coal utilization for US electricity production far exceeds other primary energies. In the US, coal supports almost thrice the amount of the next largest primary source. In the world, as the primary source of 39% of the world's electricity, its contribution is twice that of the next largest source [41].

---

<sup>f</sup> *Other gases* refer to blast furnace gas, propane gas and other manufactured and waste gases derived from fossil fuels. *Other renewables* refer to wood, black liquor, other wood waste, municipal solid waste, landfill gas, sludge waste, tires, agricultural by-products and other biomass, geothermal, solar thermal, photovoltaic and wind. *Others* refer to batteries, chemicals, hydrogen, pitch, purchased steam, sulfur, and miscellaneous technologies.

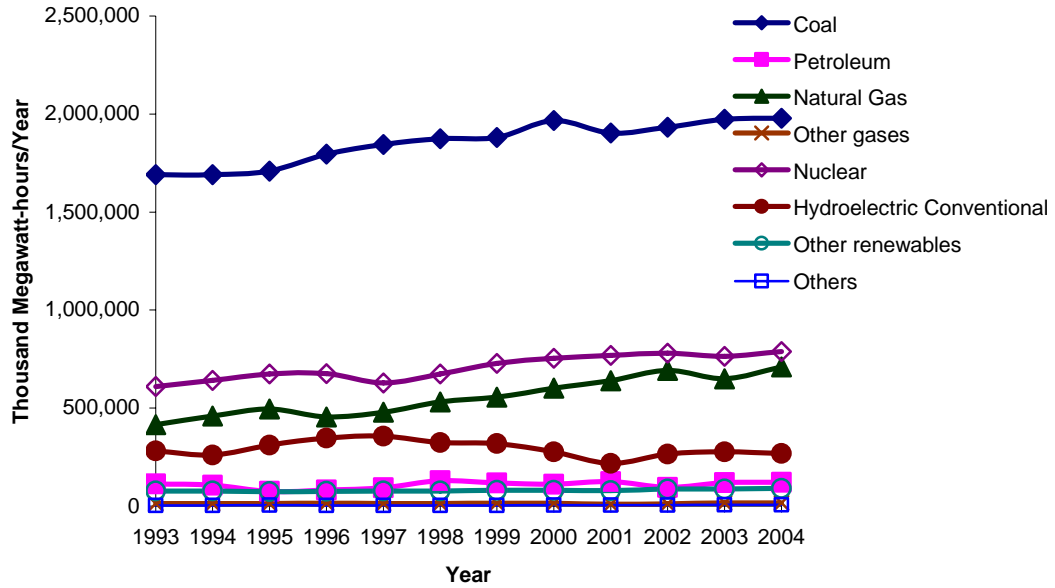


**Figure 2.6** Total net generation of electricity by energy source in the US [46].

However, the main criticism of coal utilization is the large amount of emissions released during its processing [6, 25, 41, 44]. To quote Deffeyes in his book *Beyond Oil* (2005) [6], “coal is the best of fuels; it is the worst of fuels”. While recognizing their apparent advantages, he also mentioned that coal-fired power plants emit gases, especially greenhouse gases, which could produce smog, acid rain, CO<sub>2</sub>, and mercury pollution [6]. According to Hodgson, a typical coal power plant will emit in a year about 11 million tons of carbon dioxide, 16 000 tons of sulfur dioxide, 29,000 tons of nitrous oxide, 1,000 tons dust and smaller amounts of other chemicals such as aluminum, calcium, potassium, titanium and arsenic [47]. The management of these pollutants through improved technologies (i.e. the goal of zero emission), especially for CO<sub>2</sub>, is this resource’s greatest challenge. The development of technologies for carbon capture and

sequestration is necessary for coal to be environment-friendly. Indeed, the heavy dependence of US to coal-fired power plants is one of the reasons it did not accept the Kyoto Protocol – an international agreement on world climate change which includes setting limit to the amount of greenhouse gases that could be released to the environment [44].

#### ***2.1.4 Natural Gas***

Natural gas is a combustible mixture consisting of methane and other hydrocarbons with other inert gases that is found in porous rocks of the Earth's crust [48, 49]. It is usually associated with deposits of crude oil [44, 48]. It is the third largest primary energy source in the world, next to crude oil and coal [19, 37, 49]. It is considered to be the fastest growing primary energy source – with a projected rate from 2002 to 2025 that is higher than the demand for petroleum and coal [37]. As of 2005, it was reported that the world natural gas reserve is about 6,040 trillion cubic feet [37]. Similar to petroleum, emerging economies are expected to have a higher demand rate for this commodity [37]. This projection is seen on Figure 2.7.

In 2003, the IFP (French Oil Institute)-sponsored international colloquium *Panorama 2003* noted that there was nothing that can be considered as a world gas market, as opposed to a world oil market [50]. They noted that while 50% of oil was transported from one continent to another, only a measly 5% of marketed natural gas production was traded inter-regionally. This is probably due to the fact that accessibility to a pipeline infrastructure as well as proximity to population centers are important

considerations for transportation of natural gas to be economical [6, 37]. However, transporting natural gas in the form of liquefied natural gas (LNG) as well as compressed natural gas (CNG) seems to be addressing this problem nowadays.

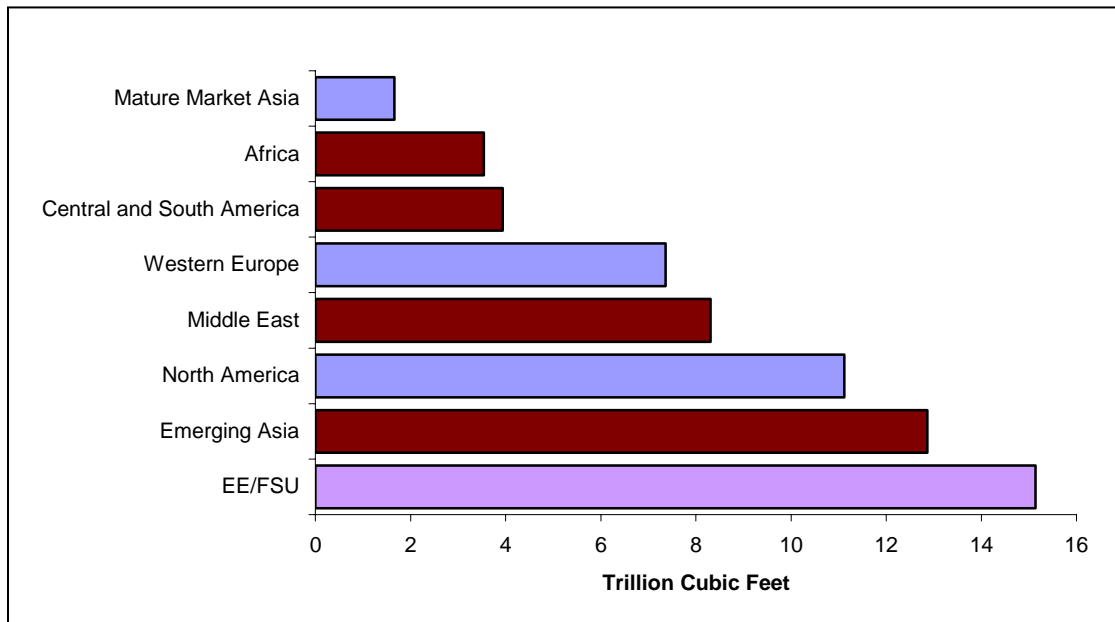


**Figure 2.7** Projected incremental increase in natural gas consumption by region and country group [37] (light blue = mature economies; lavender = transition economies; maroon = emerging economies)

Natural gas is primarily used for generation of electricity and space heating<sup>g</sup>. Currently, it is being tapped to replace diesel/gasoline as transportation fuel for what are known as alternative fuel vehicles [51]. Other potential applications include using it for hydrogen production for lower emissions [52]. According to the US DOE website, natural gas is

---

<sup>g</sup> One barrel of oil is equivalent to about 6000 cu. ft of natural gas. See Deffeyes, 2005.

clean burning and has significantly lower harmful emissions than reformulated gasoline. Like other fossil fuels though, its use releases large amounts of CO<sub>2</sub> and possibly H<sub>2</sub>S, depending on the technologies used.

#### ***2.1.5. Nuclear Energy***

In the paper Hubbert delivered in 1956 discussing the oil peaking year for the US, he also mentioned the possibility of using nuclear power to compensate for the expected decline in crude oil production [23]. Since the demonstration of its power in the bombing of Hiroshima in 1945, the awesome energy contained in the nucleus of these radioactive materials has been harnessed by some countries as a primary resource [44, 47]. In 2003, there was a total of about 2.5 trillion kilowatthours of electricity that was sourced from nuclear reactors all over the world [31]. Currently, there are a total of 493 commercial nuclear generating units in the world, capable of supplying 364.9 gigawatts [53]. By 2025, EIA projected that the total would be increased to 421.8 gigawatts – 63% of which is expected to be produced in mature economies [37].

Nuclear reactors use uranium as fuel. World production of this element was reported to be 102.17 million pounds U<sub>3</sub>O<sub>8</sub> in 2004 [54]. According to this data, Canada was the largest producer at 30.15 million pounds – around 30% of total production, followed by Australia. However, it was noted that uranium (a finite resource in itself) supply might eventually become a problem for energy sourcing from nuclear reactions [44, 55].

Utilization of nuclear reactors decreases the amount of CO<sub>2</sub> emission associated to energy generation. As an example, France, which has around 80% of its total electrical energy source as nuclear (data for 1999), has halved its carbon emission per unit energy produced since 1970 [47]. In the US, nuclear power plants helped avoid 90% of the total carbon emissions from 1981 to 1994 [56].

Shown in Figure 2.8 is a chart of the growth of nuclear power in the world from 1960 to 2002. During this period, there was not much growth for North America, Europe and the former Soviet Union. However, Japan and the developing countries, mostly in Asia, showed growth in nuclear power generation during the same time frame. Aside from immense capital and operational cost [57], a serious impediment to the proliferation of nuclear power plants for most countries is the fear of the people of the possibility of a nuclear accident, with its far-reaching effects – such as one in Chernobyl (now part of Ukraine) in 1986 [47]. So far, there were a total of seven nuclear reactor accidents that have resulted to radiation release [57]. Another important consideration is the hazards associated with the disposal of the nuclear wastes and spent fuel from the process.

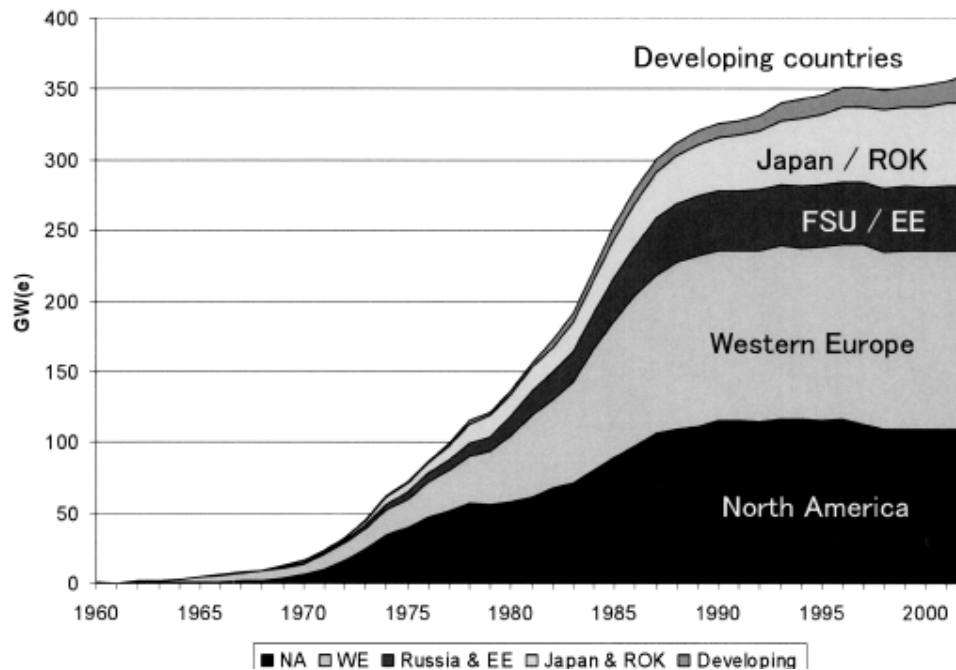


**Figure 2.8** Growth of world nuclear power [58]

### **2.1.6 Renewable Sources**

Hydroelectric, geothermal, solar, wind and biomass are considered renewable sources of energy. According to the EIA, a total of 6.117 quadrillion Btu of consumed energy in the US was supplied by these five in 2004 [59]. This translates to only about 6% of the total 2004 US energy consumption while 86% was from cumulative fossil fuels. Despite this, it is expected that we would be relying more on the renewables as the fossil fuels become more expensive by reason of its depleting existence.



### 2.1.6.1 Solar Energy

The sun is a large burning mass of hydrogen and helium about 92.96 million miles from earth on average<sup>h</sup> [44, 60]. It radiates in all regions of the spectrum. However, its energy is concentrated only in the range of 300 to 3000 nm [61, 62]. Direct-normal radiation and diffuse radiation make up the two components of solar radiation that we can harness. The first one refers to the radiation that arrives from the sun that is not scattered by dust and other particles. On the other hand, diffuse radiation is that which has undergone scattering due to contact with these objects in the atmosphere before it reaches the earth's surface [61]. Because of scattering, the latter has less energy. On a very overcast day however, only diffuse radiation is available [61].

The sun is considered a source of “free, non-polluting and infinitely renewable energy [44].” Possible energy that can be harvested from sunlight is enormous. Unfortunately, it is only available during the day – around 30 to 40 percent of an average year [61]. Energy will also vary depending on location. Shown in Figure 2.1 are solar intensity values on horizontal plates from different parts of the world [44]. Aside from this, problems encountered by a solar-based energy source include low intensity radiation at ground level and the need for efficient and economic energy extraction, conversion and storage<sup>i</sup> [44].

---

<sup>h</sup> The distance from the sun to the earth (average: 92.96 million miles) is equivalent to 1 astronomical unit.

<sup>i</sup> In England, an interesting paradox exists. Here, energy from the sun is highest during the summer season. However, electricity requirements were actually the lowest at this time of the year. See Ref. 44.

**Table 2.1** Solar intensity values (on horizontal surface) [44]

		kWh/m <sup>2</sup>					
Location	Latitude	Max. bright day		Min. dull day		Yearly Total	
		(1)	(2)	(1)	(2)	(1)	(2)
Equator	0°	6.5	7.5	5.8	6.8	2200	2300
Tropics	23.5°	7.1	8.3	3.4	4.2	1900	2300
Mid-earth	45°	7.2	8.5	1.2	1.7	1500	1900
Central UK	52°	7.0	8.4	0.5	0.8	1400	1700
Polar circle	66.5°	6.5	7.9	0	0	1200	1400

(1) Direct sunlight

(2) Direct + diffuse sunlight

#### 2.1.6.2 Hydroelectric Energy

Hydroelectric energy was the second largest contributing renewable primary energy resource in the US in 2004 [59]. It supported about 2.7% of the total energy consumption of the US during that year. Energy generation from water was not a new technology. Early water turbines were used for irrigation purposes. Water wheels were used to grind/mill grains [44]. These applications were usually of the run-of-river type wherein the energy of a moving stream of water is utilized [44, 61].

Present large-scale hydroelectric power stations are of the reservoir type. This application utilizes dam structures. From an elevated reservoir, water is allowed to fall onto the blades of a water turbine which rotates the shaft of an electric generator. In the case of the Shasta Dam in California, the spillway is three times higher than that of the Niagara, considered as the world's first large-scale hydroelectric power-station [44].

Shown in Figure 2.9 is the hydroelectric dependency of the different regions of the world up to 2004 as reported by BP in 2005.

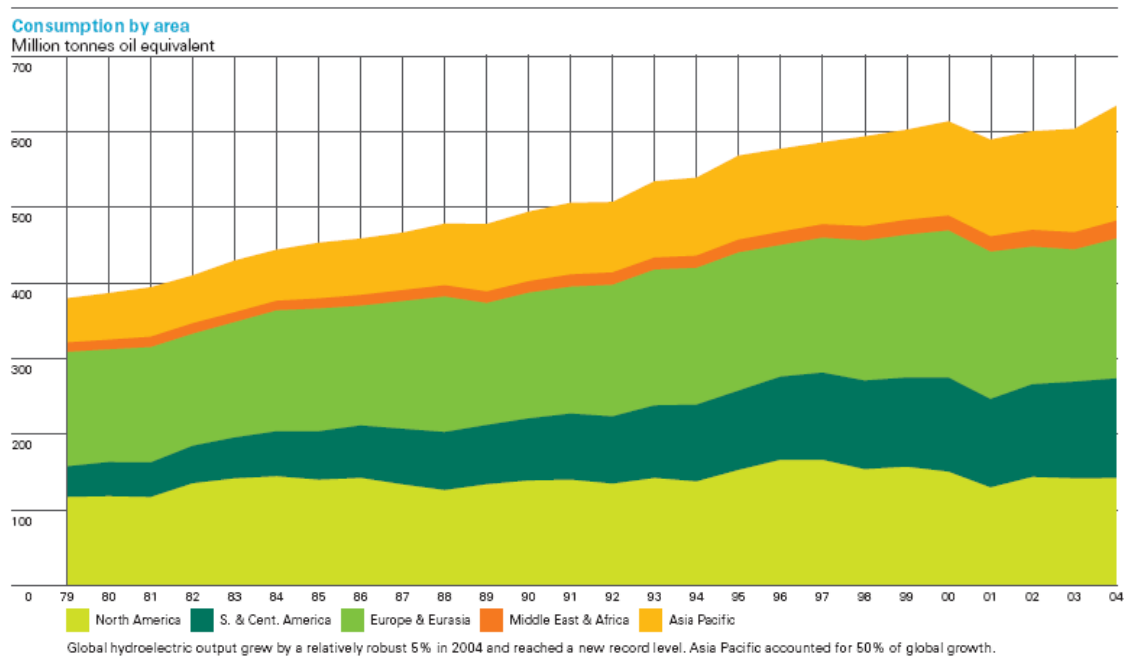


**Figure 2.9** Hydroelectricity consumption from 1979 to 2004 [63]

The main advantage of hydroelectric power generation over petroleum-based energy is that hydroelectric plants use a free fuel. With the ever-increasing petroleum prices, investing in a hydroelectric plant might become more attractive. The downside for this is the fluctuations in flow and water height depending on the season – e.g. long summer months might cause water level to go down, making it less efficient.

### 2.1.6.3 Geothermal, Wind and Biomass Energy

According to the Annual Energy Review 2004 done by the EIA, only about 1.5% of the total world energy consumption in 2003 was sourced from geothermal and other renewable sources (hydroelectric not included) [20]. This is a very small amount. However with some projections of as much as 70% of energy sourced from renewable resources by the year 2050 [55], much growth is expected in the utilization of these resources.

The first utilization of wind energy came with the use of sailboats. Since then, wind mills have been built and utilized, especially in Holland [44, 62]. Most of the currently operational wind turbines are of the lift-type configuration wherein the wind generates a force perpendicular to the direction it blows [62]. The mechanism is similar to that of sailboats that sail cross wind. Positive points for wind-generated electricity include (1) the fuel is free (as in hydrothermal); (2) no CO<sub>2</sub> emission; (3) leaves no dangerous residues; and, (4) the land where wind farms are located can be developed as an agricultural land as well [62]. On the other hand, the intermittent supply of wind is the problem.

The term geothermal came from two Greek words: *geo* which means “Earth” and *therme*, which stands for “heat”. As this implies, geothermal energy is sourced from the heat of the earth, coming from the outer core that is made up of magma. Water that has seeped through the permeable layers of the earth becomes heated, and by convection, may travel again upwards towards the surface to emerge as hot water springs or streams (geysers). In a geothermal power plant using the hot rock method [44], two holes are

drilled into the earth up to a depth where it can tap the earth's heat. One is a cold water inlet and the other one, an outlet for the heated water or steam. The heated water or steam is then directed to the power plant where turbines and heat exchangers are operated to recover the heat energy. It is said that the stored amount of energy that can be harnessed through a geothermal route far exceeds that of total fossil and nuclear resources. Geothermal energy is considered to be as immense as that of solar energy [44]. However, as it stands, its utility has not been much exploited in most countries capable of harnessing it.

Lastly, biomass energy accounts for the largest portion of US total energy sourced from renewable sources at 2.859 quadrillion Btu – about 47% of the renewables [59]. In the world, it is currently second to hydroelectric energy. More detailed discussion about biomass is given in the following sections.

## **2.2 BIOMASS**

Since the discovery of fire, humans have been using biomass as a source of energy. From dried twigs for camp fires to charcoal for barbequing to waste bark, low quality wood chips and sawdust for hog-fuel boilers, biomass materials have been utilized to produce much-needed light, heat and energy. However, throughout the years, other sources of energy have become more utilized, foremost of which are the fossil fuels, and burning plant materials has been considered inefficient. In the past decade or so, utilization of biomass has become of keener interest – not only as fuel but also as a source of chemicals which could potentially replace petroleum-based feedstock. Why is

biomass attractive? Because it is renewable, readily available and considered to give zero net emission of one of the most notorious greenhouse gases, carbon dioxide. Its utilization addresses the timely issues of sustainability, self-sufficiency and environmental consciousness. Presently biomass technologies however are not cost-effective. This is one major challenge that must be overcome for biomass energy to be commercially viable in a large scale.

### ***2.2.1 Chemical Composition of Biomass***

Biomass does not refer only to plants and plant-derived materials. It encompasses all substances from living or once-living organisms. However, plants and plant-derivatives are more intuitive and available resources in the quest for alternative sources of energy and chemical feedstock. Among the organisms, they are the first to capture the inherent energy of the sun, transforming it into forms that can be harnessed by the plants themselves and other organisms. An example of such product is starch, formed through the process of photosynthesis. Lignocellulosic plants, to which trees belong to, are so named because they are mainly constituted of the three most abundant natural polymers on earth: cellulose, hemicellulose and lignin. The following subsections deal with the description of these compounds.

### 2.2.1.1 Cellulose

Cellulose is the most abundant naturally-occurring polymer in the world. It is more commonly found on plant cell walls, constituting around 39-42% by dry weight [64] of softwoods, though some other organisms, such as the bacteria *Acetobacter xylinum*, have the capability to produce it as well [65-69]. It is a homopolysachharide consisting of repeating units of cellobiose - a dimer of  $\beta$ -D-glucose. The degree of polymerization (DP) ranges from 2000 to 14000 in cotton fibers [9]. Shown in Figure 2.10 is a representation of cellulose. Notice that two successive glucose units (ring structure) are not configured similarly – the next one “flips”. This is why strictly speaking, cellobiose is the repeating unit of cellulose and not glucose.

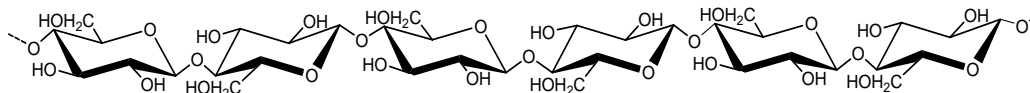


**Figure 2.10** Structure representation of cellulose

The glucose units in cellulose are linked together by  $\beta$ -1 $\rightarrow$ 4 glycosidic bonds. This allows for the formation of chains that can stack together and have closer interaction with each other, as illustrated in Figure 2.11. In plant cell walls, cellulose chains form bunches called micelles [70] or elementary fibril. These in turn aggregate into microfibrils. The microfibrils form macrofibrils which interact with the hemicelluloses and lignin in order to form the composite plant cell wall (see Figure 2.12 a).

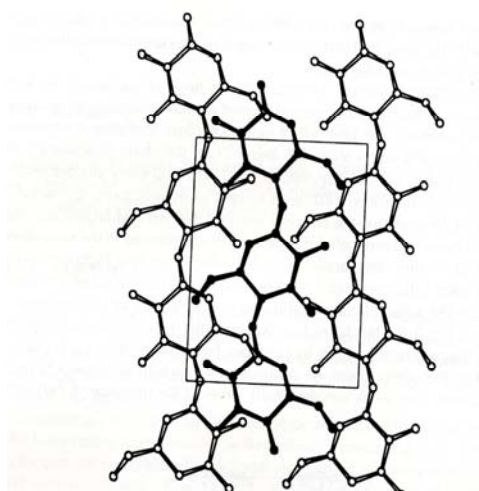


**Figure 2.11** Interaction between chains in native cellulose I. (Reproduced from [71])

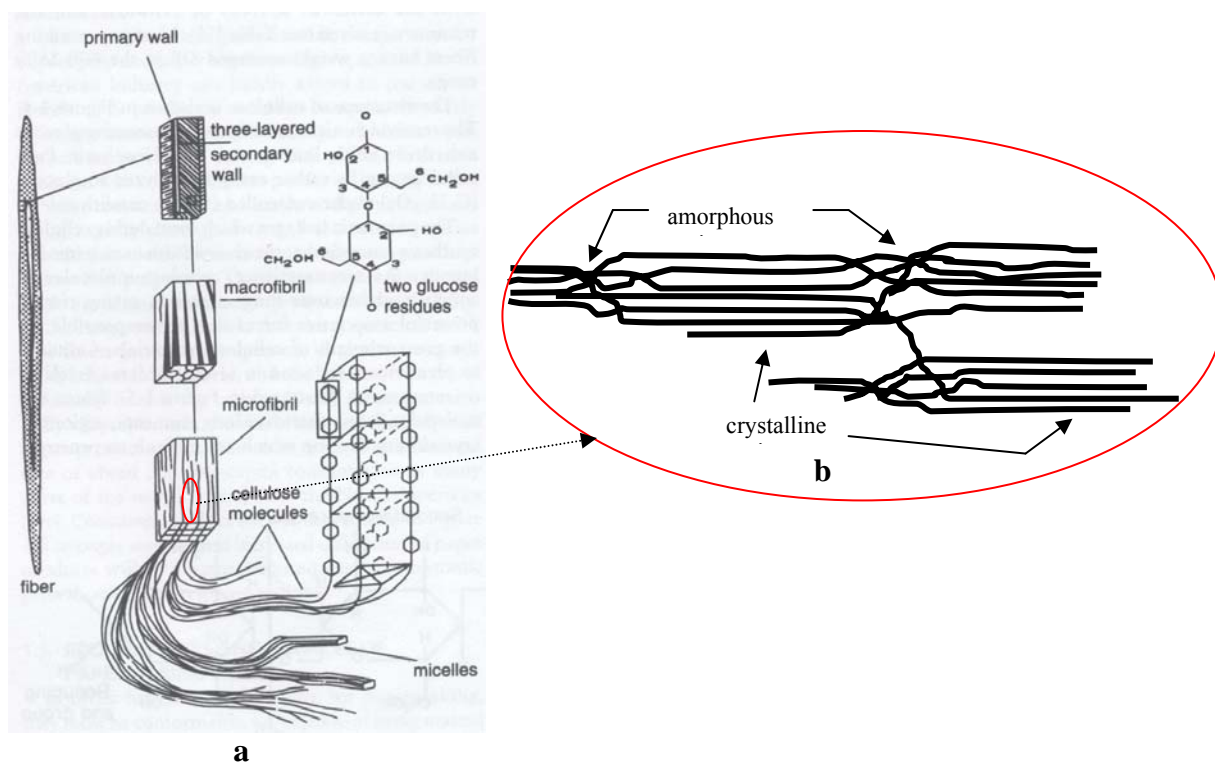


**Figure 2.12** Cellulose ultra-structure in plants. (a) organization from micelles to cell wall (Reproduced from [70] ); (b) illustration of crystalline and amorphous regions in microfibrils.



Cellulose is found to be insoluble in most solvents [72]. The elementary cellulose fibrils can have close association with each other such that they form ordered, linear, crystalline structures (Figure 2.12b). However, a small portion of the chains may become disordered and thus have a more random arrangement. These are found in the amorphous regions. Due to the strong interaction of cellulose chains in the crystalline region, it is difficult for solvents and other chemicals to penetrate through the structure while the amorphous regions are more susceptible [70].

Cellulose can be derived from cotton linters by removing the associated waxes by solvent extraction [72]. The pulp and paper industry have long been utilizing cellulose from lignocellulosic materials. Fibers for paper production are preferentially made up of cellulose and some remaining hemicellulose from pulping. A special type of cellulose called *alpha-cellulose* is used for more high-end products such as films, absorbent products and membranes. Cellulose can also be derivatized into its acetate and xanthate forms for use in specialty polymer applications. The higher the value of the end-product, the more stringent are raw material requirements, the lesser the yield and the more are considered as process waste.

#### 2.2.1.2 Hemicellulose

Hemicelluloses make up around 35% by weight of hardwoods and 25% by weight of softwoods [70]. Together with cellulose, they are referred to as holocellulose. Hemicelluloses are a group of heteropolysaccharides consisting of combinations of glucose, galactose, mannose, xylose and arabinose. The predominant type of hemicellulose in softwoods is different from hardwoods. These biopolymers are

branched, with chains that are much shorter than cellulose (DP  $\sim$  150 [9]). Aside from the sugar components, some hemicellulose fractions may also be in acetylated or in uronic acid forms [71-73]. Figure 2.13 shows the two most abundant groups of hemicelluloses in softwoods. Galactoglucomannans (Figure 2.13a) are the major component of softwoods followed by arabinoglucuronoxylans (Figure 2.13b) [71, 74]. For hardwoods, the major hemicellulose group is glucuronoxylans or O-acetyl-4-O-methylglucurono- $\beta$ -D-xylan.

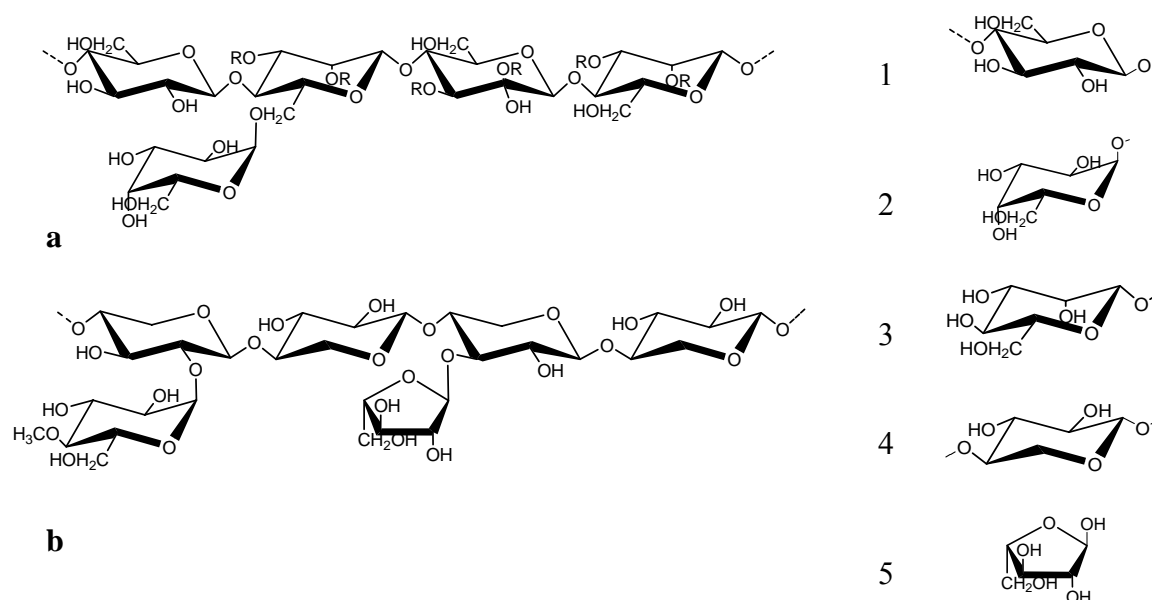


**Figure 2.13** Hemicelluloses. (a) Galactoglucomannan; (b) Arabinoglucuronoxylans. (1)  $\beta$ -D-glucopyranose; (2)  $\alpha$ -D-galactopyranose; (3)  $\beta$ -D-mannopyranose; (4)  $\beta$ -D-xylopyranose; (5)  $\alpha$ -L-arabinofuranose

The branching in hemicelluloses causes them to be more accessible and thus more susceptible to the action of solvents and chemical reactions. For example, Garrote et al. [75] noted that for hydrothermal treatments, hemicelluloses were best hydrolyzed within the range of 150 – 230°C. On the other hand, cellulose hydrolysis was favored above 210-220°C. Indeed, the process of pre-hydrolysis, be it by acid or steam, aims at removing the more labile hemicelluloses to have a higher yield of fractionated cellulose (glucose) in the next step [64, 73, 76-78]. The hydrolyzed sugars could then be purified for production of higher-value products [27].

#### 2.2.1.3 Lignin

The complete structure of lignin, the third most abundant component of biomass, still remains elusive up to this day [79]. The reason for this is the lack of extraction methodology that will leave lignin structure intact during or after extraction from biomass. However, lignin researchers agree that it is an amorphous macromolecule, mostly made up of phenyl propane units and cross-linked by ether and carbon-carbon bonds [9, 71, 79]. Shown in Figure 2.14 is a proposed structure of this biopolymer [71].

Lignin is considered to be made up of three phenylpropane building block units: p-coumaryl, sinapyl and coniferyl. Their relative abundances are different for softwood and hardwood lignins. Softwood lignin is called guaiacyl lignin – predominantly from coniferyl alcohol units. On the other hand, hardwoods contain both syringyl (from sinapyl alcohol) and guaiacyl lignin. The three lignin precursors are shown in Figure 2.15.

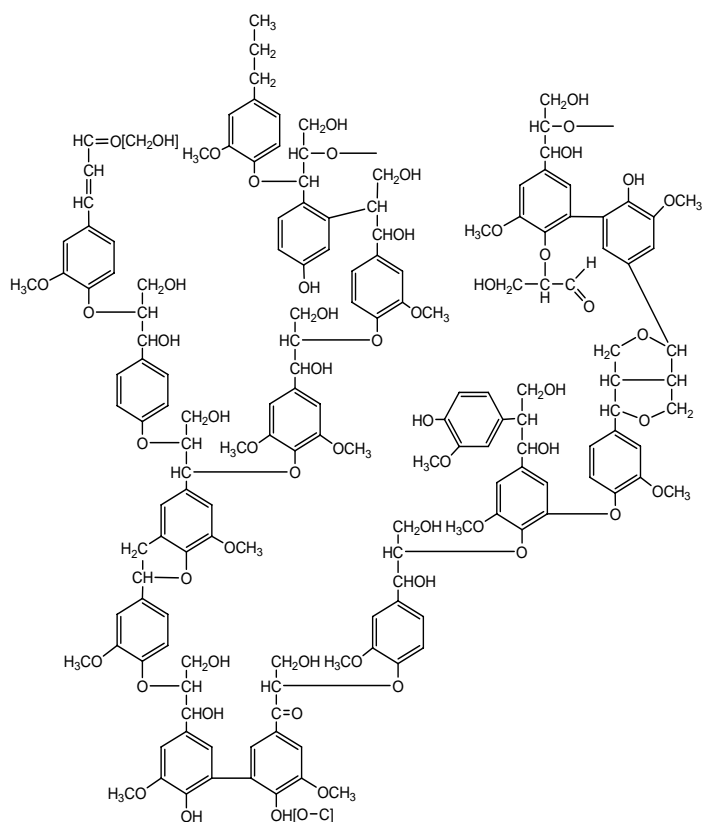


**Figure 2.14** Proposed structural segment of softwood lignin [71]

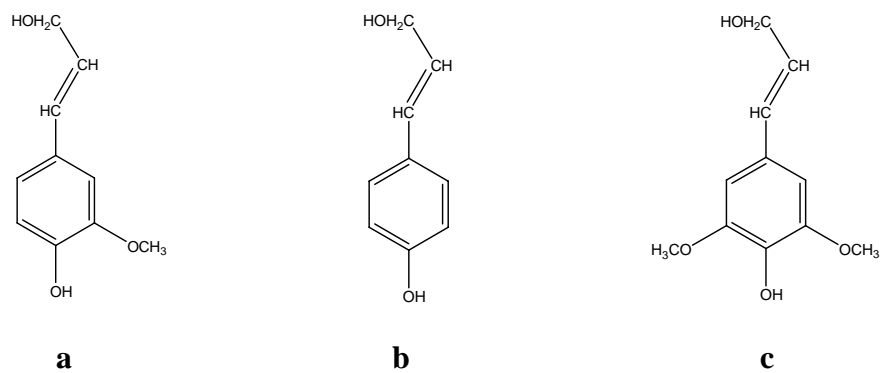


**Figure 2.15** Lignin precursor units. (a) coniferyl alcohol; (b) p-coumaryl alcohol; (c) syringyl alcohol

For the most part, lignin is unwanted in paper making. Chemical pulping is done to remove this polymer which causes stiffness and the unwanted dark color in fibers. The most commonly used process in the United States is the Kraft process. This makes use of the combined power of sodium hydroxide and sodium sulfide in order to lower the lignin content to 4-5% for softwoods [70]. Lignin degradation usually occurs in basic conditions, though acid can also be used to remove it from wood chips. Acid sulfite pulping for papermaking was widely used before the chemical recovery process in Kraft pulping became cost-effective. The active components of the acid sulfite process are sulfite-bisulfite ions which attack the lignin. Unfortunately, if conditions of the acid sulfite process were not controlled<sup>j</sup>, the reverse process of lignin degradation, i.e. lignin re-condensation, could readily occur [70, 71]. Re-condensation will cause the previously fragmented lignin to form cross-linked molecules and redeposit onto the fibers. The insolubility of lignin at high acidity conditions is exploited in the most accepted method of quantitative lignin determination, the Klason method. Klason lignin is the residue product after digesting milled wood samples in 72% H<sub>2</sub>SO<sub>4</sub>.

Lignin, in the form of lignosulfonate, has been studied for application as acidic ion-exchange resin [80, 81], cationic surfactant, dispersant and retention aid [82-85], as catalyst for coal gasification in its sodium- and calcium-sulfonate forms [86, 87] and precursor for silica-carbide [88, 89]. Pye [90, 91] summarized lignosulfonate applications in Table 2.2.

---

<sup>j</sup> This can also result in low fiber yields as well as fibers that are structurally weak because of the damage. The relative non-selectivity of the sulfite-bisulfite ions is one of the main reasons why Kraft pulping, which produces stronger fibers (less holocellulose degradation, higher selectivity towards lignin solubilization), is preferred presently.

**Table 2.2** Summary of lignosulfonate major applications [90]

<b>Applications of crude spent liquor lignosulfonates</b>	<b>Applications of refined lignosulfonates</b>
Feed and pellet binders Feed molasses extenders Dust suppression and road stabilization Granulation and agglomeration Plant micronutrients and horticulture Agricultural dispersants and emulsifiers Grinding aids Metal ore processing	Oil well drilling fluids Dye and pigment dispersants Protein precipitants Tanning agent Gypsum board manufacture Cement manufacture Concrete admixtures Refractory clays and ceramics Carbon black Phenolic resins Lead acid storage battery plates

#### 2.2.1.4 Extractives

Extractives consist of wood components which are soluble in neutral organic solvents or water. They are typically in the order of 2-8% of dry wood weight, depending on species and, location in the tree, among other criteria [64, 70]. These compounds are important to maintaining the tree's biological functions [71]. Terpenoids, steroids, fats, waxes as well as phenolic constituents such as stilbenes, lignans, tannins and flavonoids comprise the wood extractives. The phenolics have fungicidal properties and affect natural wood color. Fats and waxes, as in other biological systems are utilized as energy source while terpenoids and steroids are what are known as oleoresins. The last group also has anti-microbial as well as insect-resistance properties. Some extractives are pharmaceutically important. For example, flavanoids are used as antioxidants and as antivirals [92-94]. Some extractive structures are shown in Figure 2.16.

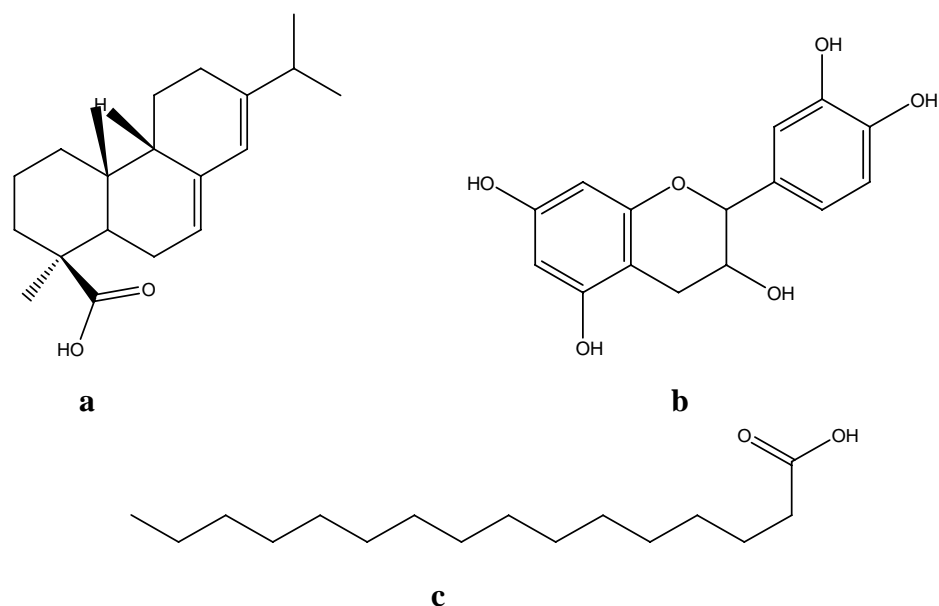


**Figure 2.16** Examples of wood extractives. (a) abietic acid (oleoresin); (b) catechin (flavonoid); (c) palmitic acid (fatty acid)

#### 2.2.1.5 Ash

Similar to extractives, the inorganic components of biomass usually function in some biological pathway in plants. Trace metals are usually complexed with wood constituents such as magnesium in chlorophyll. Other inorganics come from metal salts that are deposited in the plant cell walls and lumens. Calcium is commonly the most abundant metal followed by potassium and magnesium. Typically, ash is less than 1 wt% of most wood [71].

### ***2.2.2 Biomass as a renewable resource***

Before the petroleum industry became almost the sole source of industrial chemicals in the 1930's, bulk products were sourced from biomass. These include fuel (ethanol, butanol) and organic acids (acetic, citric and lactic acids) [95]. However, the advent of petroleum refineries changed all these. Synthetic polymers replaced natural ones such as hemp, wool and cotton. Furniture usually made from wood and metal also started using plastic. The use of polymers has proved its advantages and natural fibers lost the limelight for bulk applications. Biomass, as an energy source, became limited to incineration/burning to produce heat.

Amidst the current trends in petroleum prices as well as environmental concerns, utilization of biomass is again being reviewed with a recognition that the inherent chemical value of each component exceeds their collective heating value [96]. Willke and Vorlop noted that Shell Oil intends to produce 30% of the world's chemical and oil needs with biomass while DuPont projected in 2001 that it would try to achieve sourcing of 25% of its product from biomass by the year 2010 [95]. The biorefinery concept addresses the realization of these targets. Ragauskas et al. defined biorefinery as “a facility that integrates biomass conversion processes and equipment to produce fuels, power and chemicals from biomass” [64]. It has similarities with a petroleum refinery which is the source of most of the chemicals used presently. Kamm et al. [27] identified four biorefinery systems, namely:

- (a) *lignocellulosic feedstock biorefinery*, which uses “nature-dry” raw material



- (b) *whole crop biorefinery*, which is applied to raw materials such as cereals and maize
- (c) *green biorefineries*, which use “nature-wet” biomass such as grass, alfalfa, clover or immature cereal
- (d) *biorefinery two platforms concept*, which is divided into the sugar platform and the syngas platform

Shown in Figure 2.17 is the schematic for a lignocellulosic biorefinery. The focus of this biorefinery is the fractionation of lignocellulosic materials into its components, i.e. cellulose, hemicellulose and lignin by either biological or thermochemical means. The by-products (e.g. monosaccharides) are then further refined (secondary refining) to form smaller molecules which are feedstock for industries such as polymers, binders and adhesives, lubricants, and fuels, among others. In 2004, staff at the Pacific Northwest National Laboratory (PNNL) and the National Renewable Energy Laboratory (NREL) published a report identifying the twelve precursor molecules that can be produced from biomass [97]. These molecules are expected to have an impact of future chemical feedstock sourcing

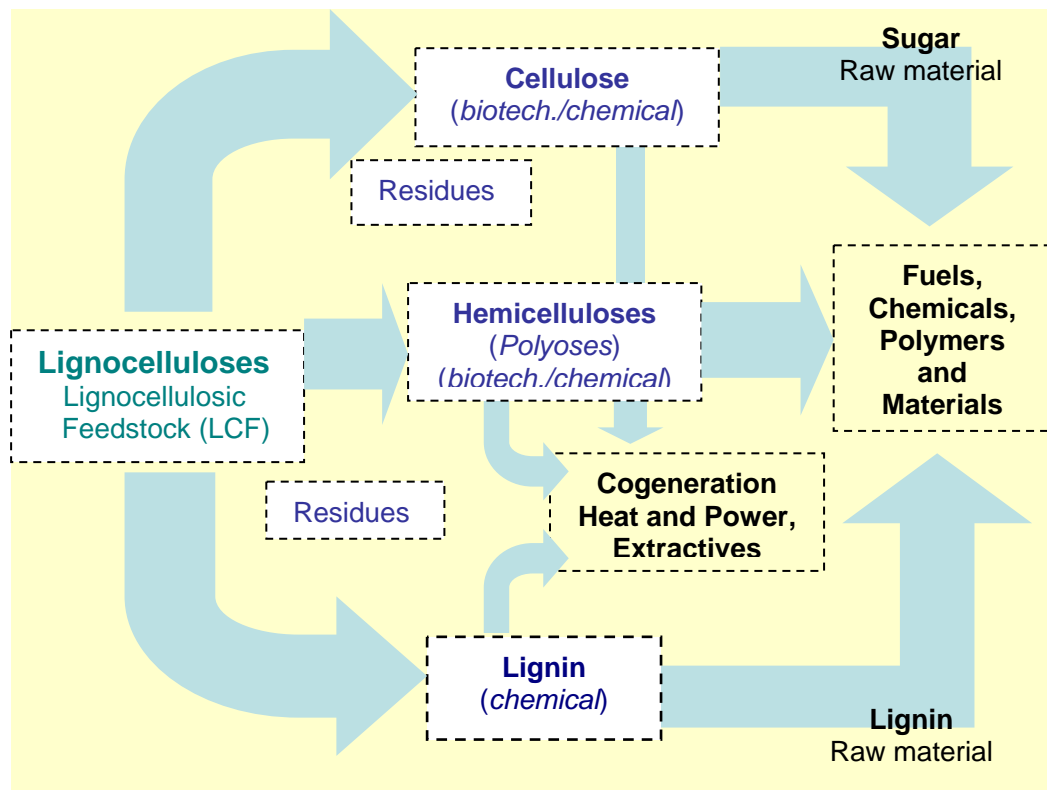


**Figure 2.17** General schematic of a lignocellulosic refinery [27, 91]

Another scheme that integrates lignocellulosic materials is the biorefinery two platform system concept. Its flowchart, slightly similar to the LCF biorefinery scheme, is shown in Figure 2.18.

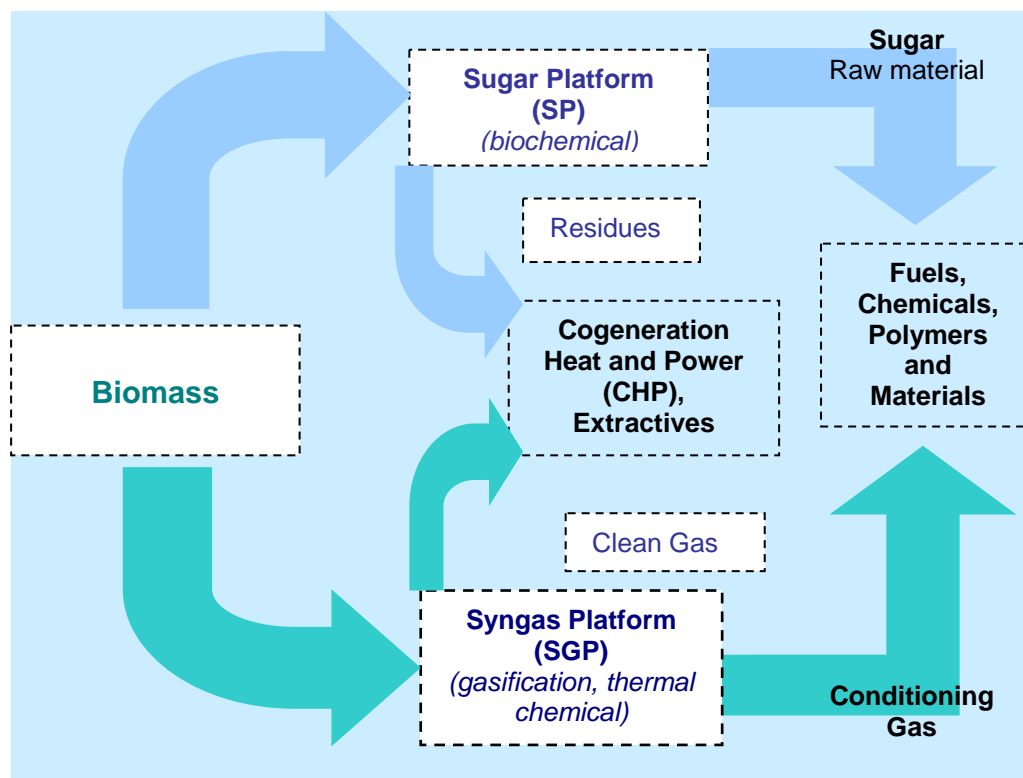


**Figure 2.18** Schematic of the two-platform biorefinery system [27]

In the sugar platform, focus is on the fermentation of sugars derived from the carbohydrate fraction of the biomass in order to produce precursor molecules. On the other hand, application of thermochemical reactions on the biomass, such as gasification, will produce syngas (CO and H<sub>2</sub>) which could be used as a feedstock for synthesis of higher value products. This is NREL's biorefinery concept [98]. Thus, the most common utilization of biomass for energy production can be classified into two: biochemical and thermochemical conversions.

#### 2.2.2.1 Biochemical Conversions

In March 2006, the EIA reported that since the beginning of the year, around 26.7 million barrels of fuel ethanol were produced [99]. If we consider an average of 0.3 million barrels of ethanol per day, an estimated 107 million barrels of ethanol will be produced for this year. With the US Energy Policy Act of 2005 [100] which requires the oil industry to blend 7.5 billion gallons of renewable fuels into gasoline by 2012, it is expected that the demand for ethanol will continue to grow.

Ethanol is sourced from agricultural starch crops such as corn and other grains [101]. Starch in the raw materials is hydrolyzed to its monomer, glucose, by action of enzymes and is then fermented to ethanol. However, full reliance on grains, especially corn, for ethanol raw material is not sustainable. There will be competing utility of corn as an energy source and as a source of food. This is why bioethanol, sourced from lignocellulosic materials, has gained importance in research.

Starch is easier to hydrolyze than cellulose, though both of them are homopolymers of glucose. This is due to the presence of branches in the amylopectin part of starch that makes the molecule more accessible to the solvent. (See Figure 2.19). Also, the  $\alpha$ -1 $\rightarrow$ 4 glycosidic linkage is not as stable as its cellulosic counterpart. Notice that the hydroxyl in C1 of the pyranose unit participating in the bond is in the axial position, crowding the bulky C6 group of the connecting monomer. As is expected, sterics play a role in the stability of the bond, even if the chains tend to curve – forming spirals to relieve some of the strain (Figure 2.19b). On the other hand, crystalline cellulose forms packed linear structures that are more difficult to penetrate by solvents.

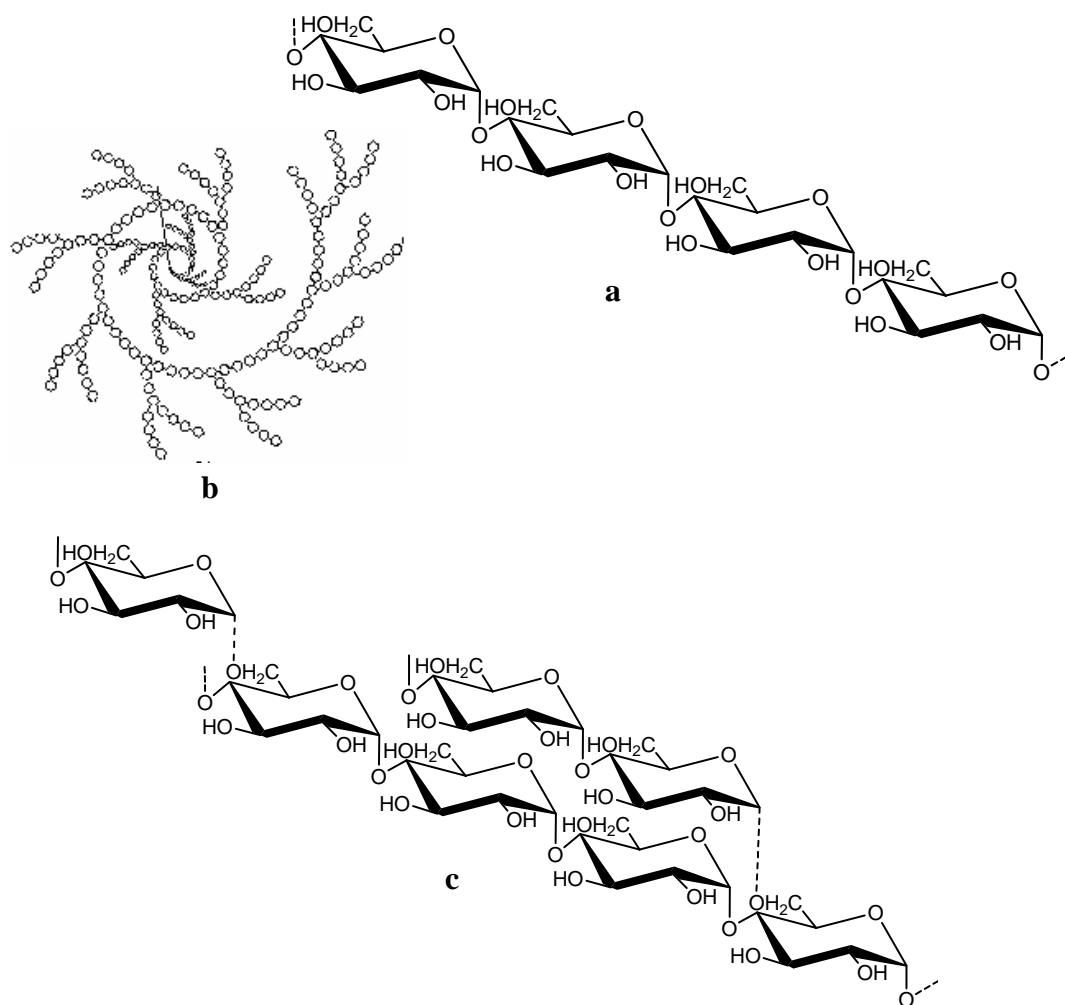


**Figure 2.19** Chemical structure of starch. (a) amylose; (b) 3-D structure representation; (c) amylopectin.

Starch processing to produce ethanol is considered a “fairly mature technology” [102]. Bioethanol production is not. Considering the much more complex chemical composition of lignocellulosic biomass, hydrolyzing the bonds holding these components will be more challenging. Gray et al. [102] noted that there are three major steps to

achieve this, namely, (1) *thermochemical pretreatment*, in order to improve enzyme access to the cellulases; (2) *enzymatic saccharification*, the use of enzymes (e.g. cellulases) to produce sugars; and, (3) *fermentation by microorganisms*.

Both cellulose and hemicelluloses are susceptible to acid hydrolysis, though hemicelluloses are more so. On the other hand, lignin is more easily attacked by alkali [70-72]. This differing solubilities would have an effect on the presence of chemicals in the hydrolysates. Acid hydrolysis will result in the formation of furfurals while acetates and ferrulates will be present if base hydrolysis is applied [102]. Aside from these, some phenolics from lignin may also be present in the acid hydrolysate [78]. These have been found to have an effect on the subsequent fermentation of the sugar hydrolysates. A recent study by Oliva et al. [103] on ethanol fermentation of *Kluyveromyces marxianus*<sup>k</sup> in a synthetic media with added furfural, acetic acid and catechol showed that furfural drastically affected the specific growth rate of the organism. Also, they noted that there was a synergistic effect between the three sample lignocellulosic degradation molecules on lowering both ethanol and biomass yield.

Another consideration with using lignocellulosics in ethanol production is the formation of pentosans in the hydrolysates. It has been reported that *Saccharomyces cerevisiae*, the most common yeast used for fermentation, is not as efficient at converting xylose into ethanol as it is with hexosans such as glucose [95, 102, 104]. Juanbaro and Puigjaner [105] noted though that many strains of bacteria are capable of utilizing pentosans. In their paper, they studied the action of *Clostridium acetobutylicum* for the

---

<sup>k</sup> A yeast strain that was found to be more heat-resistant than the commonly employed *Saccharomyces* strain. A simultaneous saccharification and fermentation (SSF) process at 42°C was used by Oliva, et al.

formation of acetone-butanol from brewing bagasse slurries. A paper by Klinke et al. [106] provides a comprehensive and fairly recent review of the inhibitory effects of pre-treatment by-products (furans, phenolics and acetate) on the ethanol production as well as specific growth rate of *S. cerevisiae*. Four pentose-fermenting organisms were also studied. Only *Thermoanaerobacter mathrani* A3M3 proliferated and produced ethanol without the need for detoxification.

Lastly, Willke and Vorlop [95] compiled a list of problems typically encountered in biochemical utilization of lignocellulosics as well as their possible solutions in Table 2.3.

**Table 2.3** Problems of biotechnological processes and possible solutions [95]

Problem	Solution
Biocatalyst not known	Screening (if required/mutation), metabolic pathway design (MPD)
Low productivities	High cell density-fermentation, cell recycle, immobilization
Cheap substrates often not suitable	Screening
Unwanted by-products	Genetic engineering, MPD
Low product and substrate concentration	Mutation/selection
Product recovery	In situ processes
Process control	On-line analytics

Gray et al. [102] recently published a review of the current advances done in the field of biotechnology with the objective of making commercialization of bioethanol possible, especially through genetic manipulation of organisms.

#### 2.2.2.2 Thermochemical Conversions

Clements and Dyne identified [107] three types of thermochemical conversions: (1) pyrolysis – refers to biomass processing between 300 to 600°C in the absence of oxygen; (2) gasification – treatment of biomass at temperatures higher than 700°C, the reaction of which can be catalyzed or not; and, (3) liquefaction – production of simpler compounds from the feed. The last one can be divided into *thermochemical* and *hydrolytic* liquefaction. Thermochemical liquefaction is a pyrolytic processing coupled with addition of H<sub>2</sub>, CO and CO<sub>2</sub> in the presence of catalysts to produce hydrocarbons, phenols and light gases. On the other hand, hydrolytic liquefaction uses acids, bases or enzymes to produce the smaller molecules from biomass. Of the three types of conversions, the first two are the most common in harnessing energy from biomass.

##### 2.2.2.2.1 Pyrolysis

Pyrolysis was previously employed mainly to produce solid char [71]. The feed, usually wood, was slowly heated up to its target set temperature. As mentioned previously, pyrolysis occurs at temperatures between 300 - 600°C in the absence of oxygen. Aside from the char, tar and gases were also evolved in the process. Other terms used for pyrolysis includes carbonization, wood distillation, destructive distillation and dry distillation [71]. In the 19<sup>th</sup> century, chemicals such as methanol, acetic acid, acetone and turpentine were extracted from wood through destructive distillation. In ancient Egypt, pyrolysis was used to produce caulking agents as well as some embalming chemicals [9].



Presently, instead of the solid char, the target product of pyrolysis is the bio-oil through flash/fast pyrolysis. Bio-oils are “dark brown, free-flowing organic liquids that are comprised of highly oxygenated compounds [9]”. Other terms synonymous to bio-oils are pyrolysis oils, pyrolysis liquids, bio-crude oil (BCO), wood liquids, wood oil, liquid smoke, wood distillates, pyroligneous acid and liquid wood. Mohan et al. described their formation as a “freezing in” of the condensable thermal degradation products of cellulose, hemicellulose and lignin, preventing them from further degradation [9]. Additionally, they identified bio-oils as being a “complex mixture of water, guaiacols, catechols, syringols, vanillins, furancarboxaldehydes, isoeugenol, pyrones, acetic acid, formic acid and other carboxylic acids, hydroxyaldehydes, hydroxyketones, sugars, carboxylic acids and phenolics [9]”. These fractions are still very reactive due to the presence of easy-to-polymerize compounds containing double bonds, as well as the tendency for esterification and etherification reactions over time. Aside from this, the organic acid degradation products cause the bio-oil pH to be quite low. These are prompting concerns on polymerization and storage [108, 109]. Several studies attempted to identify and quantify pyrolysis oil components through HPLC, GC, etc. of such substrates as beech wood [110]; aspen poplar, maple, spruce, hog fuel, Western hemlock, pine and fir [111]; and unspecified bio-oil samples from three laboratories [108]. In his paper, Yaman lists other pyrolysis studies using varied substrates [8].

Bio-oil has been considered as fuel oil substitute. It was reported [8] that pyrolysis oils can be burned effectively in standard or slightly modified engines and boilers though their heating value is only 40-50% of the hydrocarbon fuels. However, bio-oils are very corrosive to most metals due to the presence of the organic acid degradation products

mainly from the breakdown of hemicelluloses [109]. It also contains a lot of water. Lastly, solids/char in the oil can block injectors if they are not removed [8].

Another way of utilizing bio-oil is through steam reforming or gasification to produce hydrogen or syngas. Panighari et al. reported production of syngas at 75-80 mol% ( $H_2$ : 48-52 mol%) with  $CH_4$  at 12 to 18 mol% when a commercial bio-oil was steam gasified at 800°C, under atmospheric pressure, in a flow reactor. They also reported of producing small amounts of  $C_2$ ,  $C_3$  and  $C_4$  hydrocarbons. Rioche et al. [7] used supported catalysts (Pt, Pd, Rh on alumina and ceria/zirconia) in the steam reforming of bio-oil derived from the fast pyrolysis of beech wood. They found that catalysts supported on alumina are less reactive than the ones on ceria/zirconia. Their study showed that an average of 65%  $H_2$  yield can be produced with 1% Pt/Ce- $ZrO_2$  at 795°C in a span of 125 minutes. However, increasing the O/C ratio in the feed with adding  $O_2$  caused significant decrease in the amount of  $H_2$  evolved over time at the same temperature (850°C  $\pm$  30°C). On the other hand, molecular  $O_2$  eliminated the problem of coking.

A novel way of upgrading bio-oil is through fermentation as this is a rich source of precursor chemicals such as levoglucosan. However, as mentioned earlier, pretreatments have a huge impact on the success of the action of the microorganisms and studies show that pyrolysis oils contain compounds that have been identified as inhibitory to most microorganisms [102, 109]. Some progress has been done on developing ways of pretreating the bio-oil before being subjected to biological process, such as neutralization or even directly fermenting levoglucosan but large scale process has yet to be developed [109].

#### 2.2.2.2.2 Gasification

The Energy Efficiency and Renewable Energy (EERE) agency of the US DOE defines biomass gasification to be a process whereby “biomass is converted into a gaseous mixture of hydrogen, carbon monoxide, carbon dioxide, and other compounds by applying heat under pressure in the presence of steam and a controlled amount of oxygen (in a unit called a gasifier) [112]”. Temperature for gasification is generally higher ( $> 600^{\circ}\text{C} - 700^{\circ}\text{C}$ ) than that used for pyrolysis [107, 113]. Unlike pyrolysis, gasification may proceed in the presence of some  $\text{O}_2$  or steam. Supercritical water gasification (SCWG), including near- and subcritical ones are also being investigated [12, 113-117]. Catalysts are added to the process to lower operating temperatures [10, 12, 117]. The gaseous products are usually composed of  $\text{H}_2$ ,  $\text{CO}$ ,  $\text{CO}_2$  and possibly some alkanes.

Dalai and coworkers [10] gasified cedar wood, aspen and cellulose to produce  $\text{H}_2$  in the presence of steam. They used a packed-bed tubular quartz reactor. Maximum hydrogen production for an uncatalyzed reaction was accomplished at around  $825^{\circ}\text{C}$  for cellulose (no data for the other feeds). However, with the addition of  $\text{CaO}$ , optimal temperature for  $\text{H}_2$  generation was lowered to  $675^{\circ}\text{C}$ .

In 2005, Matsumura, along with several other authors, published a review on biomass gasification in near- and super-critical water [117]. They have divided the efforts in this field into two: low temperature catalytic gasification from  $350$  to  $600^{\circ}\text{C}$  and high temperature supercritical water gasification from  $500$  to  $750^{\circ}\text{C}$ . As can be noticed, operation at near- or super- critical temperatures greatly decreased the temperature requirement of gasification. However, these processes require higher pressures and thus need more consideration regarding reactor construction and set-up [117].

Modell [113] pioneered the treatment of biomass in supercritical water. First, he studied glucose gasification at subcritical ( $T = 150, 200, 300^{\circ}\text{C}$ ) conditions. He reported that the process produced gas, liquid and solid by-products, with 40% of the carbon feed in the solid product at  $300^{\circ}\text{C}$  and 0.3% in the gas. He further noted that increasing the temperature from  $150^{\circ}$  to  $300^{\circ}\text{C}$ , the amount of char also increased. However, when supercritical conditions ( $T = 374^{\circ}\text{C}$  and  $P = 218\text{ atm}$ ) were used, no char was formed. From a set of experiments, it was shown that maintaining the density of water, that is, maintaining the supercritical pressure as well as the temperature, was necessary so that no char would be formed. Such was the case also for cellulose and for maple sawdust. It was the first time that char was not formed during heat treatment of biomass. In the SCWG of maple sawdust in the absence of a catalyst, the highest  $\text{H}_2$  percentage was 18% (CO was the major gas component) after 15 minutes of reaction time. Though he varied the reaction time in five runs, it was difficult to conclude as to the effect of time with  $\text{H}_2$  production since the amount of carbon in the feed was varying. In the presence of catalyst, his glucose gasification recorded a highest percentage of 45%  $\text{H}_2$  after 30 minutes of reaction in the presence of seven mixed catalysts: five of which are Ni-based, and then  $\text{Pt/Al}_2\text{O}_3$  and  $\text{Co/Mo}$  catalyst.

Other catalysts used for supercritical gasification include carbon [12, 114, 118] which the group of Antal had successfully used for the gasification of biomass such as potato and corn flour as well as sawdust at  $650^{\circ}\text{C}$ . Their studies showed no production of solid chars at pressures higher than the critical pressure of water (22MPa).  $\text{K}_2\text{CO}_3$  was also used as a catalyst for supercritical gasification [115, 116]. The presence of  $\text{K}_2\text{CO}_3$  was found to increase  $\text{CO}_2$  and  $\text{H}_2$  composition in the gas phase. CO concentration was

minimized due to water-gas shift reaction promoted by  $K_2CO_3$ . At  $280^\circ C$ , the presence of  $K_2CO_3$  in hydrothermal processing of biomass was reported to promote formation of long-chain carbon compounds in the liquid phase [119]. Ru/C was found to be also active in catalyzing hydrogen production from cellulose in supercritical water – more active than Pd/C,  $CeO_2$ , nano- $CeO_2$  and nano- $(CeZe)_xO_2$  particles [120].

Some authors have studied the mechanisms of biomass- or biomass-derived compound-degradation during gasification. Kabyemela et al. [121] had studied cellobiose decomposition in sub- and supercritical water during short residence times of 0.04 to 2 seconds. Products formed include glucosyl-erythrose, glucosyl-glycoaldehyde, glucose, fructose, glyceraldehydes, erythrose and pyruvaldehyde as well as acids that were not characterized. They reported that between 300 to  $400^\circ C$  at pressures from 20 to 40 MPa, cellobiose undergoes both hydrolysis and pyrolysis. Glucose is formed through hydrolysis while pyrolysis forms glucosyl-erythrose and glucosyl-glycoaldehyde. The last two undergo hydrolysis to form their monomeric sugars. Pressure did not affect the hydrolysis rates. However, it had an inverse relationship with pyrolysis.

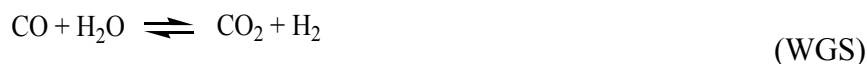
Kruse and Gawlik in 2003 [122] studied the conversion of biomass in sub- and supercritical water. Due most probably to their longer reaction time (15 minutes), they were able to identify acid degradation by-products such as HMF. In this study, they identified phenols, furfurals, acids and aldehydes as key components in their liquid by-product. Their biomass was baby food which has the formula  $CH_{1.87}O_{0.98}N_{0.02}S_{0.001}$  (through elemental analysis). They monitored gas production and found that increasing the temperature increased the amount of carbon (mainly  $CO_2$  in the gas phase). Alkanes and alkenes up to cis/trans butane were identified through GC. They contend that at

temperatures lower than 374°C, intermediate compounds are formed and are preferred over gas formation itself at ionic water conditions. However, at supercritical conditions where the lower density of water encourages free-radical reactions, gases are formed preferably.

Karagoz et al. [119] probed the effect of K<sub>2</sub>CO<sub>3</sub> and biomass/water ratio on the hydrothermal treatment of biomass at 280°C for 15 minutes. They gave a relatively comprehensive analysis of three liquid extracts: acetone-soluble, ether-soluble and ethanol acetate-soluble. In the presence of alkali, polymerization occurred with compounds having carbon backbone as high as C<sub>17</sub>.

## 2.3 AQUEOUS-PHASE REFORMING

With the report of Dumesic et al. (University of Wisconsin-Madison) of the aqueous-phase reforming (APR) process in 2002, the possibility of producing hydrogen at much lower temperatures than either gasification or pyrolysis was demonstrated. From the typical gasification temperature of above 500°C, APR was shown to be capable of producing H<sub>2</sub> at around 500K using oxygenate model compounds such as ethylene glycol [13]. In the presence of a suitable catalyst such as platinum, APR is anchored on two important H<sub>2</sub>-generating reactions: reforming and water gas shift (WGS).



They based their findings on the thermodynamic favorability of reforming oxygenated hydrocarbons at much lower temperatures than those required by alkanes as illustrated in Figure 2.20.

From the figure, it could be seen that the lowest temperature at which steam reforming of  $C_6H_{14}$  would be favorable ( $\Delta G_{rxn} \leq 0$ ) is at around 680K. This temperature becomes higher as the carbon backbone shortens to methane. On the other hand, for oxygenated hydrocarbons, reforming is favorable at as low as 340K. At this temperature, it must be noted that the water gas shift (WGS) reaction has a negative Gibbs free energy of reaction. Hence, operating at lower temperatures has two major advantages for oxygenates: (1) lower temperatures mean lower energy consumption to heat up/maintain temperature of the reactor and (2) taking advantage of the low temperature activity of two  $H_2$ -producing reactions.

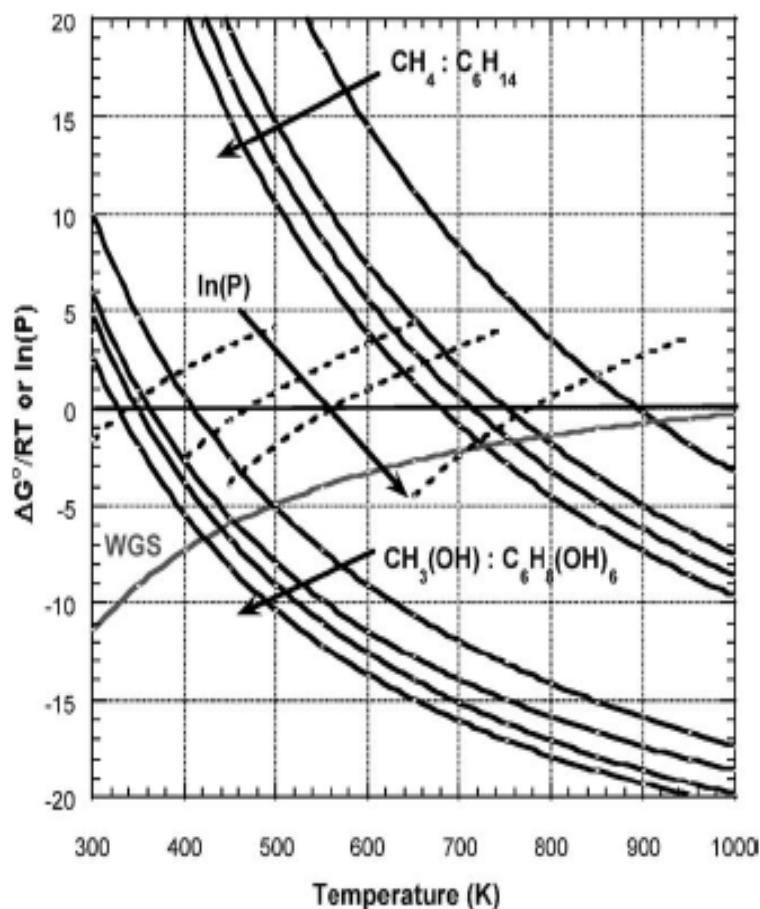


**Figure 2.20** Thermodynamics of alkane and oxygenate reforming [123]

In their first article published in *Nature* [13], the group of Dumesic reported that APR of methanol and ethylene glycol could have as high as 96% H<sub>2</sub> selectivity<sup>1</sup> while the more “oxidized” glucose only had a selectivity of 50%. They concluded that the ratio of oxygen to hydrogen in the molecule affects hydrogen selectivity – the more reduced the

<sup>1</sup> Dumesic et al. defined selectivity as (molecules H<sub>2</sub> produced)/(total C atoms in gas phase) x 100/RR . Reforming ratio (RR) refers to the ratio of theoretical moles of H<sub>2</sub> that can be produced per mole C in the feed molecule. (RR for ethylene glycol is 2.5 while for glucose is 2.0)



molecule, the better is its H<sub>2</sub> selectivity with APR. The authors accounted for this finding by noting the comparative likelihood of breaking a C-C bond and C-O bond on the metal catalyst used. The first occurrence will form the desired product (i.e. H<sub>2</sub>) while the latter will cause formation of alkanes or dehydrated oxygenates. These proposed mechanisms are illustrated in Figure 2.21.

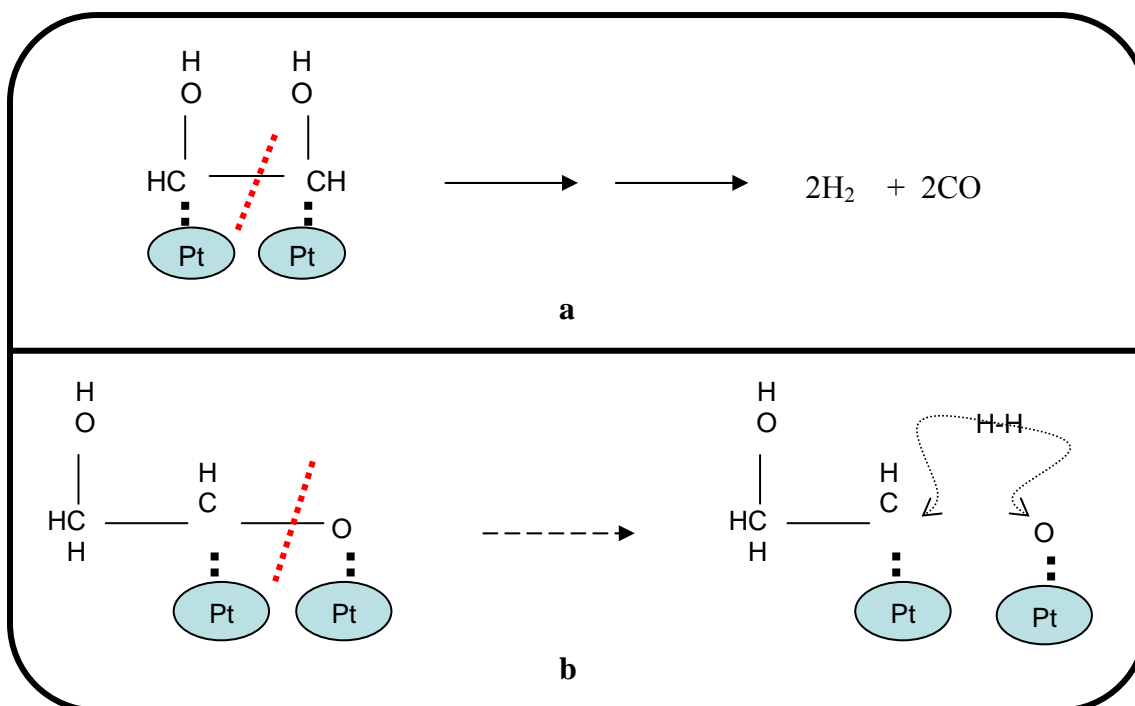


**Figure 2.21** Possible pathways of competing bond breaking on Pt. (a) C-C bond breakage leading to formation of H<sub>2</sub> and CO. (b) C-O bond breakage leading to formation of alkane/dehydrated molecule through reaction of intermediate with hydrogen. (Adapted from [13])

In order to increase the selectivity from glucose, Davda and Dumesic [17] developed a two-stage system consisting of a hydrogenation reactor coupled to a reforming reactor. In the hydrogenation reactor, the glucose feed stream was reacted with H<sub>2</sub> to form sorbitol. After this, the stream was directed onto the reforming reactor where

APR occurred. From an initial H<sub>2</sub> selectivity of 10.5%, they were able to increase the selectivity to 62.4% by incorporating the hydrogenation reaction [17].

Ideally, the metal catalyst used in the process should catalyze both of the aforementioned reactions. Before the group started using bimetallic catalysts, Pt/Al<sub>2</sub>O<sub>3</sub> was identified to have the highest hydrogen selectivity [15, 16]. They have studied APR of ethylene glycol and methanol using platinum and the less expensive Sn-Ni catalysts on different supports (acidic, basic and neutral) [14-16, 124-127] and found that Pt/Al<sub>2</sub>O<sub>3</sub> by far gave the best selectivity among the catalysts. Addition of Sn on Ni was found to lower methanation on Ni [15] and thus increase hydrogen selectivity. Recently, Huber et al. applied bimetallic Pd and Pt catalysts on ethylene glycol APR [128]. Using a high-through-put reactor, they were able to screen more than 130 bimetallic catalysts. After identifying the promising ones, they then subjected these to flow reactor APR conditions with ethylene glycol. Results showed that combining PtFe<sub>9</sub>/Al<sub>2</sub>O<sub>3</sub> gave TOF values that are three times higher monometallic Pt/Al<sub>2</sub>O<sub>3</sub>. This increase was much higher for Pd. TOF for PdFe<sub>9</sub>/Al<sub>2</sub>O<sub>3</sub> were 39-46 times higher Pd/Al<sub>2</sub>O<sub>3</sub> at the same reaction conditions [128].

Lastly, the group was able to develop protocols for preferentially producing alkanes [18] through APR as well by employing aldol-condensation after acid catalyzed dehydration to produce long chain alkanes (C<sub>7</sub> to C<sub>15</sub>) [129].

Recently, a group from China published a report of their study on modification of Pt/Al<sub>2</sub>O<sub>3</sub> with Ce and Mg for ethylene glycol APR. At 498K and 2.58 MPa, they saw higher H<sub>2</sub> selectivity as well as conversion in the presence of both Ce and Mg than in plain Pt/Al<sub>2</sub>O<sub>3</sub> [130].

To date however, there has not been any report of applying aqueous-phase reforming to actual biomass. In using lignocellulosic materials, the current APR protocol would have to be modified in order to accommodate the more complex chemical composition of real biomass. As Kruse and Gawlik noted in their study of the reactions of biomass conversion in near-critical and supercritical water conditions, “results from experiments with model compounds cannot be adapted easily to understand the reaction network of real biomass [122]”.

## **CHAPTER 3**

### **OBJECTIVES OF THE STUDY**

Concerns about the sustainability of our current energy sources are unavoidable considering the heavy dependence of society on fossil fuels. With the expected peaking of world conventional oil reserves in the near future [6, 23, 34], it has been contended though that current reserves of other sources of fossil fuel energy can make up for the deficit, for at least a few more decades [35, 37]. Growth in other existing primary energy sources (nuclear and renewable) is also expected to carry their share of the load to keep up with the increasing demand for energy brought about by increasing world population and economic developments. Biomass energy, though currently contributing only a small fraction to world energy supply, is considered to be a vast and promising resource due to its availability, sustainability and CO<sub>2</sub>-neutrality [64, 131, 132]. Though existing technologies for bioenergy production are plagued with concerns about economic feasibility and applicability in the short term, various studies all over the world are on-going to find a way to build upon the information base we currently have.

Aqueous-phase reforming is a promising and attractive technology for hydrogen production from biomass considering its much lower energy requirement and the possibility of utilizing biomass in its wet form. It is the objective of this study to employ this technology to actual biomass by modifying the metal-catalyzed APR protocol to include acid hydrolysis in order for APR to be feasible. The biomass (Southern pine sawdust) used in the study was a by-product in one of the manufacturing processes of Georgia Pacific. This study was aimed at determining the effect of acid concentration and

addition of Pt/Al<sub>2</sub>O<sub>3</sub> on the hydrogen production as well as overall gas evolution of biomass APR. Since existing studies deal with model compounds, comparison with other feed was made in order to determine the performance of biomass APR with other substrates such as wastepaper, glucose and ethylene glycol in a batch system.

It is anticipated that the results of this could further enhance our understanding of the aqueous phase reforming process and its applicability to biomass. Ultimately, the objective of this study is to contribute to the body of knowledge that could help develop a solution to averting future energy crisis that might not be too-far-fetched when the non-renewable fossil fuels resources of the world are finally depleted.

## **CHAPTER 4**

### **EXPERIMENTAL METHODS**

This chapter describes the experimental techniques, apparatus used, as well as the analytical methods undertaken in the course of this study to achieve the objectives mentioned previously.

#### **4.1 RAW MATERIAL PREPARATION AND CHARACTERIZATION**

Southern pine is a collective term for ten species of pines that grow in the Southern part of the United States, from East Texas to Virginia [133]. It has four major species: longleaf pine (*Pinus palustris*), slash pine (*P. eliottii*), loblolly pine (*P. taeda*), and short-leaf pine (*P. echinata*) [134]. The minor species are: Virginia pine (*P. virginiana*), pond pine (*P. serotina*), sand pine (*P. clausa*), spruce pine (*P. glabra*) and pitch pine (*P. rigida*) [134]. The lignocellulosic material used here was not specifically identified. They were received from Georgia Pacific just as Southern pine chips.

The chips were then milled using a Wiley mill. The underflow was allowed to pass through Tyler screens mounted on a mechanical shaker. The -35 +60 fraction (average aperture: 375  $\mu\text{m}$ ) was used in the experiments. Moisture content was measured by TGA – averaging triplicate samples. Elemental and proximate analyses were done by outside laboratories: Desert Analytic Laboratory for the elemental analysis of the wood and the IPST Wood Chemistry Laboratory for its proximate analysis.

Proximate analysis accounted for the different groups present in the sample. The sample was first extracted with dichloromethane to remove the extractive content of the pine saw dust. The extractive-free wood was then treated with 72%  $\text{H}_2\text{SO}_4$ . Carbohydrates (glucan, mannan, galactan, xylan and arabinan) were measured using HPLC-Pulsed Amperometric Determination (HPLC-PAD) of the 72%  $\text{H}_2\text{SO}_4$  hydrolyzate. Some of the hydrolyzate was loaded in a UV-Vis spectrometer to determine the acid-soluble lignin at 205 nm. On the other hand, the residue in the reaction of the wood sample with 72%  $\text{H}_2\text{SO}_4$  accounted for the acid-insoluble lignin (Klason lignin). Some remaining whole sawdust was put in a muffle furnace set at 525°C for ash content

One of the objectives of the research was to compare biomass APR with other substrates. In line with this, office wastepaper, ethylene glycol (certified, Fisher), and D-glucose (anhydrous, certified A.C.S., Fisher) were also investigated.

Catalysts used were 2M sulfuric acid (diluted from concentrated stock, 36M, Fisher), platinum on alumina ( $\text{Pt}/\text{Al}_2\text{O}_3$ ) pellets (0.5 wt.% Pt, Engelhard) and gamma-alumina ( $\gamma\text{-Al}_2\text{O}_3$ ) powder (Strem Chemicals).

Deionized water used in the study was primarily from a Barnstead EASYpure® RODI water purifier which is maintained at 18.1 ohms.

## **4.2 REACTION METHOD**

### ***4.2.1 Reactor***

A 100-mL stainless steel Parr batch microreactor (SS 316) was used for all the runs in this study. The assembly included a magnetic drive for the mechanical stirrer and a temperature controller with a PID controller and J-type thermocouple. The reactor was

outfitted with a gas collector at the outlet, using two pieces of 1/8" stainless steel tubing, arranged into a J-shape and attached by a Swagelok T-connector. A Swagelok connection with absorber inside was attached to remove condensed water in the sample volume. Lastly, a check valve was attached at the end to contain and control gas sample exit from the sample volume. Diagrams and a picture of the reactor are presented in Figure 4.1

The pressure of the collected product gas was allowed to equilibrate to atmospheric pressure in a balloon and samples were taken using gas tight syringes. Two modes of sampling were done during the research. In the early part of the study, intermittent sampling was done every 30 minutes. However, the disturbance this method caused to the system precluded having good reproducibility. As such, sampling was then done by extracting the gas product at the end of a three-hour reaction.

Removal of the solid residue of the previous run from the reactor was considered important. Washing protocol included overnight base wash at 50°C followed by scraping of adhering residue and then washing with copious amounts of de-ionized (dI) water. An acid wash for about 3 hours followed. After this, the reactor was cleaned with detergent and then washed again with copious amounts of dI water.



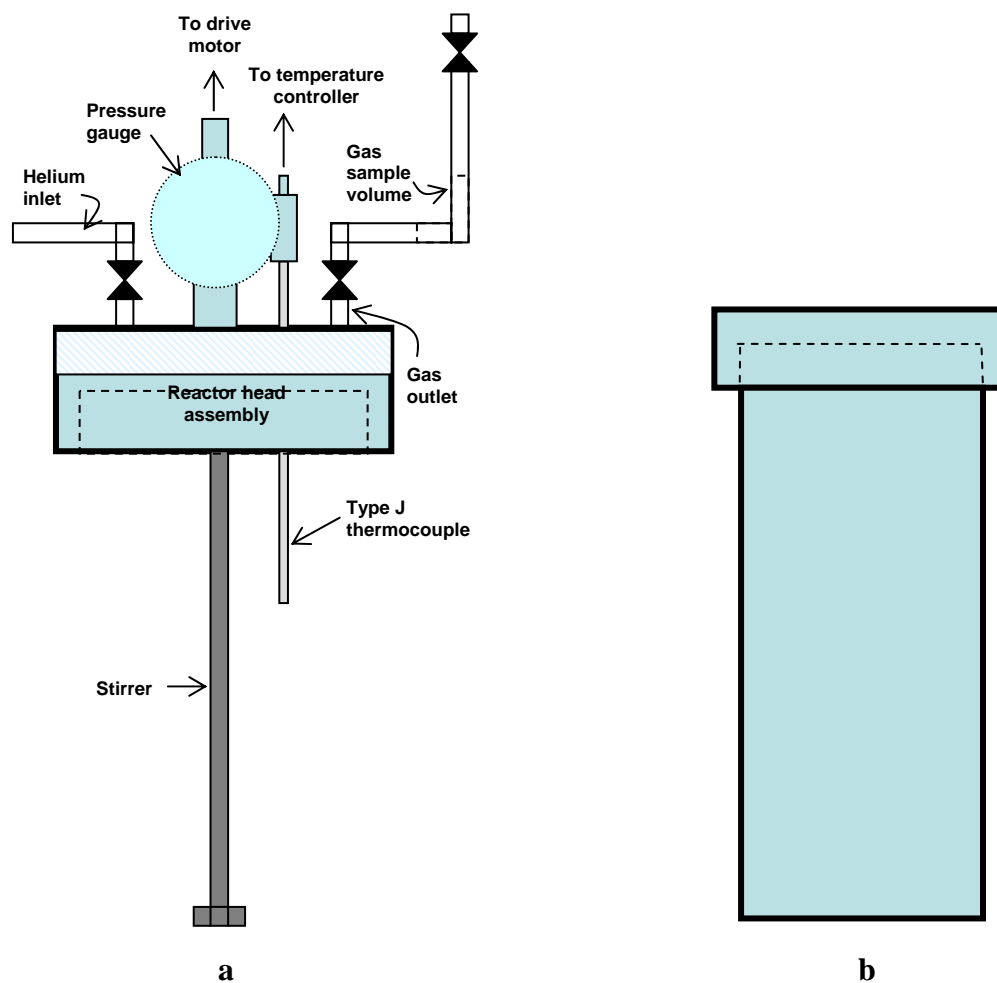


**Figure 4.1** Parr reactor assembly. (a) Top assembly (valve for liquid sampling not included; actual pressure gauge much larger); (b) bottom bomb; (c) picture of the actual set-up.

## 4.2.2 Process Description

### 4.2.2.1 Acid hydrolysis

To date, published studies of aqueous-phase reforming (APR) have dealt with the processing of model compounds [13-18, 123-128, 135-137] which include ethylene glycol, methanol, glycerol, sorbitol and glucose. All of these readily dissolve in or are very miscible with water, thus forming homogeneous feed to the APR reactor

In contrast, the present study dealt with heterogeneous substrates (i.e. pine sawdust and office wastepaper). Because of this, acid hydrolysis was employed in order to breakdown the feed to smaller molecules (e.g. monomeric sugar units such as glucose) for the platinum-catalyzed APR to proceed. To determine the effect of sulfuric acid ( $\text{H}_2\text{SO}_4$ ) hydrolysis on gas production, different acid concentrations were added to the biomass-water mixture without the  $\text{Pt}/\text{Al}_2\text{O}_3$  catalyst. Shown in Table 4.1 are the quantities used for this part of the study.

**Table 4.1** Quantities used for run with different acid concentrations

	1%	5%
<b>Wood (g)</b>	5.54	5.54
<b>dI water (g)</b>	44.31	43.3
<b>2M <math>\text{H}_2\text{SO}_4</math> (mL)</b>	0.253	1.263

A preliminary study done on this topic [138] used a liquid-to-wood (L/W) ratio of four. However, a few previous studies [119, 139, 140] showed that L/W ratio can have an effect on the reaction of and product formation from biomass. Barth [139] found that a high water-to-biomass ratio increased the yield of bio-oil during aqueous pressurized pyrolysis of softwood pulp. Karagoz et al. [119] noted that in hydrothermal upgrading of

wood biomass at 280°C, lowering the L/W ratio from six to three caused a decrease in gas production and an increase in residue weight. In view of this, an L/W ratio of nine was included. This gave a 10 wt.% feed which was comparable to the concentration used by Dumesic et al. [13].

#### 4.2.2.2 Pt-catalyzed reforming

Catalysts that have already been used for APR include platinum on alumina modified with cerium and magnesium [137], bimetallic platinum and palladium catalysts with metals such as iron, nickel and cobalt [128], Raney-nickel and modified nickel catalysts [15, 123, 125-127], palladium supported on silica-alumina [18] and platinum supported on different substrates such as alumina, carbon and silica [13-18, 123, 124, 135, 136]. Dumesic et al. found that excluding the bimetallic catalysts, Pt/Al<sub>2</sub>O<sub>3</sub> gave the highest hydrogen selectivity among all other catalysts tested for APR activity [15, 16].

In a typical experiment using sawdust, 5.54g of biomass (10.63 % moisture content via TGA) and 0.498g Pt/Al<sub>2</sub>O<sub>3</sub> pellets were loaded into the reactor. The reactor configuration used did not allow for pre-reduction of the platinum catalyst before the reaction without exposure to ambient conditions. In order to obtain a L/W ratio of nine, 44.57 mL of water was added. Using a micropipette, 1.263 mL of 2M H<sub>2</sub>SO<sub>4</sub> was transferred into the reactor for a 5% acid concentration run (wt% based on dry biomass). The pH of the resulting mixture was then recorded. After securing the reactor head, helium gas was allowed to flow through the reactor and to purge out air from the headspace. After about 1.5 minutes, the reactor was pressurized with 30 psig of He, sealed and then heated to 225°C (498 K). The temperature and pressure of the system

were recorded every 5 minutes. For runs where wastepaper was used, an additional 30 minutes of soaking in water was performed before the addition of acid and platinum. This was done for the easy defiberization of the paper. Each run was repeated at least twice.

At the end of the reaction and after sampling, the remaining by-product was centrifuged to separate the liquid from the solid residue.

Several baseline experiments were carried out to probe the possibility that the catalysts (both  $\text{H}_2\text{SO}_4$  and  $\text{Pt}/\text{Al}_2\text{O}_3$  in concert or separately) could catalyze the production of hydrogen from water. In these runs, only water and the catalyst(s) in question were put inside the reactor. Before the system was heated to the target temperature ( $225^\circ\text{C}$ ), the reactor was also pressurized with helium in each baseline runs as mentioned above.

## **4.3 GAS-PHASE ANALYSIS**

### ***4.3.1 Thermal Conductivity Detector: Brief Background***

Analysis of the gas phase was done using two gas chromatographs (GC). Expected gases in the sample were permanent gases including hydrogen, carbon monoxide, carbon dioxide, methane and possibly other low molecular hydrocarbons (such as ethane). Of the commonly available GC detectors, the thermal conductivity detector (TCD) is well-suited for the application.

TCDs operate on the basis of thermal conductivity differences between the analytes in the gas phase and a pure gas carrier. (Table 4.2 lists the thermal conductivities of the different gas species typically found in the sample gas at  $25^\circ\text{C}$ .) Inside the metal block of the TCD assembly, cavities through which the gas flows contain resistance wires

or filaments that are mounted on holders. These can also be placed concentrically in a cylindrical cavity. Filaments are either made of tungsten or tungsten-rhenium (WX) alloy. These materials cause the filaments to have high resistance. A typical TCD usually have four filaments, arranged in a Wheatstone bridge assembly as shown in Figure 4.2. [141-143]

The Wheatstone bridge is considered “a classic method for measuring resistance”[142]. Application of a direct current (DC) through the filaments causes them to heat above the temperature of the cell block, thus creating a temperature gradient. The larger the temperature differential, the more sensitive is the detector [142]. If it is only the carrier (R) that passes over the filaments, the circuit is balanced and there is no voltage gradient at the corners of the bridge. However, when the analyte (S) with a different thermal conductivity from the carrier is introduced, there would be a corresponding change in the filament temperature. This will cause the filament resistance to increase and a voltage drop develops across the bridge. This differential voltage value is recorded and comes out as a peak. As soon as all of the analyte has eluted, only the carrier is now in contact with the filaments and the bridge is balanced once again. [142, 143]

**Table 4.2** Thermal conductivities of the different gas species in the study [144]

Gas	Thermal Conductivity cal/°C-s-cm
He	351.2
H <sub>2</sub>	417.22
N <sub>2</sub>	61.02
O <sub>2</sub>	62.8
CO	59.3
CO <sub>2</sub>	40.3
CH <sub>4</sub>	80.4
C <sub>2</sub> H <sub>6</sub>	51.1

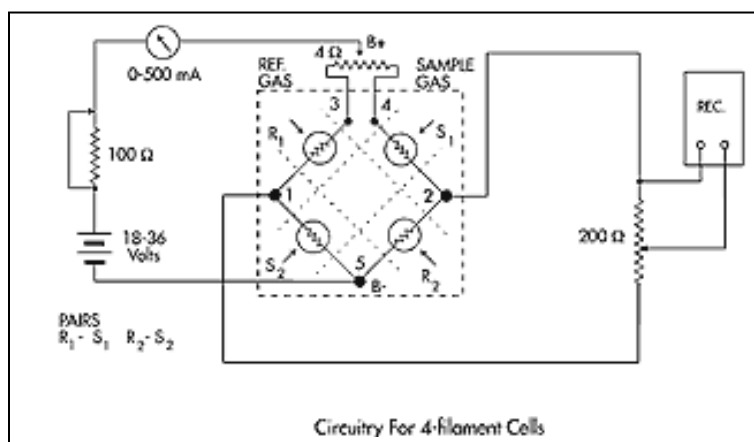


**Figure 4.2** Wheatstone bridge circuit for a TCD [141]

Quantification of carbon monoxide, methane, carbon dioxide and for some runs, ethane, was done using a Buck Scientific (BS) 910 gas chromatograph<sup>m</sup>. The BS-GC had a Carboxen 1000 packed stainless steel column (1/8" x 15 ft) from Supelco and helium as

<sup>m</sup> BS-GC can sense hydrogen. However, the peak is not quantitative. Split (negative) peaks for hydrogen also occurred.

carrier gas. Temperature programming was done to shorten CO<sub>2</sub> elution time. Data collection and analysis was done using PeakSimple 2000. Helium is not a good carrier for hydrogen considering their close thermal conductivity values (see Table 4.1 again). As such, two gas chromatographs with TCD were used in quantifying the amount of gases evolved in the study. The other GC, a Hewlett-Packard (HP) 6890, used nitrogen as a carrier gas. This had a stainless steel column packed with Carbosieve S-II (60-80 mesh) (1/8" x 4 ft) and was capable of detecting and separating helium, hydrogen, oxygen, methane and carbon dioxide. Negative polarity was turned on. Software used for data collection and analysis was HP ChemStation.

In both GCs, the presence of water was unwanted as this usually registered a wide tailing peak which overlapped with other peaks making quantification erroneous.

#### ***4.3.2 GC Calibration***

A certified gas mixture from Airgas was used to calibrate the two GCs used in this study. The mixture contained: 25.50% H<sub>2</sub>, 4% C<sub>2</sub>H<sub>6</sub>, 3% CO<sub>2</sub>, 2% CO, 1.02% CH<sub>4</sub> and the balance N<sub>2</sub>. Calibration of the BS-GC required injecting different concentrations of a certain gas and recording the corresponding area units as reported by the data software. Various concentrations were prepared by mixing different flowrates of the gas mixture and pure helium. Calibration of air in the GC was also done to check for contamination due to unavoidable leaks. Because of the high starting oven temperature (100°C), O<sub>2</sub> and N<sub>2</sub> peaks eluted as a single peak. Figures 4.3 to 4.7 show the calibration curves for air, CO, CO<sub>2</sub>, CH<sub>4</sub> and C<sub>2</sub>H<sub>6</sub>, respectively. However, typical concentrations of CO<sub>2</sub> in the samples are much higher than 3% so an extended calibration using 100% certified gas from Airgas was used. There was not much difference between the

calibration values obtained (Figure 4.8). For the study, the slope derived can the from the calibration curve of the pure CO<sub>2</sub> gas was used.

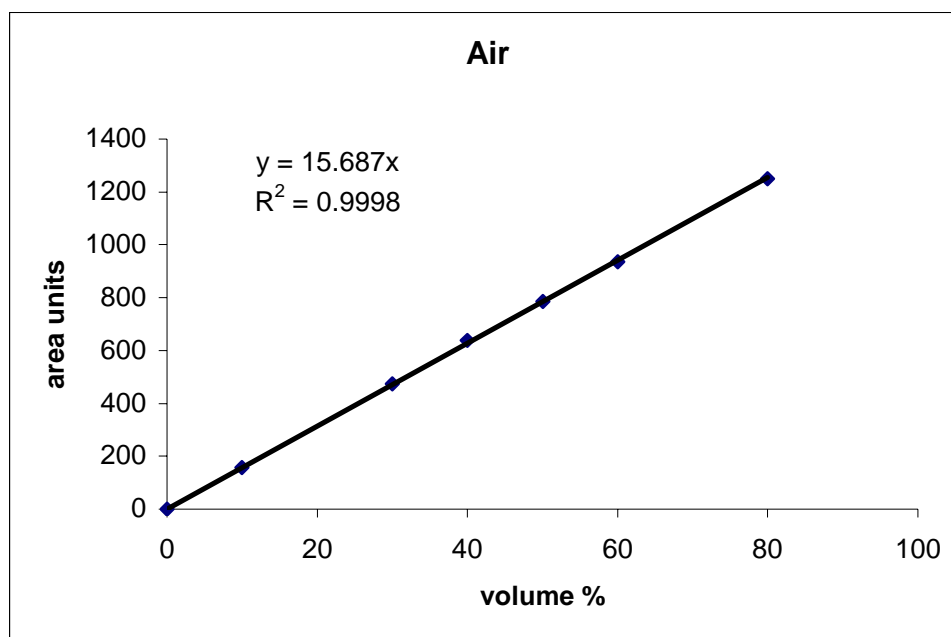


**Figure 4.3** BS-GC calibration curve of air



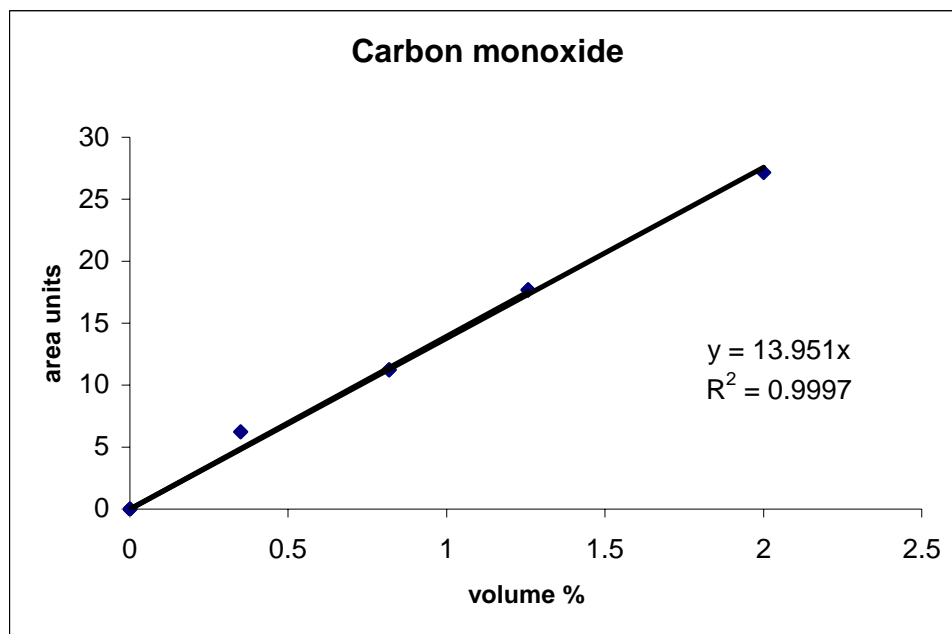


**Figure 4.4** BS-GC calibration curve of carbon monoxide

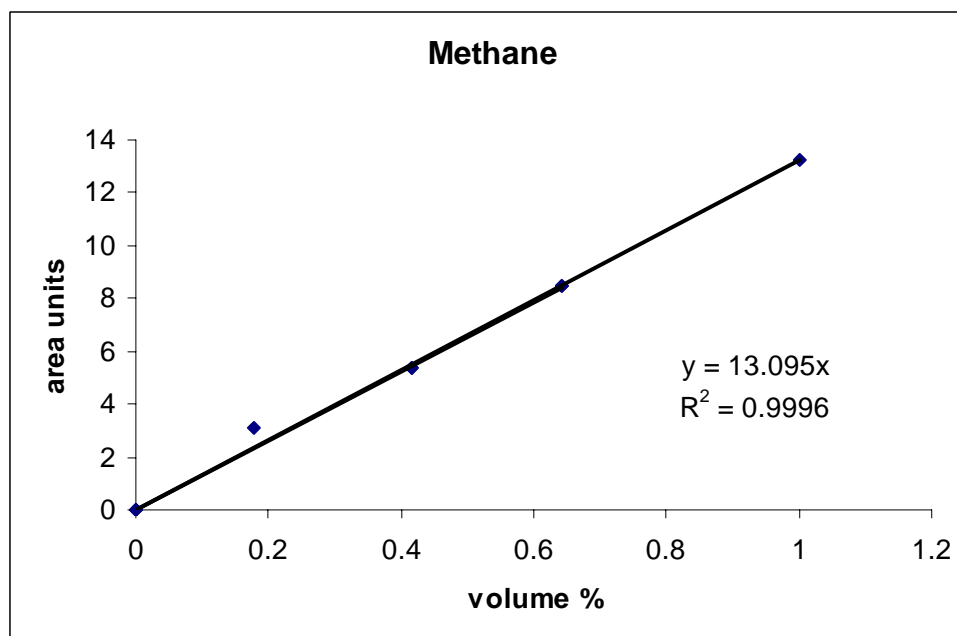


**Figure 4.5** BS-GC calibration curve of methane

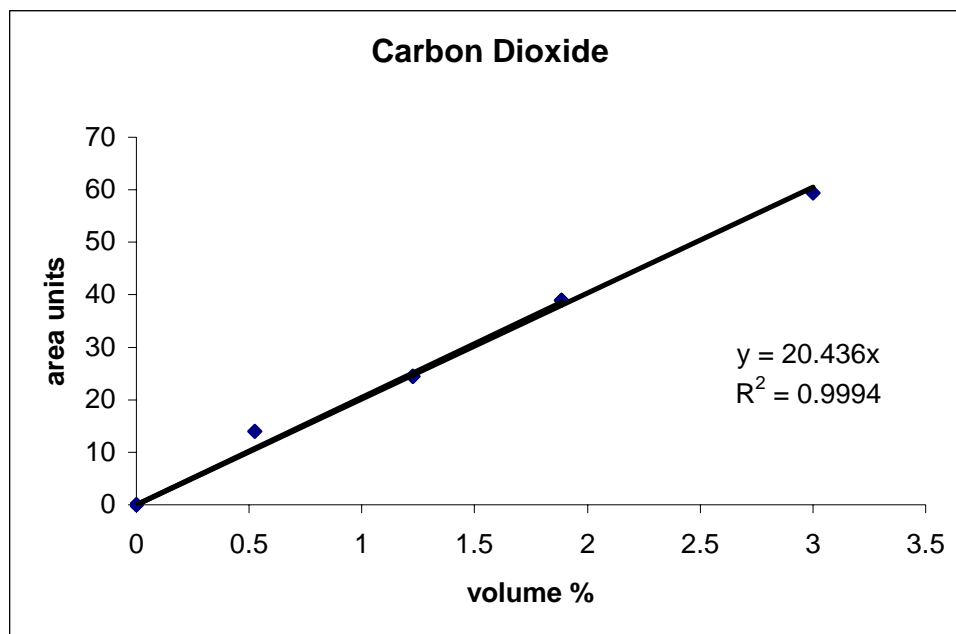


**Figure 4.6** BS-GC calibration curve of carbon dioxide

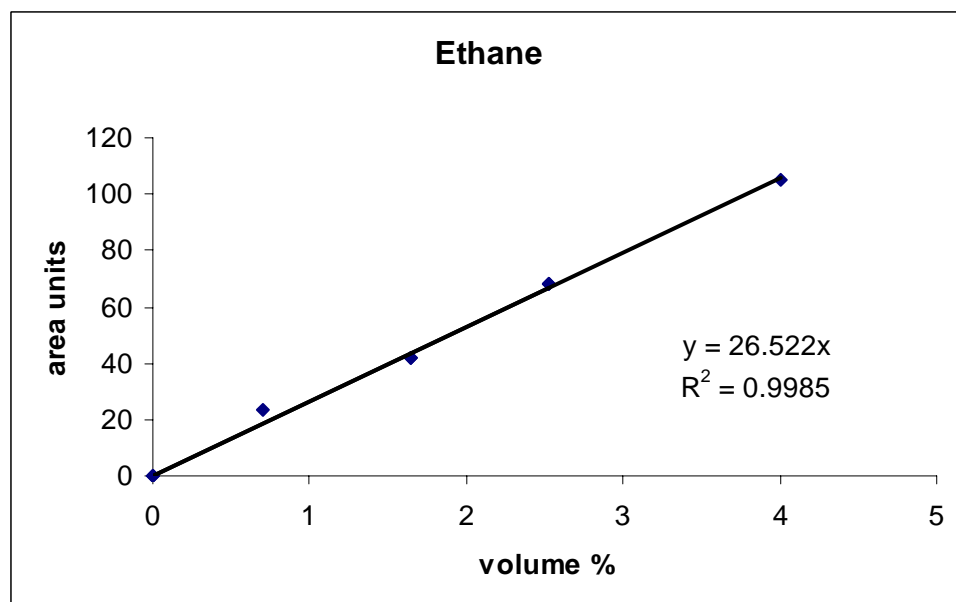


**Figure 4.7** BS-GC calibration curve of ethane

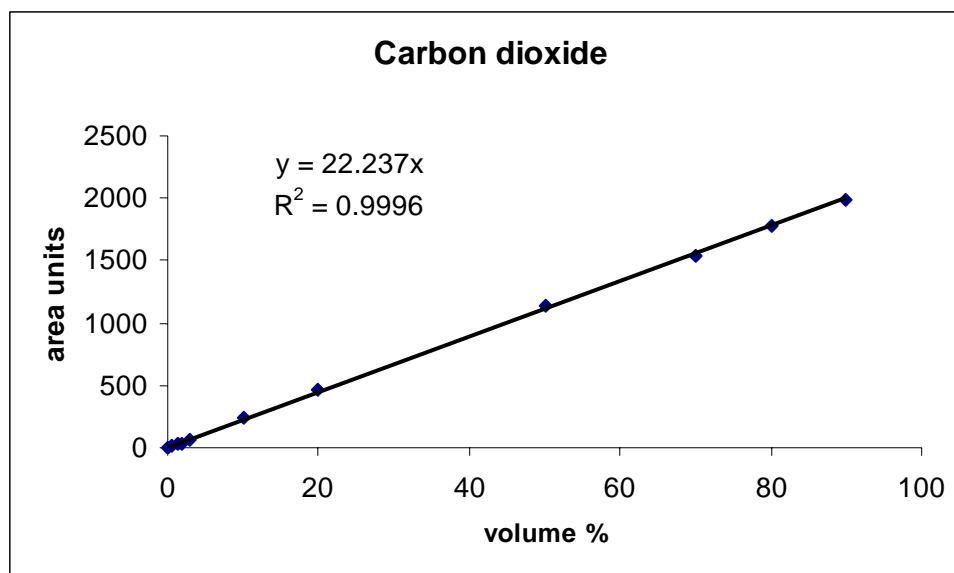


**Figure 4.8** BS-GC calibration curve of carbon dioxide at higher concentrations

For the HP-GC, calibration curves for He, H<sub>2</sub>, air (O<sub>2</sub>) and carbon dioxide were obtained from pure certified CO<sub>2</sub>, certified 90% H<sub>2</sub> – 10% ethylene gas mixture and ultra-high purity grade He – all from Airgas. Figures 4.9 – 4.12 show these calibration curves.

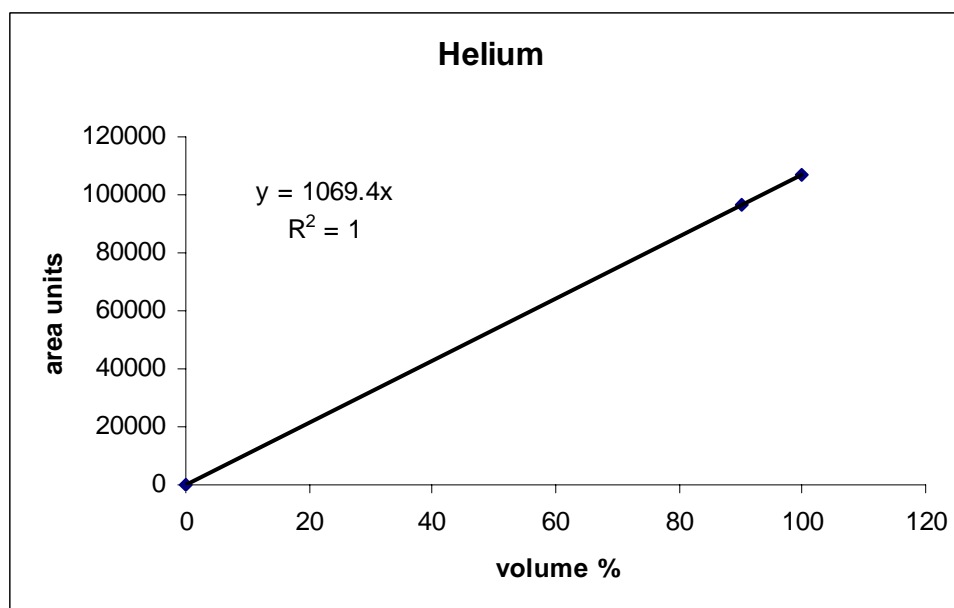


**Figure 4.9** HP-GC calibration curve of helium

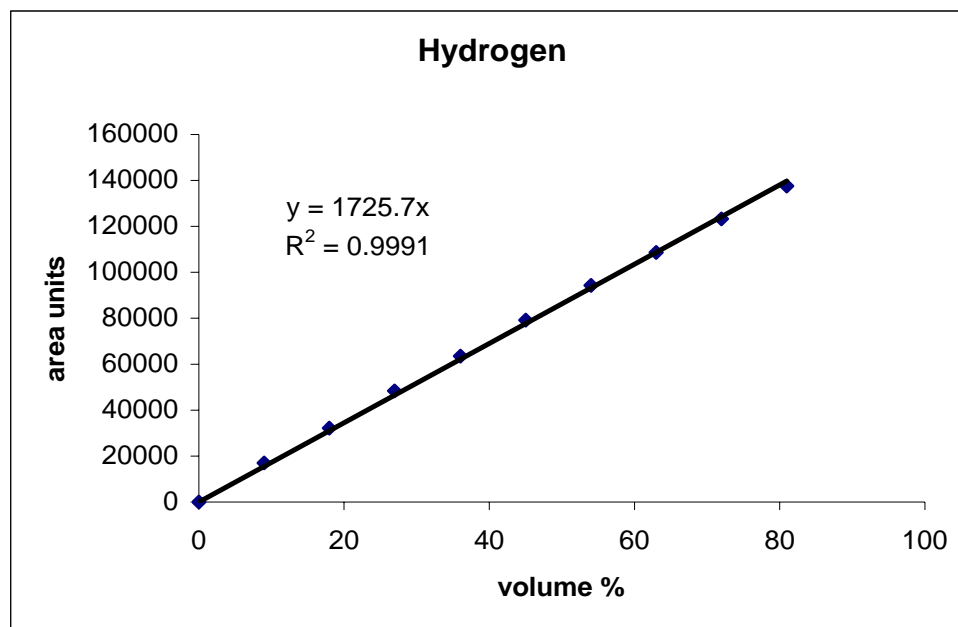


**Figure 4.10** HP-GC calibration curve of hydrogen

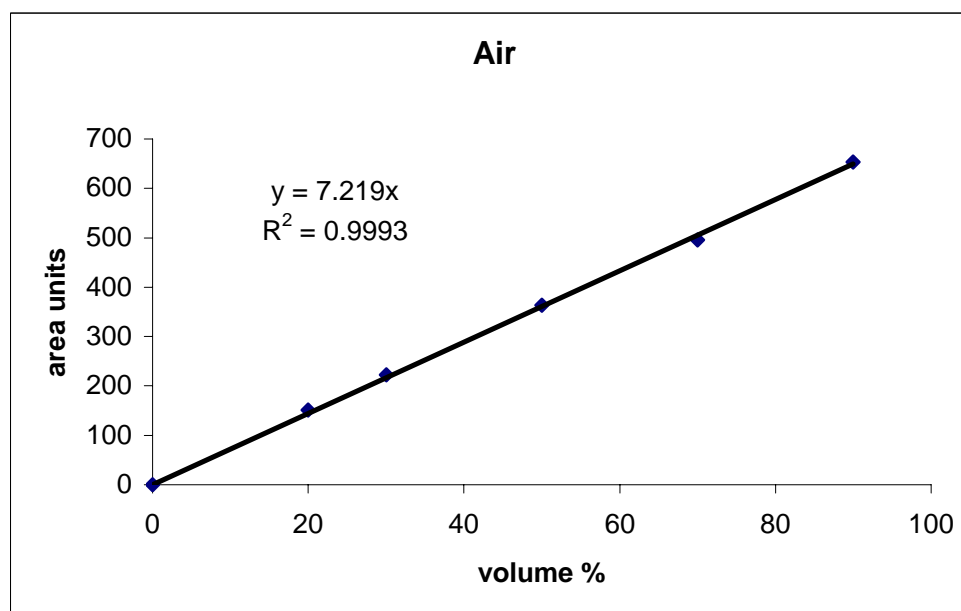


**Figure 4.11** HP-GC calibration curve of air

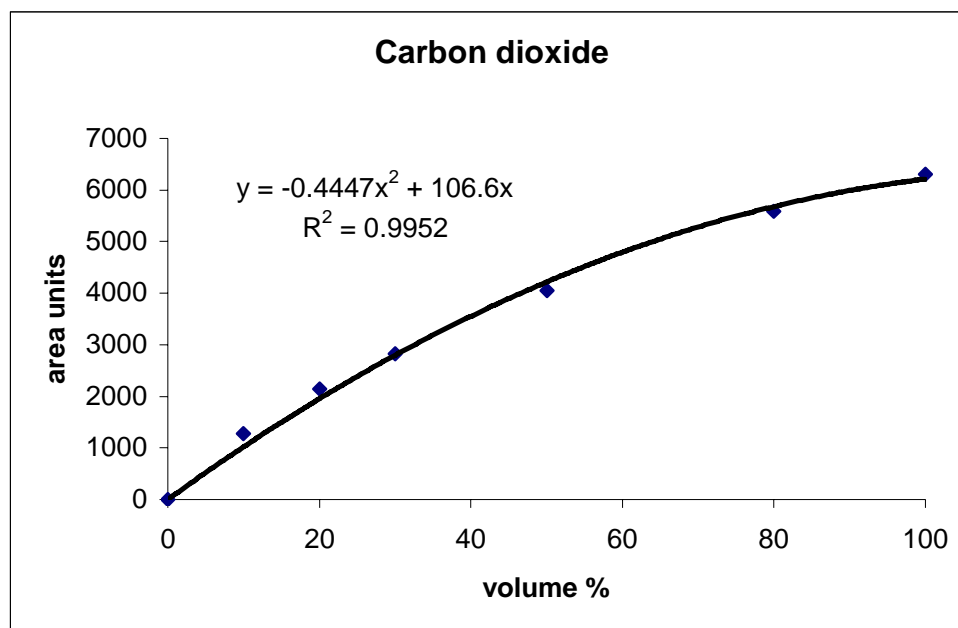


**Figure 4.12** HP-GC calibration curve of carbon dioxide

For each calibration, at least four measurements were made. Percent difference<sup>n</sup> was never more than  $\pm 8\%$  of the average

## 4.4 SOLID BIOMASS RESIDUE ANALYSIS

### 4.4.1 Proximate Analysis

After hydrolysis and APR reactions at process conditions, solid residues were recovered from biomass through centrifugation of the reaction by-product after extracting most of the liquid filtrate. The solids are then dried in an oven set at 105°C for 72 hours

---

<sup>n</sup> Percent difference (% difference) in this calculation was taken to equal  $|X_{\text{average}} - X_i| / X_{\text{average}} * 100\%$ .

(until constant weight). Dried solids, one batch each of hydrolysis and APR, are sent to IPST for analysis. Analyses done are similar to what was applied to the biomass raw material as mentioned before. Residue analyses were important because they give an indication on the effect of treatment on the biomass.

## **4.5 SPENT CATALYST CHARACTERIZATION**

Catalyst stability is an important consideration for reactions that involve catalysts – especially those that use expensive metal catalysts. With this in mind, the spent catalyst was characterized using elemental analysis, X-ray photoelectron spectroscopy (XPS), hydrogen chemisorption experiments and nitrogen physisorption measurements.

### ***4.5.1 Elemental Analysis***

Samples of fresh catalyst pellets as well as spent ones were sent to Galbraith Laboratories, Inc. for elemental analysis. Platinum, aluminum as well as sulfur contents were determined using inductively coupled plasma-optical emission spectrometer (ICP-OES) method.

### ***4.4.2 Hydrogen chemisorption***

Samples of fresh Pt/Al<sub>2</sub>O<sub>3</sub>, spent reaction, calcined spent and acidified catalysts were sent out for H<sub>2</sub> chemisorption. A Micromeritics ASAP 2020 at an analysis temperature of 308 K. Before the isotherms were recorded, samples were evacuated at 623 K followed by reduction in flowing H<sub>2</sub> at the same temperature.

#### ***4.5.3 Nitrogen physisorption***

Samples of fresh Pt/Al<sub>2</sub>O<sub>3</sub>, spent reaction, calcined spent and acidified catalysts were degassed under vacuum for eight hours at 175°C. Nitrogen physisorption experiments to determine surface area of the pellets were done using a Micromeritics ASAP 2000 system. A data acquisition and analysis program were used to calculate BET surface area and pore volume.

#### ***4.5.4 X-ray Photoelectron Spectroscopy (XPS)***

A PHI 1600 X-ray photoelectron spectroscopy unit was used to determine the surface species on fresh Pt/Al<sub>2</sub>O<sub>3</sub>, spent reaction, calcined spent and acidified catalysts. Elemental analysis of the surface is also possible. Peak alignment was done on C1s peak at 284.5 eV.

## CHAPTER 5

### RESULTS AND DISCUSSION

Contained in this chapter are the results and information gathered from the experiments described in the previous chapter. An attempt to give meaning and relevance to these data in the context of the objectives of the study is also presented.

#### 5.1 BIOMASS CHARACTERIZATION

##### *5.1.1 Elemental analysis*

Monosaccharides have an empirical formula of  $(\text{CH}_2\text{O})_n$ . This was the reason why they were misleadingly referred to before as “hydrates of carbon”. As two monomers form a disaccharide, a water molecule is lost between the two units in order to form a glycosidic bond through condensation. For example, cellobiose, which is the repeating unit of cellulose, consists of two D-glucose units and has a molecular formula of  $\text{C}_{12}\text{H}_{22}\text{O}_{11}$ . Cellulose can be represented as  $(\text{C}_6\text{H}_{10}\text{O}_5)_n$  [145] while glucose has a formula of  $\text{C}_6\text{H}_{12}\text{O}_6$ . Notice that though the C/O and C/H ratios have changed for the polysaccharide, the H/O ratio remains the same, i.e. 2.

The Southern pine sawdust used in this study contained mostly carbon, hydrogen and oxygen – as shown in the elemental analysis in Table 5.1. These three elements comprise more than 99% of the sample – making it comparable to the model oxygenated compounds that the group of Dumesic used in their studies with respect to elemental composition. Converting the resulting mass percentage from the analysis to mole ratios, the biomass used could be represented as  $\text{C}_{1.69}\text{H}_{1.90}\text{O}$ . Its H/O ratio was close to that of



carbohydrates. However, other components, most notably lignin, are present and these caused a slightly different ratio.

Dumesic et al. reported that a correlation exists between the hydrogen and oxygen ratios and the trend in hydrogen production of the various feeds that they used. They noted that as the H/O ratio decreased, i.e. 4, 3, 2.67, 2.33 and 2 for methanol, ethylene glycol, glycerol, sorbitol and glucose, respectively, the lower was the hydrogen production of a certain feed [13]. Interestingly though, this trend was not observed in the system used in this study (to be discussed later).

**Table 5.1** Elemental analysis of Southern pine sawdust used in the study

<i>Elemental analysis constituent</i>	<i>Weight percentage of component (wt% dry basis)</i>
<b>C</b>	52.87
<b>H</b>	4.96
<b>O</b>	41.81
<b>N</b>	0.15
<b>S</b>	< 0.06
<b>Ash</b>	0.15

### **5.1.2 Proximate analysis**

Lignocellulosic materials are more commonly sourced from trees. As previously mentioned, they are principally made up of cellulose, hemicelluloses and lignin. Cellulose is a homopolymer consisting of  $\beta$ -D-glucopyranose units while hemicelluloses

are branched polysaccharide chains of  $\alpha$ - and  $\beta$ -D-glucopyranose,  $\alpha$ - and  $\beta$ -D-galactopyranose,  $\beta$ -D-mannopyranose,  $\beta$ -D-xylopyranose, and  $\alpha$ - and  $\beta$ -L-arabinofuranose with some acetyl, methoxy and uronic acid substituents. Lignin, on the other hand, is composed of phenyl propanoid units linked together by ether, ester and aryl-alkyl bonds. Amounts of these components may vary depending on species, age and location of the tree as well as the location of the sample in the tree itself. For example, softwoods are generally known to have higher lignin contents than hardwood while the bark has more extractives and lignin per weight than the wood itself. Chemical composition of the tip of the branches is different from that of the trunk. Average ranges of values for typical composition are reported in the literature, for example [64, 71, 146].

Presented in Table 5.2 is the chemical analysis of the pine sawdust used in the study. The method categorized the carbohydrate content into five groups: arabinans, galactans, glucans, xylans and mannans. Glucans include glucose units from both cellulose and hemicellulose fractions. Approximation of specific hemicellulosic group percentages is possible from the data obtained [76, 147]. Average molar ratios of constituting monosaccharides have been reported such as those given by Sjöström [71] in Table 5.3 can be used. Other more rigorous methods of analysis are available to separate cellulose from hemicellulose directly [148] but for the purposes of the research, determination of the total carbohydrate content is sufficient.

**Table 5.2** Chemical composition of Southern pine sawdust used in the study

	<i>Weight percentage of component (% dry basis)</i>
<b>Carbohydrates</b>	
<b>Arabinan</b>	1.00
<b>Galactan</b>	2.30
<b>Glucan<sup>+</sup></b>	39.00
<b>Xylan</b>	5.30
<b>Mannan</b>	11.70
<b>Lignin</b>	
<b>Acid insoluble</b>	27.50
<b>Acid soluble</b>	0.40
<b>Extractives</b>	3.70
<b>Ash</b>	0.30

+ comes from both cellulose and hemicelluloses

**Table 5.3** Constituent monosaccharides of softwood hemicelluloses

<b>Hemicellulose</b>	<b>Constituents</b>	<b>Average molar ratio</b>
Galactoglucomannan	$\beta$ -D-mannopyranose	3
	$\beta$ -D-glucopyranose	1
	$\alpha$ -D-galactopyranose	1
	acetyl	1
(Galacto)glucomannan	$\beta$ -D-mannopyranose	4
	$\beta$ -D-glucopyranose	1
	$\alpha$ -D-galactopyranose	0.1
	acetyl	1
Arabinoglucoronoxylan	$\beta$ -D-xylopyranose	10
	4-O-Me- $\alpha$ -D-glucopyranose	2
	$\alpha$ -L-arabinofuranose	1.3

The hydrogen produced in the biomass APR as well as acid hydrolysis is expected to have come mainly from the reforming of the soluble holocellulose or carbohydrate fraction. It must be noted though that the proximate analysis from the laboratory did not close the balance to 100%. The analysis result for carbohydrate content was below what was expected [64, 71, 146]. This may be attributed to an incomplete hydrolysis of the wood constituents before carbohydrate determination by HPLC-PAD. Dimers or oligomers of glucose were most likely not completely digested. This might be due to the relatively more recalcitrant crystalline cellulose in the biomass.

Shown in Figure 5.1 is the HPLC chromatograph of the hydrolyzate from pine sawdust. It shows that the method used was calibrated to determine only glucose, arabinose, galactose, xylose and mannose, with fucose as the internal standard. The method was terminated after mannose eluted. Presence of dimers/oligomers would not be detected.

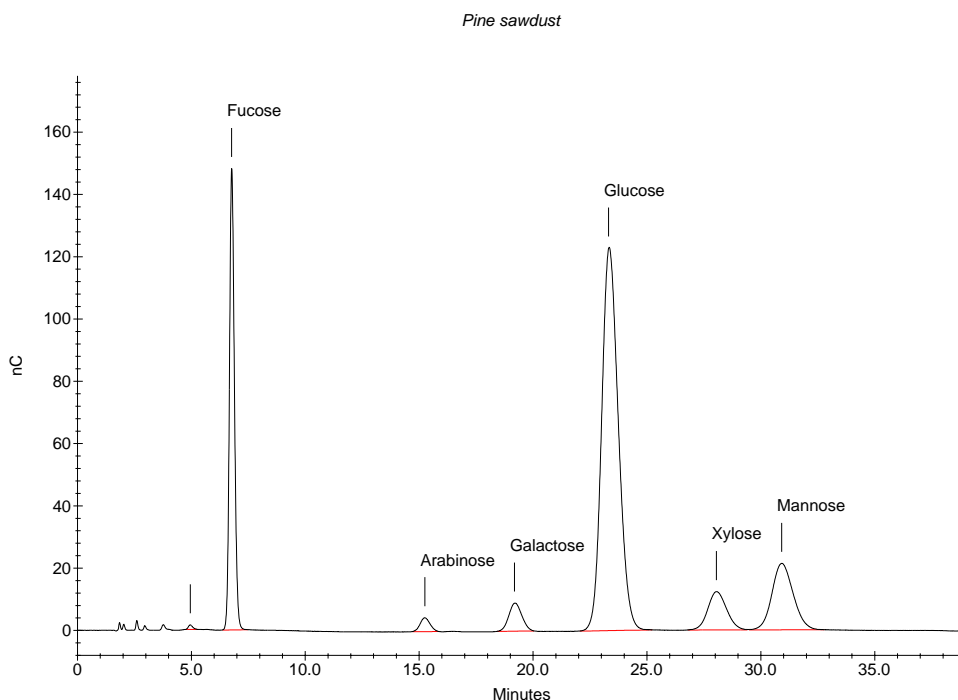


**Figure 5.1** HPLC-PAD chromatogram of wood monosaccharides from pine sawdust

## 5.2 BATCH REACTION

### 5.2.1 *Batch reaction with intermittent sampling*

Studying the kinetics of the biomass APR reaction was considered to be important. As such, intermittent sampling of the gas phase was done during the early phase of the project. In this set-up, gas samples were taken from the reactor every 30 minutes in a three-hour run of a single charge of feed, aqueous medium and catalyst. The thirty minute interval sampling was dictated by the analysis time in the Buck Scientific GC. It was assumed that the amount taken from the reactor was small enough so as not to cause too much system disturbance. However, this was proven wrong later on.

Reactions with varying acid concentrations were probed. Unfortunately, not much gas was evolved during the runs such that the actual amount of hydrogen produced could not be calculated. During sampling, usually there was not enough gas pressure other than that due to steam in the reactor at a certain temperature. As expected, the pressure of the system would go down after every sampling but would go back to steam temperature readily. This attested to the capability of water in the vapor phase to be replenished.

On the other hand, volumetric percentages of the gases could still be quantified (moisture-free) using the gas chromatographs. Runs with varying acid concentrations showed an increasing trend with respect to volumetric percentage. It was noted that the hydrogen volumetric composition stabilized after about 1.5 to 2 hours. However, good repeatability of the tests was difficult to achieve. This could be attributed mainly to the heavy dependence of sampled gas volume on the prevailing temperature and pressure, as well as the depletion of the gas products due to sampling and to some extent, the variability of the biomass sample. Because of this, it was decided to change the sampling protocol to sampling at the end of a complete three-hour batch run, allowing the gas product to accumulate. It must be noted though that in these system, products already formed may become depleted through some side reactions due to this accumulation [16].

### 5.2.2 Acid Hydrolysis

Due to lignocellulosic biomass' non-solubility in water as well as its chemical complexity, aqueous-phase reforming of pine saw dust cannot proceed as readily as that of the model compounds [13-18, 123-128, 135, 136]. Previous studies usually had feeds containing 1 to 10 wt% of the substrates which were readily soluble or miscible with the aqueous medium. As such, the metal-catalyzed reforming reactions which produce H<sub>2</sub>, CO, CO<sub>2</sub> as well as some alkanes could readily proceed at the reaction conditions of the process at around 500 K.

Two processes are available for biomass breakdown: acid-catalyzed and base-catalyzed hydrolysis. Lignin and hemicelluloses are susceptible to extraction by base. This principle is used during the Kraft pulping for paper manufacturing [70, 149]. The objective is to delignify as much lignin as possible from the wood chips without damage to the fiber (cellulose and hemicelluloses). Unfortunately, yield is usually only about 45-50% of the initial feed [70], signifying hemicellulose dissolution as well as cellulose degradation through the *peeling reaction*. Base-catalyzed hydrolysis of wood is generally considered to occur at a slower rate compared to acid hydrolysis and requires higher concentrations [71].

Acid hydrolysis mainly affects the carbohydrate component of the biomass. This process has been used as a means to produce monosaccharides for other applications [74, 76], such as glucose for ethanol fermentation and even polymers. As a pretreatment, dilute acid pre-hydrolysis has been tapped to preferentially degrade the more susceptible hemicelluloses<sup>o</sup> and keep the cellulose more or less intact [73, 75-77]. On the other hand, concentrated acid hydrolysis had been used to directly attack the crystalline cellulose fraction of biomass [150].

---

<sup>o</sup> Formation of furfural from pentosan degradation tends to inhibit the growth of microorganisms in the substrate thus lowering the yield of alcohol.

Lignin, on the other hand, is not solubilized in dilute acid to any significant degree. Indeed, the chemical analysis of the pine sawdust (Table 5.2) showed only 0.40 wt% as acid soluble lignin compared to 27.5 wt% lignin that was insoluble in 72% sulfuric acid. As a way of confirming the expected hydrolysis extent of the varied biomass fractions, chemical analyses on the solid residue of a sample batch were done. Results are shown in Table 5.4.

**Table 5.4** Proximate analysis of pine sawdust solid by-products due to hydrolysis (5% H<sub>2</sub>SO<sub>4</sub>) and APR (5% H<sub>2</sub>SO<sub>4</sub>) + 10% Pt/Al<sub>2</sub>O<sub>3</sub>)

	<i>Hydrolysis residue<sup>1</sup></i>	<i>APR residue<sup>1</sup></i>
	<i>(wt% based on dry residual solid)</i>	<i>(wt% based on dry residual solid)</i>
<b>Carbohydrates</b>		
<b>Glucan</b>	4.30	1.80
<b>Xylan</b>	-nd- <sup>2</sup>	-nd-
<b>Galactan</b>	-nd-	-nd-
<b>Mannan</b>	-nd-	-nd-
<b>Arabinan</b>	-nd-	-nd-
<b>Lignin</b>		
<b>Acid insoluble</b>	82.90	86.60
<b>Acid-soluble</b>	0.70	0.70
<b>Extractives</b>	6.70	4.40
<b>Ash</b>	3.90	4.30
<b>Total Carbon</b>	64.70	63.30

<sup>1</sup> Analyses samples taken from a single representative batch treatment

<sup>2</sup> nd- not detected

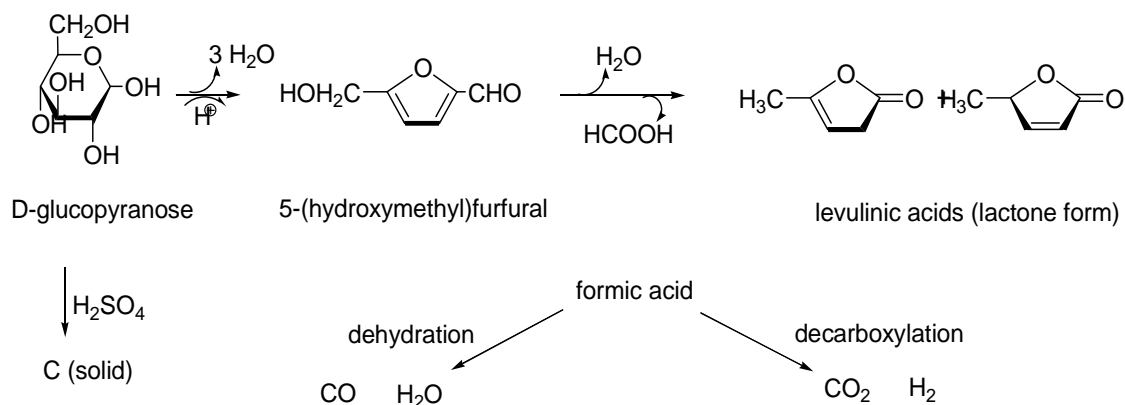
#### 5.2.2.1 Cellulose and hemicelluloses

As can be seen from the table, no monosaccharide other than glucose was found to be present in the residue. This is not surprising if we consider the remaining glucose to have come from the more recalcitrant crystalline region of cellulose and all the other carbohydrates were already hydrolyzed and were in the solution – as saccharides or their acid and/or thermal degradation products. As mentioned before, the ordered, linear arrangement of the crystalline cellulose region makes it more resistant to chemical reactivity compared to the more branched hemicellulose or the amorphous cellulose [71].

Early researchers had recognized that breakdown of hemicelluloses and cellulose in the presence of acid will produce sugars that are subject to further degradation upon continued exposure to acid [151]. Monosaccharides undergo dehydration reactions in acidic conditions giving rise to formation of what was previously referred to as “humic substances of indefinite composition”[151], the furfurals: 5-hydroxymethyl-2-furaldehyde (HMF) (from hexoses) and 2-furaldehyde (from pentoses and hexuronic acids) as well as some low molecular weight organic compounds [70, 71, 152]. Some of the earliest studies of the mechanism for this degradation were by Feather and Harris [153-155]. However, their suggested mechanism for HMF formation from fructose was later refuted by Antal et al.[156-158]. Antal further reported the presence of other degradation products such as levulinic acids. A path has been established between HMF and the formation of levulinic acid, which involves formation of formic acid through decarboxylation [71, 72]. Scheme 1 summarizes a possible pathway of degradation from glucose.



**Scheme 1.** Proposed pathway of degradation of D-glucopyranose in the presence of acid [71, 72]



It has been suggested that the decomposition of formic acid results in the formation of  $\text{H}_2$  in the processing of carbohydrates [115, 116]. Parallel pathways for formic acid decomposition have been reported in the literature: (1) *decarboxylation*, to  $\text{CO}_2$  and  $\text{H}_2$ ; and, (2) *dehydration*, to form  $\text{CO}$  and  $\text{H}_2\text{O}$ . Several studies on gaseous formic acid decomposition [159-161] showed that production of  $\text{CO}$  was favored over  $\text{CO}_2$ . On the other hand, it was noted that decarboxylation was preferred in aqueous-phase conditions [162-164]. At subcritical and supercritical conditions, Yu and Savage [164] found that formation of  $\text{CO}_2$  and  $\text{H}_2$  was favored over  $\text{CO}$  and  $\text{H}_2\text{O}$ . Corollary to these findings, computational studies showed a lower energy barrier for decarboxylation in the presence of water than for dehydration [161, 162, 165, 166].

To determine the effect of acid on hydrogen production, acid concentration was varied. Two concentrations were considered: 1% and 5% by weight of the feed. The results are shown in Figure 5.2.

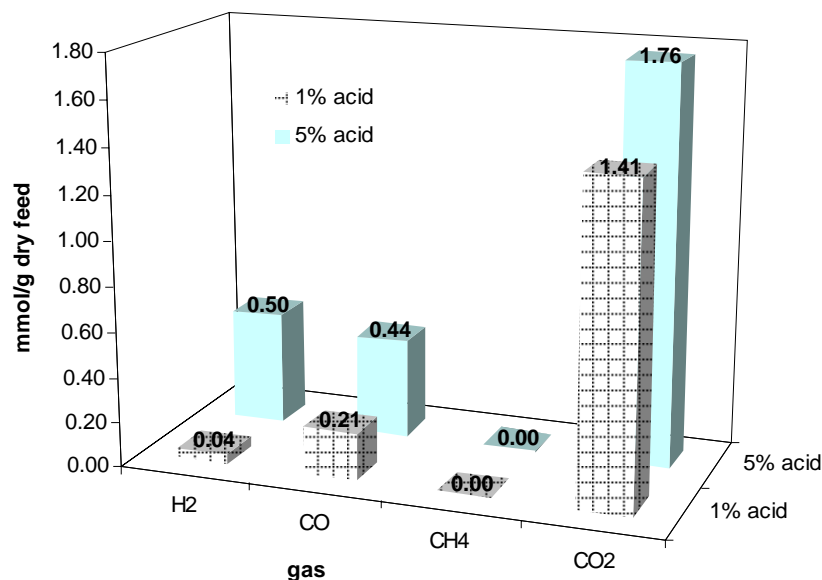


**Figure 5.2** Gas production due to acid hydrolysis of biomass in the absence of reforming catalyst.

Based on Figure 5.2, an increase in sulfuric acid concentration from 1% to 5% caused an increase on the amount of hydrogen produced. From 0.04 mmol/g dry biomass at 1% acid, hydrogen production increased by an order of magnitude to 0.50 mmol/g dry biomass at 5% acid. There were also corresponding increases in the CO and CO<sub>2</sub> production but not as dramatic as the hydrogen production.

Considering the mechanism suggested by Sinag et al., [115, 116] it could be said that the increase in acid concentration caused an increase in biomass degradation, forming more degradation products in the process (i.e. formic acid, among others) and thus releasing more hydrogen. However, it must be noted that production of hydrogen through formic acid degradation is not the only possible mechanism operating in our reaction conditions. This is illustrated by the non-stoichiometric increase of H<sub>2</sub> and CO<sub>2</sub>

from 1% acid to 5% acid concentration. Watanabe et al. [167] mentioned two major reactions that could occur: *dehydration*, wherein the bond between C and O breaks (i.e. Scheme 1) forming furans and phenols and *C-C bond-breaking reactions*, which forms low molecular acids, aldehydes and gases. Further study is required to elucidate the mechanism of the reactions in the system dealt with in this study.

The relationship between hydrogen evolution and acid concentration agree with observations from a study done by Parajo et al. [77] In that work, they monitored the amount of xylose (derived from the hemicellulose fraction) produced in the prehydrolysis of *Eucalyptus* wood with sulfuric acid at much lower temperatures of 113°C and 130°C. In their study, they found that at short times (0.25 to 1 hr), there was a significant increase in xylose concentration with increasing acid concentration from 2% - 6%. Increasing the reaction temperature also improved xylose yield. However, by increasing reaction times (up to 6 hours), the amount of xylose produced decreased, starting with an acid concentration of 4% acid at 113°C. Under harsher conditions at 130°C, a decrease of xylose occurred even with just 3% of acid. They attributed these results to degradation reactions which consumed the monosaccharide. These reactions, as mentioned earlier, could result in the formation of H<sub>2</sub>, among other by-products.

#### 5.2.2.2 Lignin

Lignin was not solubilized in dilute acid to any significant degree. Though some small fraction was acid-soluble, this was almost negligible compared to the acid-insoluble part. Indeed, the weight of the lignin fraction in the solid residue increased after subjecting the pine to hydrolysis conditions in this study (operating temperature: ~498K). Depolymerization of lignin occurs only to a limited extent during the initial stages of

hydrolysis due to the presence of some acid labile bonds that are readily hydrolyzed, especially the splitting of  $\alpha$ - and  $\beta$ -ether or ester linkages [152, 168, 169]. However, the liberated fragments are quite reactive and tend to form insoluble condensation products of high molecular weights with longer contact with acid [70, 71, 152]. For softwoods, Matsushita and Yasuda reported that the condensation of gymnosperm lignin in acidic conditions is due to the intermolecular dehydrations between benzylic carbons and the guaiacyl aromatic ring [170]. In another study, Hasegawa et al. reported the cross-linking effect of sulfuric acid on lignin, thus producing ligneous polymeric products with higher molecular weights [88].

### *5.2.3 Addition of reforming catalyst: Aqueous-phase reforming (APR)*

#### 5.2.3.1 H<sub>2</sub> production

Platinum on alumina was identified by Dumesic et al. as a very selective catalyst for the production of hydrogen [15, 16]. As previously mentioned, platinum could catalyze both the C-C bond and C-O bond cleavage, generating species such as H<sub>2</sub>, CO<sub>2</sub>, CO, methane and other alkanes through reforming, dehydrogenation and hydrogenation reactions. Also, it could catalyze the water-gas shift reaction which produces H<sub>2</sub> and CO<sub>2</sub> from CO and H<sub>2</sub>O.

In our experiments, the addition of platinum resulted in an increase in both the total amount of gaseous products formed as well as hydrogen volumetric percentage in the gas produced. This is illustrated in Figure 5.3 In the presence of only 5% H<sub>2</sub>SO<sub>4</sub>, the gas phase products contained 18.5% H<sub>2</sub> (by volume), whereas in the presence of 5% H<sub>2</sub>SO<sub>4</sub> and Pt/Al<sub>2</sub>O<sub>3</sub>, the gas phase contained 33.4% H<sub>2</sub>. On the other hand, both CO<sub>2</sub> and CO percentages decreased – from 65% to 57% and 16.3% to 9.5%, respectively. It must be

noted though that the amount of CO<sub>2</sub> produced remained almost the same while the CO yield decreased with APR – from 0.44 to 0.28 mmol/g dry feed. Together with the activation of the water gas shift action, other liquid-phase reactions probably occurred concurrently with the reforming, water-gas shift and hydrolysis reactions. These reactions may have produced liquid-phase compounds, which cannot be quantified through gas sampling and analysis. Liquid phase analysis could give indicators of some of these reactions. However, a comprehensive survey of the aqueous products is required in order to get meaningful mechanistic information, considering the chemical complexity of the feed.

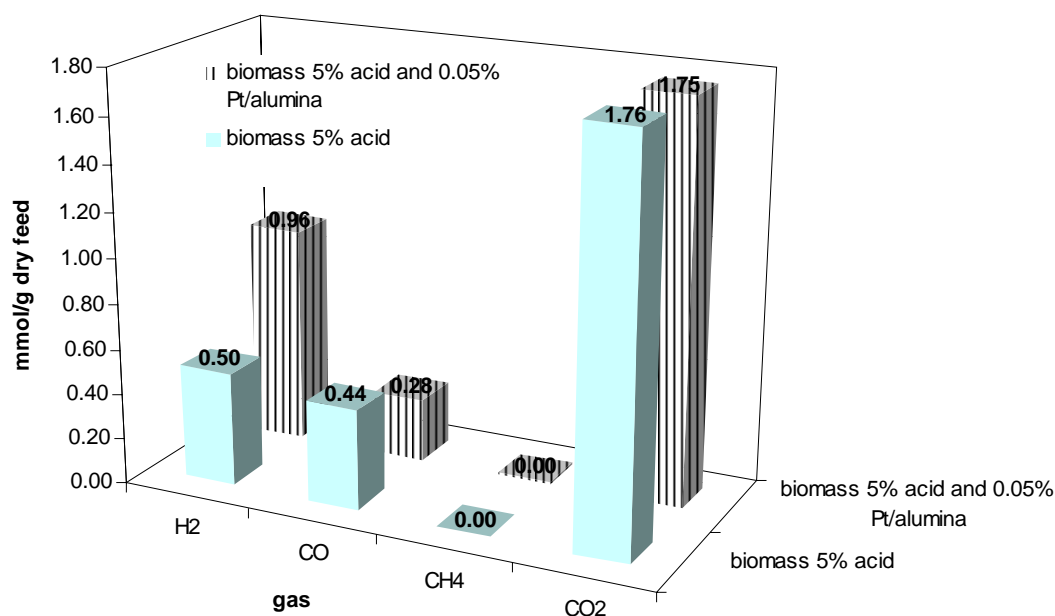


**Figure 5.3.** Comparison of gas production in the absence and presence of platinum using woody biomass as feed.

### 5.2.3.2 Characterization of spent catalyst

Catalyst stability is an important consideration in any reaction requiring a catalyst – especially those utilizing expensive noble metals. H<sub>2</sub> chemisorption of the fresh Pt/Al<sub>2</sub>O<sub>3</sub> catalyst showed Pt dispersion of about 25% with the Pt surface area 0.325 m<sup>2</sup>/g catalyst and a crystallite size of about 4.4 nm. Hydrogen absorbed was 0.00322 ± 0.00014 mmol/g. In contrast, chemisorption measurements of the spent catalysts after use in the APR reaction of biomass with exposure to sulfuric acid, water and biomass showed no measurable H<sub>2</sub> chemisorption. It was hypothesized that this could be due to either: (i) loss of Pt from the catalyst pellets due to solubilization at reaction conditions; (ii) Pt poisoning due to interaction with sulfur species; and/or, (iii) formation of carbonaceous deposits on the catalyst that make the Pt unavailable for chemisorption.

Elemental analysis of the spent Pt/Al<sub>2</sub>O<sub>3</sub> catalyst showed a basically unchanged Pt/Al ratio compared to that of the fresh catalyst (see Table 5.5). It also confirmed the presence of platinum in the catalyst after APR to nearly the same extent as the fresh catalyst.

**Table 5.5** Platinum, aluminum and sulfur content of fresh and spent Pt/Al<sub>2</sub>O<sub>3</sub> catalyst

	Fresh Catalyst		Spent Catalyst	
	wt %	no. of atoms	wt %	no. of atoms
<b>Pt</b>	0.35	1.1 x 10 <sup>21</sup>	0.33	1.0 x 10 <sup>21</sup>
<b>Al</b>	39.6	8.8 x 10 <sup>23</sup>	38.7	8.6 x 10 <sup>23</sup>
<b>S</b>	2.24 x 10 <sup>-4</sup>	4.2 x 10 <sup>18</sup>	1.32	2.5 x 10 <sup>22</sup>
<b>Pt/Al</b>	<b>1.2E-03</b>		<b>1.2E-03</b>	

This therefore eliminates the first of the probable causes, i.e., of the loss of H<sub>2</sub> chemisorption of the spent catalyst due to loss of Pt. It must be noted though that the ratio does not automatically imply that not even a small amount of platinum particles were lost in the process. It is possible that some catalyst particles were torn off due to abrasion during agitation of the mixture.

ICP-OES was used to analyze the liquid phase of a reaction by-product. Analysis of the supernatant after a reaction of formic acid, water and Pt/Al<sub>2</sub>O<sub>3</sub> catalyst pellets showed an aluminum concentration of 28.7 ppm. This is about 0.5% of all the aluminum in the catalyst. However, it was noticed that some solids settled at the bottom of the jar containing the aqueous phase product. These were not analyzed. It is expected though that there would be a small amount of catalyst particles in there as well but not to the extent, however, that it can explain the lost chemisorption capacity of the spent catalyst. This leaves us with the possibility of poisoning – either by sulfur species or by coke.

Coking is a very important factor in the catalytic cracking and reforming of petroleum. It is considered to be both a technological and economic problem. A large amount of savings could be had if it can be reduced significantly or avoided altogether by using more resistant catalysts [171]. Previous studies [171-175] noted two types of coke occurring on reforming catalysts such as Pt/Al<sub>2</sub>O<sub>3</sub>. They are identified by their differing response to temperature-programmed oxidation (TPO).

The first type of coke is that which is deposited onto the metal crystallites. According to the literature, it is removed earlier during a TPO. Removal of this coke from the catalyst was reported to cause a regeneration of activity of the metal [171]. Combustion temperatures for the coke associated with the metal surface slightly varied

from one author to another for Pt/Al<sub>2</sub>O<sub>3</sub>: about 300°C [171, 176]; 123° to 370°C (catalytic cracking of naphtha using Pt/Al<sub>2</sub>O<sub>3</sub>-Cl) [174, 175]; and, 350° to 370°C (reforming of *n*-hexane and methylcyclopentane on Pt/Al<sub>2</sub>O<sub>3</sub>) [173]. For nickel supported on alumina, Chen et al. reported the first CO<sub>2</sub> evolution peak around 380°C [172]. Based on these previous data, it was considered that calcination of the spent catalysts at 400°C should be sufficient to remove coke that is associated with the metal catalyst.

The second type of coke is associated with the support. Coking reaction is reported to be structure sensitive [176] and will thus vary depending on the reactant, catalyst as well as the reaction conditions. The zone of combustion for this type of coke varies from around 400°C [171] to 370° to 550°C [173, 175]. As such, there was a possibility that this type of coke might still be present in the calcined catalyst samples sent for H<sub>2</sub> chemisorption test. However, as mentioned before, catalyst chemisorption capacity should not be affected if the coke deposited on the metal has already been completely oxidized [171].

In the case of biomass APR, coking might come from formation of solid carbon due to prolonged exposure to sulfuric acid [177]. Thermal gravimetric analysis (TGA) data of spent catalyst shows two exothermic peaks: a big one peaking around 220°C and a small one at 520°C. However, these cannot be positively assigned to coke oxidation per se. On the other hand, hydrogen chemisorption measurement of the calcined spent catalyst pellets revealed basically no activity at all ( $0.02 \pm 0.05$  μmol/g). This leaves poisoning due to sulfur species as the possible reason.

The bulk elemental analysis of the spent catalysts showed quite a large amount of sulfur species – the spent catalyst has about 6000 times more sulfur than the fresh one



due to exposure to sulfuric acid (Table 5.5). Indeed, the S:Pt elemental ratio was 24.3, showing that there is likely enough sulfur present to potentially allow a complete poisoning of the platinum atoms with sulfur atoms and then some. Certainly, the interaction of sulfur with the platinum would result in reduced hydrogen chemisorption.

X-ray photoelectron spectroscopy (XPS), also known as ESCA (electron spectroscopy for chemical analysis) was used to have a survey of the chemicals on the surface of the catalyst pellets. XPS is a surface analysis technique that relies on the signature spectra of an element when it is bombarded by an excited ray of monoenergetic soft X-rays. Electrons become excited and are released through the photoelectric effect. The energies of these electrons are analyzed according to the equation

$$KE = h\nu - BE - \phi_s \quad (3)$$

where KE is the kinetic energy of the electron,  $h\nu$  is the energy of the photon, BE is the binding energy of the atomic orbital from where the electron came from and  $\phi_s$  is the spectrometer work function. The energy of the electron is the quantity measured by the spectrophotometer. However, this is dependent on the energy of the photon and is thus not intrinsic to the element. Both photon energy and the  $\phi_s$  are dependent on the instrument. As such, the binding energy identifies the electron and the element under consideration [178, 179].

Aside from elemental analysis, this technique also has the ability to identify what oxidation state/compound type does a particular element exists. For example, different binding energy ranges are available for Pt metal, PtSi, Pt<sub>2</sub>Si, PtCl<sub>2</sub>, etc. As such, more

qualitative information relevant to surface Pt crystallites can be obtained compared to elemental analysis.

Fresh Pt/Al<sub>2</sub>O<sub>3</sub>, APR spent, calcined spent as well as acidified catalysts were analyzed. As expected, no sulfur species was found on the fresh catalyst while sulfur was detected for the other samples that were exposed to sulfuric acid during the course of the experiments. Shown in Figure 5.4 is a comparative spectra of the three samples with sulfur species on them, namely spent, calcined and acidified catalyst. The intensities (y-axis values) of the spectra were adjusted to have a staggered and thus clearer spectrum of each. Also shown are the expected shifts for S2p<sub>3/2</sub> depending on the functional group.

As expected, no S was found on the fresh catalyst. On the other hand, the spent catalyst spectra (blue) showed a peak around 169 eV. In pure sulfur, this peak is situated at 164 eV. A look at the expected binding energy shift table for sulfur (Figure 5.4 insert) showed that it corresponded to either a sulfate or a sulfone structure on the surface [179]. A quick survey of sulfone syntheses did not come up with any route that might explain its existence on the sample, considering the condition and all the possible reactants in the reactor [180]. As such, the sulfur species on the spent catalyst were most likely to be sulfates from the acid.

The peak for 169 eV was also present in the calcined and acidified pellets. Sulfates, being already in the oxidized form, were not expected to show any change after calcination at 400°C. Thus, no line shifting was expected. On the other hand, the spectra of the acidified pellets showed a noticeable broadening of the peak. This might signify a possible double peak in that region but nothing can be said conclusively with the available data on hand.

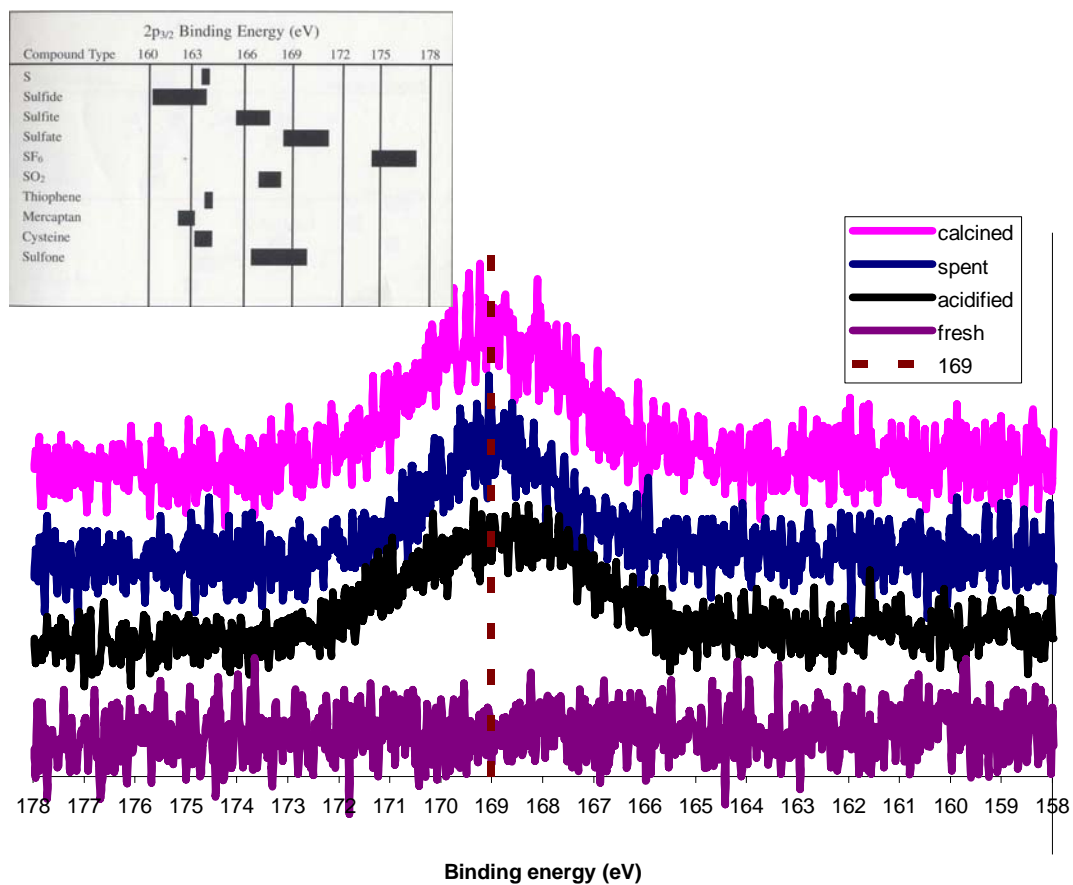


**Figure 5.4** S<sub>2p<sub>3/2</sub></sub> spectra of calcined, spent and acidified Pt/Al<sub>2</sub>O<sub>3</sub> catalyst pellets. Insert: Tabulated expected line shift for sulfur species based on compound (Reproduced from [179] )

Reports of sulfate association with alumina are found in the literature [181-184]. In a study done by Deng and An [181], Pd-Pt/Al<sub>2</sub>O<sub>3</sub> and Pt/Al<sub>2</sub>O<sub>3</sub> catalysts for hydrogen removal from carbon dioxide were exposed a feed gas which contained both O<sub>2</sub> and H<sub>2</sub>S. Hydrogen sulfide was converted to SO<sub>4</sub><sup>2-</sup> (verified by XRD) which was earlier reported to have an affinity to alumina. The authors reported that exposure of the catalysts to the sulfate caused a decrease in both activity and surface area of the spent catalysts. Through depth profiling with energy dispersive X-ray spectroscopy (EDX), they showed that sulfate was mainly concentrated in the outer shell.

In order to verify if pore blockage occurred in our system, nitrogen physisorption experiments were carried out. Samples include fresh Pt/Al<sub>2</sub>O<sub>3</sub> catalyst pellets, spent catalyst pellets, calcined spent catalyst pellets and acid-treated Pt/Al<sub>2</sub>O<sub>3</sub> pellets. Results of the study showed no significant decrease in the BET surface area for the catalysts, precluding the sulfate blocking hypothesis. Summary of the BET results are shown in Table 5.6

**Table 5.6** Summary of physisorption tests of several catalyst pellets

<b>Pt/Alumina catalyst pellets</b>	<b>SA (m<sup>2</sup>/g)</b>	<b>V (cm<sup>3</sup>/g)</b>
Fresh	104	0.23
Spent	94	0.24
Acidified	98	0.22
Calcined Spent	101	0.25

#### 5.2.4 APR of different substrates

As mentioned earlier, previous studies on aqueous-phase reforming dealt with flow reactor studies of representative model molecules that can be derived from biomass. Ethylene glycol ( $\text{C}_2\text{H}_6\text{O}_2$ ) was found to be a good molecule for APR. Previous studies reported as high as 96% hydrogen selectivity with  $\text{Pt}/\text{Al}_2\text{O}_3$  [13] and 95% with Sn-modified nickel catalyst [185] in a continuous mode. APR of other compounds with lower H/C ratio was found to be less selective to hydrogen production. Sorbitol (H/C ratio = 2.3) had a selectivity of 66% while glucose (H/C ratio = 2) was reported to have about 50% selectivity.

This varied response to APR depending on the feed source became the impetus to study the use of actual biomass for hydrogen production via APR. It is important to note that a direct comparison between the current work and Dumesic's previous work with regard to hydrogen selectivity and yield is hampered by the huge influence of reactor configuration on the results (flow vs. batch, *vide infra*). Thus, we compared the lignocellulosic APR results with other feeds to have an idea of how this system performs compared to feeds that have already been studied. Glucose was chosen as a representative compound. Waste paper was considered as another viable, alternative source. Ethylene glycol was also used as a feed but the acid catalyst was not included during its APR. This is because acid hydrolysis was deemed unnecessary since this feed has only two carbons in its backbone. The results of the study are summarized in Figure 5.5.

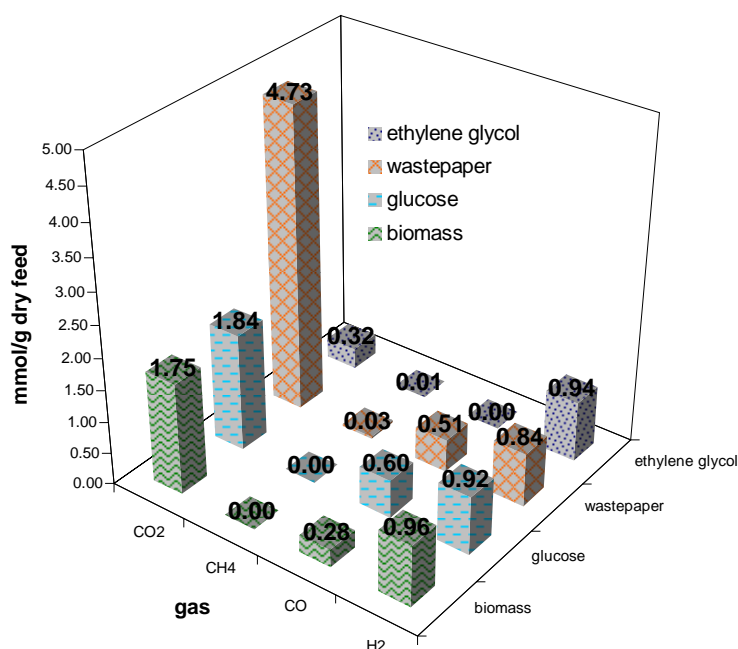


**Figure 5.5** Comparison of APR gas production using different feed sources in the presence of both acid and reforming catalysts.

As shown in Figure 5.6, the gases produced in APR were mainly H<sub>2</sub>, CO and CO<sub>2</sub>. In some runs, trace peaks of CH<sub>4</sub> were detected by the gas chromatographs but the amount of methane produced was too small to be quantifiable. In ethylene glycol runs, ethane was detected but its amount can also be considered negligible. In all the runs, the CO yield was found to be smaller compared to the H<sub>2</sub> yield. This could be attributed to the water-gas shift reaction in conjunction with other aqueous phase reaction. However, it must be noted that the total yields were not stoichiometric. For example, for every mole of glucose completely converted, it was expected that 12 moles of H<sub>2</sub> and 6 moles of CO<sub>2</sub> would be produced. As such, there should be twice the amount of H<sub>2</sub> as there were of CO<sub>2</sub>. However, such was not the case. Even for ethylene glycol runs where hydrogen was

the main gas product. This is attributed to the presence of possible H<sub>2</sub>-consuming side reactions.

Hydrogen production showed no dependence on the type of feed used in the system. The woody biomass produced the same amount of H<sub>2</sub> per dry gram of feed as the other compounds. It should be noted though that lignocellulosic materials contain lignin and our proximate analysis indicated that for the most part, it is not degraded to produce the permanent gases under our process conditions. If we consider the yield of biomass to be based only on its carbohydrate content, there would be an increase of hydrogen yield to 1.41 mmol H<sub>2</sub> per gram of dissolved feed for pine sawdust. Similarly, wastepaper gives a yield of 1.05 mmol H<sub>2</sub> per gram of carbohydrate if the inorganic content is disregarded (mass based on TGA). Thus, in this context, biomass gives a 50% higher hydrogen yield than glucose under similar conditions.

Higher cumulative production of H<sub>2</sub> from biomass over a model compound was also reported by Dalai and co-workers [10]. In their temperature-programmed gasification (TPG) study of aspen, cedar and cellulose, they found that cedar and aspen produced 32 and 26 mmol H<sub>2</sub>/g of feed, respectively. On the other hand, the maximum H<sub>2</sub> production from cellulose was only 20 mmol/g.

The APR of wastepaper showed a very high amount of CO<sub>2</sub> produced. This can be attributed to the presence of fillers and additives that go into the production of paper. CaCO<sub>3</sub> based fillers eventually produce CO<sub>2</sub> upon decomposition. However, it must be noted that CaCO<sub>3</sub> decomposition itself occurs at very high temperatures. For ground calcium carbonate (GCC) and precipitated calcium carbonate (PCC) (two forms that are usually used as fillers in the paper manufacturing industry) thermal decomposition occurs

from 1150K [186]. It is proposed that formation of CO<sub>2</sub> in the process could have been brought about by two pathways: (a) the reaction of the acid and CaCO<sub>3</sub> which directly liberates CO<sub>2</sub>; and, (b) formation of carbonic acid from the dissociation of calcium carbonate to Ca<sup>2+</sup> and CO<sub>3</sub><sup>2-</sup>, which then undergoes water-catalyzed decomposition to produce CO<sub>2</sub> [187].

#### 5.2.4.1 Batch APR of model feed compounds

It was initially expected that glucose and ethylene glycol would have produced more H<sub>2</sub> because these molecules are readily more accessible to the platinum for both the reforming and the WGS reactions to proceed. Both form a homogeneous liquid phase with water at the start of the reaction. Glucose was in solid form initially. However, their chemistries were quite different – as suggested by the difference in their product distribution. APR of ethylene glycol showed almost zero production of carbon monoxide while glucose had CO<sub>2</sub> as major product. A possible reason, aside from a possibly very efficient WGS, is the presence of reactions that have gone undetected because these products are in the aqueous phase. Reactions that were different from those which glucose and its intermediate degradation products have undergone. Note that among the feeds studied so far, only ethylene glycol had hydrogen as the major product in the gas phase rather than carbon dioxide.

Another difference between glucose and ethylene glycol APR was that the former produced a black solid residue at the end of the reaction while ethylene glycol did not. Both of them were water soluble at the beginning of the experiment though. Char production in glucose hydrothermal treatment has also been noted by others: Watanabe,



et al. in hot compressed water between 473 to 773 K [167, 188], Modell after glucose gasification at subcritical water temperatures [113], Sinag et al. in supercritical glucose gasification in a batch reactor [115] and others. The degradation reactions that glucose underwent were believed to produce this black solid residue [122, 177].

Char formation did not occur when ethylene glycol was fed to the reaction. This is believed to be due to the different solution chemistry of the ethylene glycol system and is not simply a consequence of the lack of sulfuric acid in these runs, as when even acid was used, the by-product remained homogeneous as well. The presence of acid though caused a 22% decrease in hydrogen production<sup>p</sup>.

Dumesic et al. also noted the difference between APR behavior of ethylene glycol and glucose [13]. They attributed this to further degradation reactions on the part of glucose in the liquid phase which ethylene glycol did not undergo – most probably due to ethylene glycol being a smaller molecule as well as the lack of carbonyl functionality of glucose.

Glucose can exist in a ring via hemi-acetal formation (Figure 5.6).

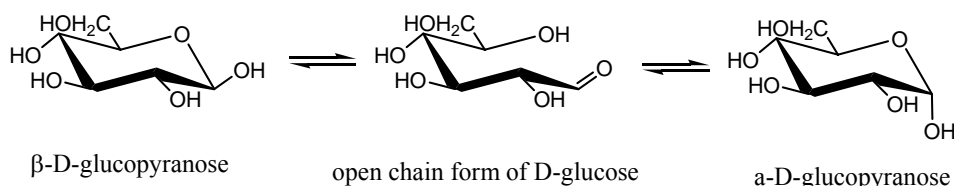


**Figure 5.6** Mutarotation of  $\beta\text{-D-glucopyranose}$  [189].

---

<sup>p</sup> Considering the complete poisoning effect of sulfate/sulfur species on platinum as demonstrated by lack of hydrogen chemisorption (Table 5.6) by the spent catalyst, this slight decrease in hydrogen production argues that the effect of the sulfates on the reforming reaction itself is not as drastic.

### 5.2.5 Baseline reactions

Experiments showed that baseline reactions in the absence of any feed (water-He and acid, water-He and Pt/Al<sub>2</sub>O<sub>3</sub>, and water-He, acid and Pt/Al<sub>2</sub>O<sub>3</sub>) did not register any increase in the total system pressure of runs with only water and pressurized with He. As such, evolution of gases other than steam was considered absent, even in the presence of platinum.

Mechanisms leading to hydrogen evolution from water on the surface of platinum have been suggested in the literature [190, 191]. However, while these published papers also indicate that although the release of two hydride species from the platinum site to form H<sub>2</sub> is favorable ( $k$  is in the order of  $\sim 10^{13}$ ), the initial reaction where water binds to an available platinum site ( $k = \sim 10^{-1}$ ) is much slower compared to the reverse reaction ( $k = \sim 10^{13}$ ). Indeed, a literature search shows platinum-catalyzed production of hydrogen from water occurs only in photocatalytic reactions [192].

An experiment with biomass with no catalysts was also performed. Even in the absence of acid, traces of hydrogen were generated. This minimal hydrogen production may be attributed to the hydrolysis due to the auto-ionization of water at elevated temperatures [116, 193]. At the beginning of the process, hydrolysis due to the release of acetic acid from acetylated hemicellulose groups was considered by some to be of a lower extent compared to the water autoionization effect [75]. However, at the latter part, acetate ions are the main sources of hydronium ions [75].

Figure 5.7 shows that the total system pressure of biomass APR became higher than the saturated vapor pressure of water at temperatures higher than 210°C. We attribute this to the onset of the reforming and/or WGS reactions that are favorable at

these temperatures [123]. In our system, the operating temperature of 225°C was usually attained at around 45 minutes. A noticeable steady increase in system pressure was noted up to about 1.5 to 2 hours, after which, pressure was more stable (i.e. rate of pressure increase was usually much slower).

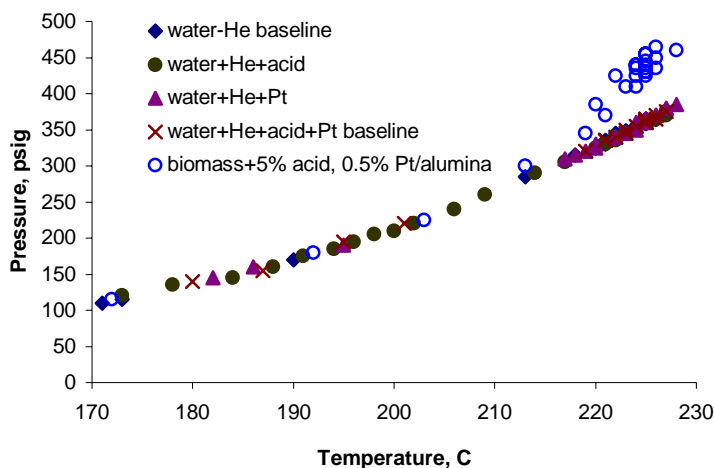


**Figure 5.7** Increase in system pressure due to evolution of gases. Pressure profiles: water-He baseline (◆); water-He-Pt (▲); water-He-Pt-acid (×); biomass with both 5% acid and Pt/Al<sub>2</sub>O<sub>3</sub> (○).

Lastly, the importance of the platinum in the production of hydrogen in the gas phase was probed with runs having  $\gamma$ -alumina and sulfuric acid acting as catalysts in the reaction. Results of these tests showed that hydrogen production was only about 5% of the total amount of hydrogen produced in the presence of Pt/Al<sub>2</sub>O<sub>3</sub> and sulfuric acid. This clearly points to the role of platinum in hydrogen production.

### 5.2.7 Comments on batch and continuous mode

Modified APR was applied to actual biomass using a batch reactor. As a proof of concept, we have shown that hydrogen can be produced from pine saw dust at a much lower temperature than traditional gasification or pyrolysis processes by using a combination of two processes: acid hydrolysis and platinum-catalyzed reforming. APR of other substrates such as glucose and ethylene glycol, using the same batch Parr reactor, showed comparable hydrogen yields. This supports contention that biomass could perform as well as ethylene glycol in a continuous reactor – if acid hydrolysis for biomass is integrated into the process.

Two parameters may be considered important in evaluating APR: turnover frequency (TOF) and selectivity. We compute TOF by considering only the H<sub>2</sub> production attributed to platinum reforming by subtracting the amount of hydrogen produced when only 5% acid is reacted with the feed. Table 5.7 presents the summary of these values. It also shows a comparison of our data from the batch reactor with the TOF values of previous studies with platinum as catalyst in a flow system [13, 128]. Interestingly, the TOFs observed in our batch system are quite similar to those observed in the previous studies of Dumesic.

**Table 5.7** H<sub>2</sub> turnover frequency (TOF) of APR of different substrates

Feed	Turnover frequencies, min <sup>-1</sup>	
		Dumesic, et al.
Pine Sawdust	2.0	--
Glucose	1.3	0.5 <sup>a</sup>

<b>Ethylene glycol</b>	8.0	7 <sup>a</sup> , 6.72 <sup>b</sup>
------------------------	-----	------------------------------------

a See ref. [13]

b See ref. [128]

The values given are calculated considering the whole 3-hour batch run. On the other hand, if the heating time to 498K is discounted (the first 45 minutes where no increase in system pressure is observed over the vapor pressure of water), TOFs for pine sawdust, glucose, and ethylene glycol (without acid) are 2.6, 1.7, and 11 min<sup>-1</sup>, respectively – showing higher H<sub>2</sub> production per surface Pt atom per minute.

With respect to H<sub>2</sub> selectivity, use of ethylene glycol in our system gave a value of 110%. This is higher compared to the previously reported ethylene glycol selectivity when Pt/Al<sub>2</sub>O<sub>3</sub> was used as the catalyst [13]. In another study using Co as catalyst, Huber, et al. [128] reported a selectivity 128.9% for ethylene glycol at a conversion of 1%. An explanation for having H<sub>2</sub> selectivities higher than 100% for ethylene glycol may be explained by revisiting the formula for selectivity as given by Dumesic et al.[13]

$$H_2 \text{ selectivity} = \frac{\text{molecules } H_2 \text{ produced}}{\text{total } C \text{ in the gas phase}} \times \frac{1}{RR} \times 100\% \quad (4)$$

where RR refers to the theoretical moles of H<sub>2</sub> that can be produced per mole C in the feed molecule. This assumes that production of H<sub>2</sub> depends only on the steam reforming-water-gas shift reactions. From equation (4), the maximum ratio between hydrogen and carbon in the gas phase is dictated by the RR term. RR for ethylene glycol is 2.5 while for

glucose is 2.0. The equation does not account for other possible reactions that might occur. For example,  $H_2$  may be liberated through dehydrogenation, leaving in the liquid phase an unsaturated species while not forming any  $CO$ ,  $CO_2$  or alkane. This also explains why our system suffers from a lower selectivity for glucose APR – 20% as opposed to a reported 50% by Cortright et al. [13]. It has been discussed before that glucose (and indeed biomass) undergoes degradation reactions which do not necessarily result to formation of  $H_2$  and  $CO_2$ . This may be due to large void spaces that are unavoidable in a batch system. Further understanding of the reaction chemistry of each substrate is necessary in order to properly quantify and evaluate product formation.

Previous studies done by Dumesic et al. used continuous reactors for APR studies of ethylene glycol as well as other model compounds [13-18, 124, 125, 127, 128, 135, 185]. They have noted the adverse effect of void space [18] on hydrogen production, especially for feeds such as glucose and sorbitol. Void space here was defined as portions of the reactor that do not contain solid catalyst. According to their reports, void spaces caused homogeneous liquid reactions that culminate in the production of acids, aldehydes and other liquid products [194-196]. These reactions compete with APR – thus, hydrogen selectivities as well as hydrogen yields were reduced. The presence of void space is essentially unavoidable in our batch system. Thus, lower hydrogen yields are to be expected. Considering this, a continuous system would be an improvement in the reported batch process. However, due to a solid feed as well as production of a solid residue in biomass APR, design of a continuous process is expected to be more challenging than for the APR of model compounds.

## **CHAPTER 6**

### **CONCLUSIONS AND RECOMMENDATIONS**

The results of this study show that hydrogen can be produced from lignocellulosic biomass at temperatures much lower than those currently used in gasification and pyrolysis processes. Increasing acid concentration from 1% to 5% by weight  $\text{H}_2\text{SO}_4$  was shown to hasten the breakdown of the biomass components as well as promote an order of magnitude increase in hydrogen production. Addition of a reforming catalyst such as  $\text{Pt}/\text{Al}_2\text{O}_3$  facilitated the formation of more hydrogen in the reaction product gas through the reforming and water-gas shift reaction. Aside from these two, other unidentified/uncharacterized reactions are expected to be occurring simultaneously as evidenced by the non-stoichiometric production of  $\text{H}_2$ ,  $\text{CO}$  and  $\text{CO}_2$ . Liquid by-product characterization may help in understanding these processes.

Comparisons between APR of different feeds (biomass, glucose, ethylene glycol and wastepaper) showed no difference in the amount of hydrogen produced per gram of feed. If hydrogen yields were to be based only on hydrolysable components of the feed (e.g. carbohydrates in biomass), biomass gave the highest yield. Additionally, differences in component gas proportions hinted at different solution chemistries for each feed molecule. Characterization of these reactions is beyond the scope of the study. An example of these is the degradation reactions that glucose is said to undergo in the presence of “void” spaces. Understanding these differences is expected to give a better

means of evaluating the sustainability of producing hydrogen directly from biomass through aqueous-phase reforming.

Catalyst characterization was considered important in this study. Through X-ray photoelectron spectroscopy (XPS), it was shown that sulfate species were present on the surface of the spent and calcined spent catalyst. These sulfur species were considered to be responsible for the observed loss of hydrogen chemisorption capacity of platinum after the APR reaction. However, addition of  $\text{H}_2\text{SO}_4$  to ethylene glycol APR resulted in about 22% reduction in hydrogen yield. This suggests that though  $\text{H}_2$  chemisorption is considered a good tool for measuring catalyst activity in a number of catalytic reactions, it is possible that it does not fully describe the effect of the modified APR reactions on the catalyst since hydrogen production was not drastically impaired by the presence of the acid.

The experiments in this study were done using a batch reactor. A limitation of a batch reactor in this process is the presence of what Dumesic et al. termed as void spaces in which glucose homogeneous degradation was said to occur. According to them, these degradation reactions do not lead to hydrogen production. However, using a continuous flow reactor is expected to improve this condition. Indeed, the similar hydrogen yields between different substrates creates an expectation that biomass can attain yields that will be comparable to previous studies for ethylene glycol.

Aside from a change in reactor configuration, optimizing the system with respect to temperature, reforming catalyst concentration as well as catalyst composition are expected to fine-tune the APR processing of biomass. The reforming reaction is favored



by increasing the temperature. On the other hand, low temperatures are favorable for the water-gas shift reaction. A balance must be achieved between them. At the same time, these reactions should also be considered when doing a survey of other potential catalysts.

The use of hydrolyzing agents other than sulfuric acid may also be considered. Other acids or a combination of these may prove to be more metal catalyst-friendly while at the same time are also effective in breaking down the polymeric components of biomass for the subsequent action of the reforming catalyst. Design of a multifunctional catalyst – capable of both catalyzing polymer degradation as well as the reforming reaction – may prove to be more efficient and environmental-friendly (less waste from homogeneous catalyst) in the long run.

Aside from Southern pine sawdust, other biomass feeds with different chemical compositions may also be studied. Studying the kinetics of their hydrogen production through APR is expected to be a useful tool in evaluating the versatility of this process.

Lastly, analysis of the liquid by-products is considered to be a very important tool in developing a better understanding of the chemistries involved in the reactions. The apparent difference in the reactivity of ethylene glycol and glucose may then be explained. The importance of the hemiacetal functionality of glucose may then be better understood as this information is expected to have an implication in the ultimate decision of whether APR can be sustainably and cost-effectively applied to biomass for hydrogen production. This is because the holocellulose fraction of biomass decomposes to monosaccharides (aldoses and ketoses that can form hemiacetal ring structures) upon hydrolysis.

## APPENDIX A

### Sample Calculations

#### I. Determination of amount of each component to maintain headspace and L/W ratio

The headspace was approximated by determining the volume occupied of 5.54g biomass and the liquid components and subtracting this from the volume of the bomb (Parr Instruments). Bulk densities of the substrates in water were roughly estimated by the volume displacement method using a graduated cylinder and equilibrating the solid (e.g. biomass) or letting the compound dissolve completely (e.g. glucose). These values were used to maintain headspace as well as L/W ratio = 9.

The reactor headspace was about 51 cc.

Liquid (water)-to-wood ratio, (L/W)	9
Density of water, $\rho_{\text{water}}$	1 g/mL
Density of wetted sawdust, $\rho_{\text{biomass}}$	1.25 g/mL
Total volume to be occupied, $v_{\text{total}}$	49 mL
Moisture content of biomass, MC%	10.63%

Total volume of slurry = volume of water ( $v_{\text{water}}$ ) + volume of biomass ( $v_{\text{biomass}}$ )

$$v_{\text{water}} = \left[ \frac{\rho_{\text{biomass}} (v_{\text{total}}) (L/W) (1 - \frac{MC\%}{100})}{1 + \rho_{\text{biomass}} (L/W) (1 - \frac{MC\%}{100})} \right] \times \left[ \frac{1}{\rho_{\text{water}}} \right]$$

$$v_{\text{water}} = \left[ \frac{1.25 \text{ g/mL} (49 \text{ mL}) (9) (1 - .1063)}{1 + 1.25 \text{ g/mL} (9) (1 - .1063)} \right] \times \left[ \frac{1}{1 \text{ g/mL}} \right] = 44.57 \text{ mL}$$

$$m_{\text{biomass}} = (v_{\text{total}} - v_{\text{water}}) (\rho_{\text{biomass}})$$

$$m_{\text{biomass}} = (49 \text{ mL} - 44.57 \text{ mL}) (1.25 \text{ g/mL}) = 5.54 \text{ g}$$

where  $m_{\text{biomass}}$  = wet weight of sawdust

$$m_{\text{dry biomass}} = 5.54 \text{ g} (1 - .1063) = 4.95 \text{ g}$$

Required amounts: 5% H<sub>2</sub>SO<sub>4</sub> + 10 wt% Pt/Al<sub>2</sub>O<sub>3</sub>

wt. of pine	5.540	g
wt. of Pt/Al <sub>2</sub> O <sub>3</sub>	0.495	g
vol. of water	44.57	ml
vol. of 2M H <sub>2</sub> SO <sub>4</sub>	1.263	ml

## II. Determination of gas phase composition

Run 70: biomass (5% acid + 10% Pt/Al<sub>2</sub>O<sub>3</sub>)

Actual amounts:

wt. of pine	5.540	g	moisture content: 10.63%
wt. of Pt/Al <sub>2</sub> O <sub>3</sub>	0.515	g	
vol. of water	44.50	ml	
vol. of 2M H <sub>2</sub> SO <sub>4</sub>	1.263	ml	
initial pressure (He)	30	psi	

At 3 hours:    Temperature: 226°C  
                   System pressure: 498 psig  
                   Steam + He pressure<sub>226°C</sub>: 364.82 psig

$$\Delta P = 133.18 \text{ psi}$$

Ideality of gas phase was assumed.

### A. GC Output

**Table A.1** Summary of GC analysis results

	Buck Scientific		HP 6890	
	Slope	Area Units	Slope	Area Units
He			<b>1071.9</b>	28251.6
H <sub>2</sub>			<b>1725.7</b>	43057.1
Air	<b>15.687</b>	67.4010	<b>7.219</b>	31.51592
CO	<b>13.951</b>	100.1800		
CH <sub>4</sub>	<b>13.095</b>		<b>736.59</b>	37.98423
CO <sub>2</sub>	<b>22.237</b>	1004.1660	*	3441.47729

\*Carbon dioxide: Area =  $-0.447 * (\% \text{ vol}_{\text{CO}_2})^2 + 106.6 * (\% \text{ vol}_{\text{CO}_2})$   
% error of 2<sup>nd</sup>-order equation (based on injected volume)

Injected volume: 80%

Area units (average): 5587.29

$$\%error = \frac{\text{Std. deviation}}{\text{Average area units}} \times 100\% = 0.38\%$$

Volume calculated based on 2<sup>nd</sup>-order equation: 77.78%

*% error of quadratic equation (based on injected volume): 2.8%*

## B. Buck Scientific GC

a.  $\text{vol}\%_{\text{air}} = \frac{\text{Area}}{\text{Slope}}$

$$\text{vol}\%_{\text{air}} = \frac{67.4010}{15.687} = 4.3\%$$

b.  $\text{vol}\%_{\text{CO}} = \frac{\text{Area}}{\text{Slope}}$

$$\text{vol}\%_{\text{CO}} = \frac{100.1800}{13.951} = 7.2\%$$

## C. HP 6890 GC

a.  $\text{vol}\%_{\text{He}} = \frac{\text{Area}}{\text{Slope}}$

$$\text{vol}\%_{\text{He}} = \frac{28251.6}{1071.9} = 26.4\%$$

b.  $\text{vol}\%_{\text{H}_2} = \frac{\text{Area}}{\text{Slope}}$

$$\text{vol}\%_{\text{H}_2} = \frac{43057.1}{1725.7} = 25\%$$

c.  $\text{Area} = -0.447(\text{vol}\%_{\text{CO}_2})^2 + 106.6(\text{vol}\%_{\text{CO}_2})$

$$\text{vol}\%_{\text{CO}_2} = \frac{106.6 \pm \sqrt{(-106.6)^2 - 4(0.447)(3441.4773)}}{2(0.447)} = 38.5\%$$

**Table A.2** Sample raw gas composition based on each GC

	<b>Buck Scientific</b>		<b>HP 6890</b>	
	<b>Slope</b>	<b>Corrected for air</b>	<b>Slope</b>	<b>Corrected for air and He</b>
<b>He</b>	-	-	<b>26.4</b>	-
<b>H<sub>2</sub></b>	-	-	<b>25.0</b>	-
<b>Air</b>	<b>4.3</b>	-	<b>4.4</b>	36.0
<b>CO</b>	<b>7.2</b>	7.5	-	-
<b>CH<sub>4</sub></b>	-	-	<b>0.05</b>	0.07
<b>CO<sub>2</sub></b>	<b>45.2</b>	47.2	<b>38.5</b>	55.6

#### **D. Resolution of volumetric percentages**

- CO<sub>2</sub> used as tie component

Ratios

CO<sub>2</sub>/H<sub>2</sub>: 1.54

CO<sub>2</sub>/CO: 6.29

CO<sub>2</sub>/CH<sub>4</sub>: 794.29

$$\% \text{CO}_2 = 100 - \% \text{H}_2 - \% \text{CO} - \% \text{CH}_4$$

#### **E. Final gas composition:**

**Table A.3** Run 70 gas phase volumetric composition

<b>Component</b>	<b>Vol. %</b>
<b>H<sub>2</sub></b>	<b>35.8</b>
<b>CO</b>	<b>8.8</b>
<b>CH<sub>4</sub></b>	<b>0.1</b>
<b>CO<sub>2</sub></b>	<b>55.3</b>

### F. Molar amount of each gas per batch

$$n \text{ (moles)} = \frac{\Delta P(V)}{RT} \left( \frac{\text{vol}\%}{100} \right)$$

$$n_{H_2} = \frac{133.18 \text{ psi} \left( \frac{1 \text{ atm}}{14.7 \text{ psi}} \right) (0.051 \text{ L}) (.358)}{0.08206 \frac{\text{L} \cdot \text{atm}}{\text{mol} \cdot \text{K}} (226 + 273.15)} = 4.04 \times 10^{-3} \text{ moles} = 4.04 \text{ mmol}$$

### G. Molar amount per gram of o.d. feed

a. Oven-dry weight of feed  
 $= 5.54 \text{ g} (1 - .1063) = 4.95 \text{ g}$

b. Moles per g feed  
 $= \frac{4.04 \text{ mmol}}{4.95 \text{ g}} = 0.82 \text{ mmol / g}$

c. Average of three runs  
Run 67: 1.01 mmol/g  
Run 69: 1.04 mmol/g  
Run 70: 0.82 mmol/g

Average moles  $H_2$  = 0.96 mmol/g  
Repeatability Std. Deviation = 0.12

d. Moles per g carbohydrates  
Wt. loss during reaction (carbohydrates) = 3.10g

$$= \frac{4.04 \text{ mmol}}{3.10 \text{ g}} = 1.30 \text{ mmol / g}$$

## APPENDIX B

### Temperature and Pressure Profile Sample Data

Run 70: biomass (5% acid + 10% Pt/Al<sub>2</sub>O<sub>3</sub>)

wt. of pine	5.540	g
wt. of Pt/Al <sub>2</sub> O <sub>3</sub>	0.515	g
vol. of water	43.30	ml
vol. of 2M H <sub>2</sub> SO <sub>4</sub>	1.263	ml

**Table B.1** T-P data of Run 70

Time	Temperature	Pressure
0	22	~30
5	31	~30
10	64	40
15	172	105
20	189	160
25	201	210
30	214	285
35	226	370
40	226	380
45	226	395
50	224	400
55	224	405
60	224	410
65	225	420
70	226	425
77	226	438
83	227	445
86	226	450
90	224	445
95	227	460
100	225	460
110	226	472
116	226	478
120	226	478
125	225	478
130	226	480
135	226	485
140	226	485
145	227	488
150	226	488
155	226	490
160	227	495
165	226	498
175	226	498
180	226	498

## APPENDIX C

### Hydrogen Chemisorption Isotherm Plots

Figure C.1 Isotherm plot of fresh Pt/Al<sub>2</sub>O<sub>3</sub> pellets

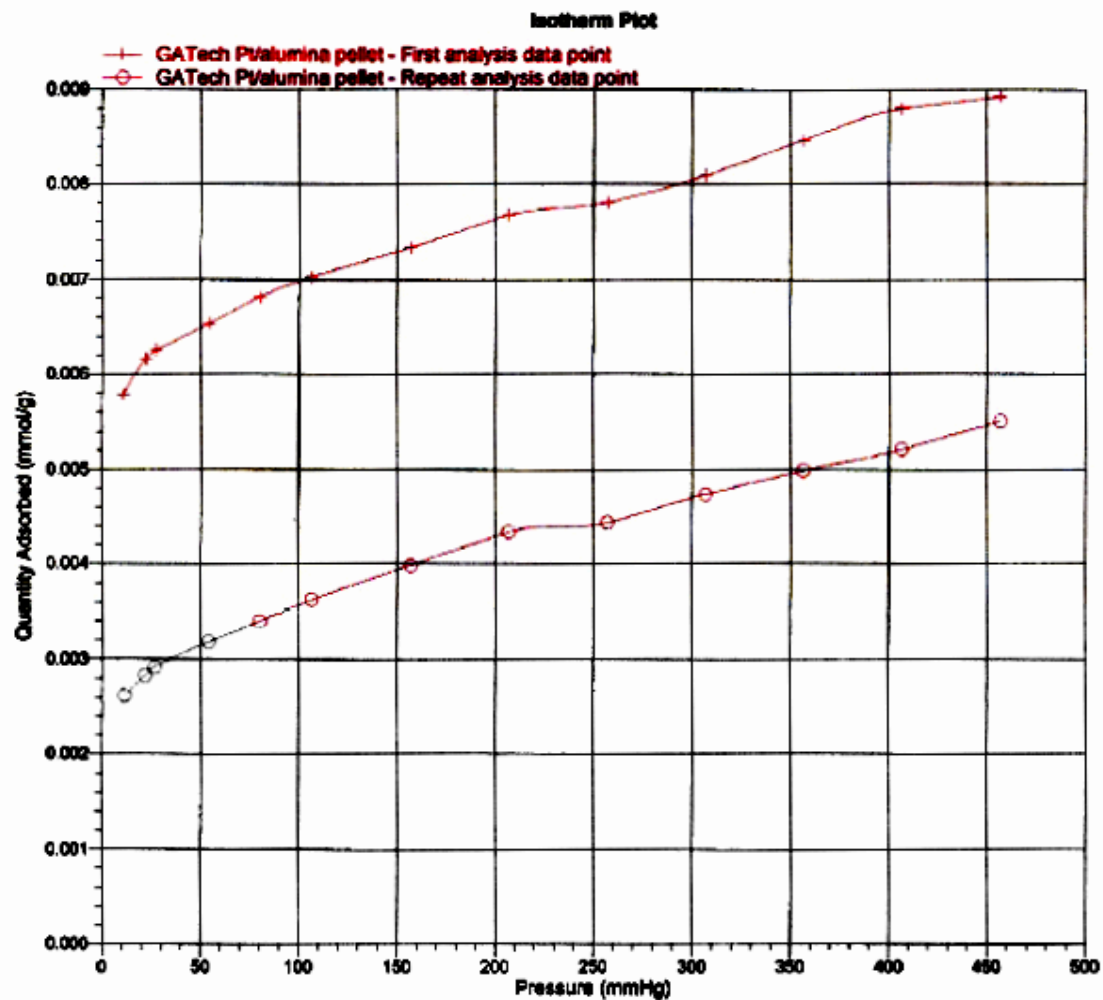
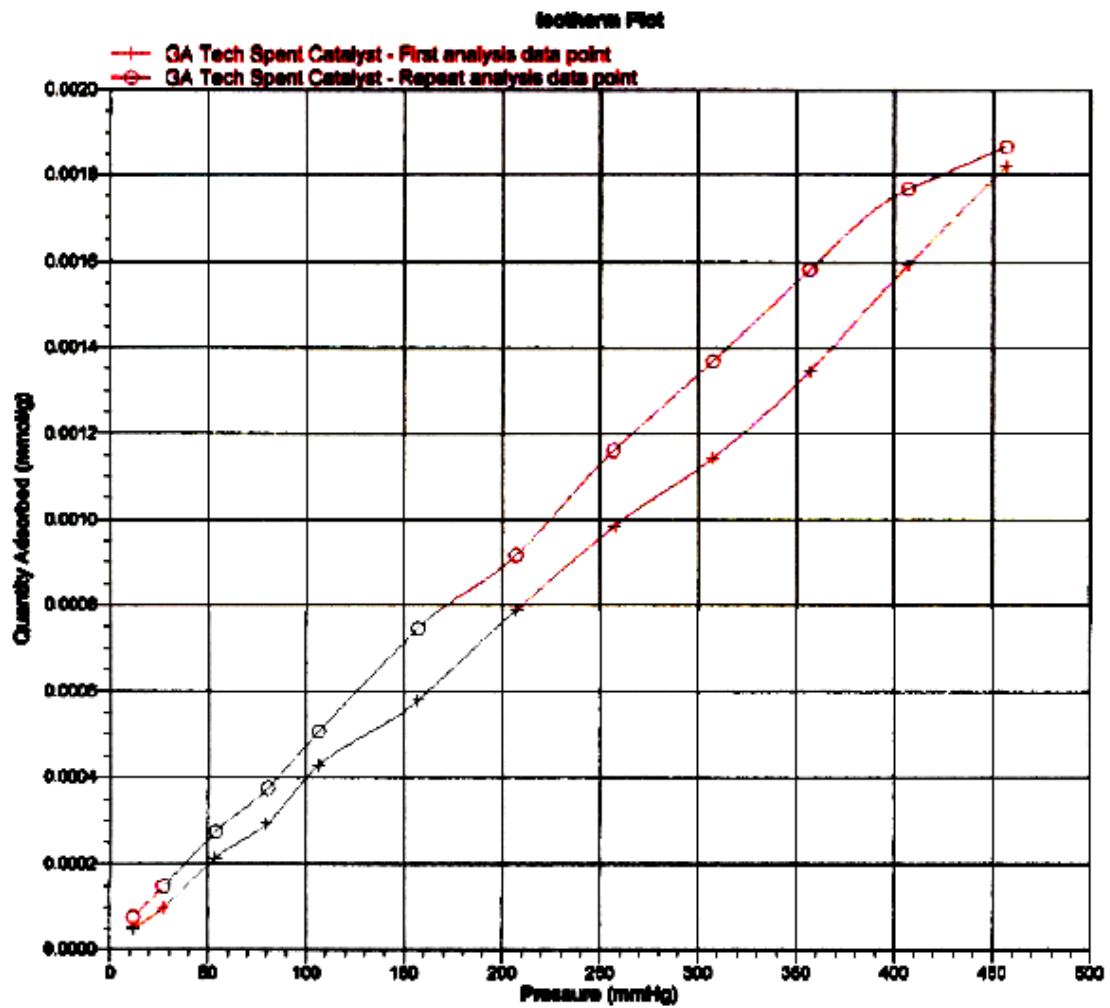
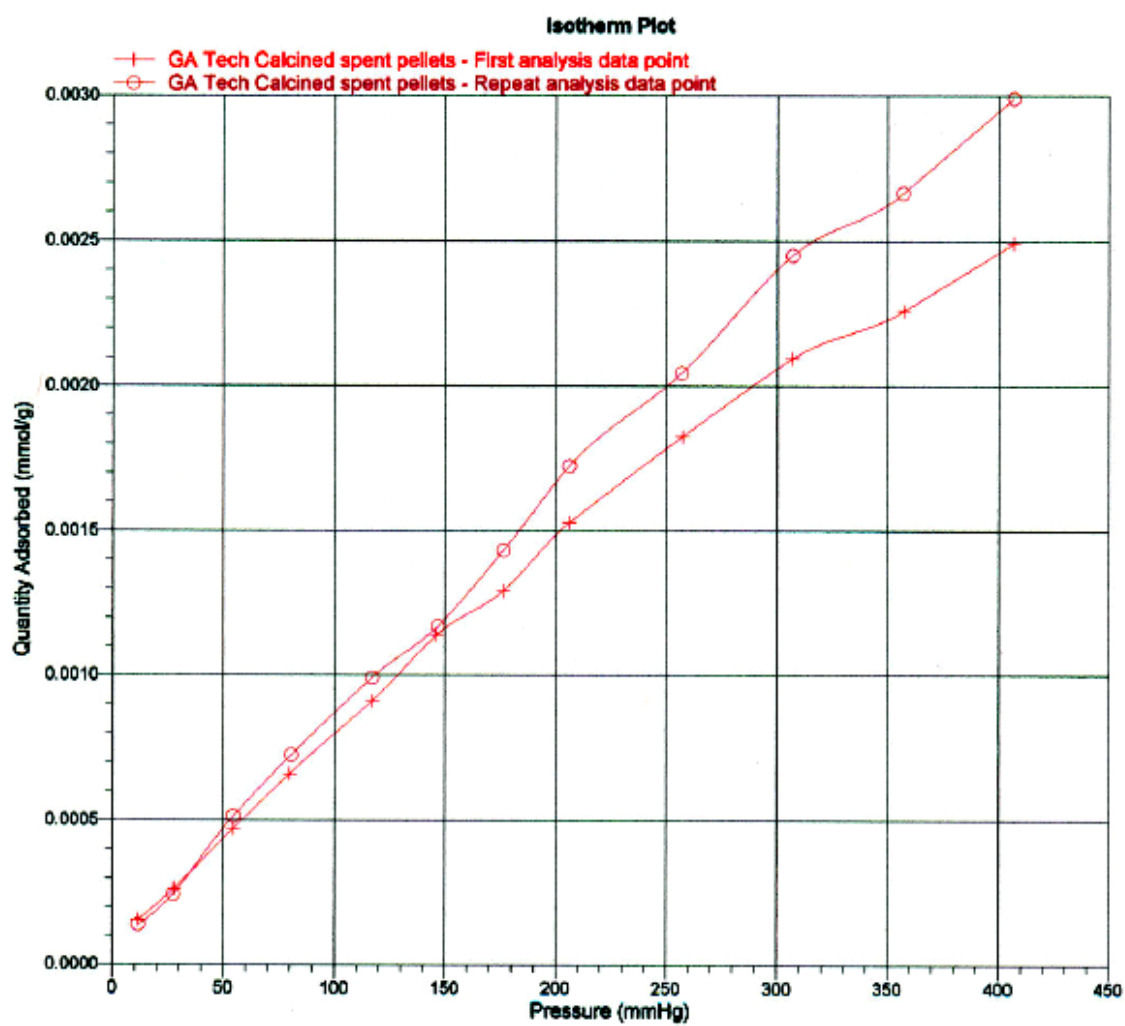




Figure C.2 Isotherm plot of spent Pt/Al<sub>2</sub>O<sub>3</sub> catalyst pellets



**Figure C.3** Isotherm plot of calcined spent Pt/Al<sub>2</sub>O<sub>3</sub> catalyst pellets



## APPENDIX D

### ICP-OES Analysis of a Liquid Sample

**Table D.1** Summary of liquid sample ICP-OES analysis of Run 117 (formic acid, Pt/Al<sub>2</sub>O<sub>3</sub>, water)

Element	Concentration
Al	28.66 ppm
Fe	1104.81 ppm
Cu	1.18 ppm
Cr	9.04 ppm
Mn	3.01 ppm

#### Typical chemical composition of SS-316

Fe, <0.03% C, 16-18.5% Cr, 10-14% Ni, 2-3% Mo, <2% Mn, <1% Si, <0.045% P, <0.03% S

## APPENDIX E

### CP-TOSS-MAS $^{13}\text{C}$ NMR of Biomass APR Residue

Nuclear magnetic resonance (NMR) spectroscopy is one of the powerful techniques used to provide useful information on functional groups present in an organic material. Solid state  $^{13}\text{C}$  NMR has been used to characterize lignin through non-destructive means [197, 198]. Shown in Figure E.1 is the CP MAS  $^{13}\text{C}$  NMR<sup>q</sup> spectrum of lignin from a softwood tree (Douglas fir). Hatcher [197] studied the chemical structure of lignins from Douglas fir and oak through solid-state  $^{13}\text{C}$  NMR. The peak at 148 ppm is characteristic of a softwood species[197]. It corresponds to  $\text{C}_3/\text{C}_4$  resonances of the guaiacyl units in lignin (See Figure E.2). For a hardwood, due to the presence of syringyl units, this peak shifts to 153 ppm (Figure E.3). Oliveira et al. [198] cited the same type of chemical shift (i.e. due to syringyl units) in Cavendish banana leaves at around 152 ppm.

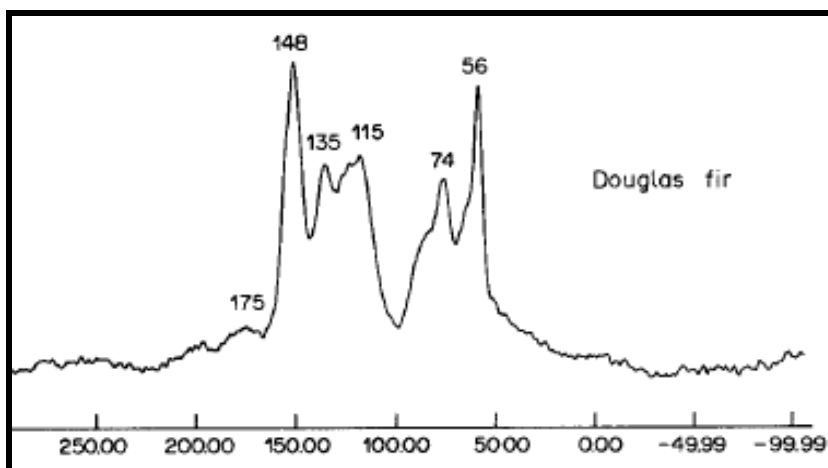


**Figure E.1** CP MAS  $^{13}\text{C}$  NMR spectra of natural lignin from Douglas fir [197]

---

<sup>q</sup> Cross-polarization Magic Angle Spin  $^{13}\text{C}$  NMR

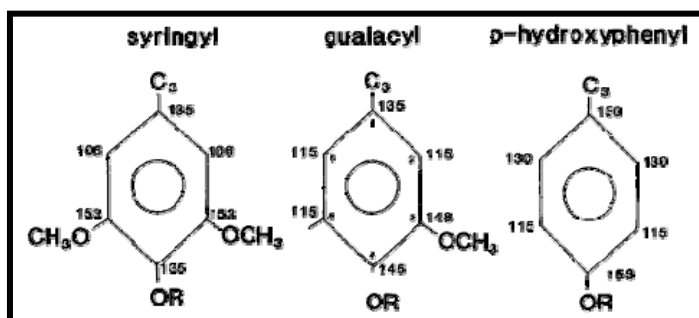


**Figure E.2** Structural units expected from lignin [197]

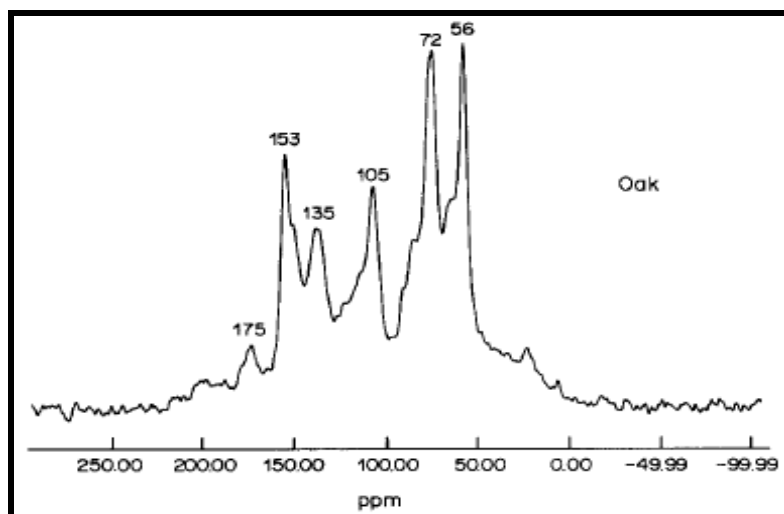


**Figure E.3** CP MAS  $^{13}\text{C}$  NMR spectra of natural lignin from oak [197]

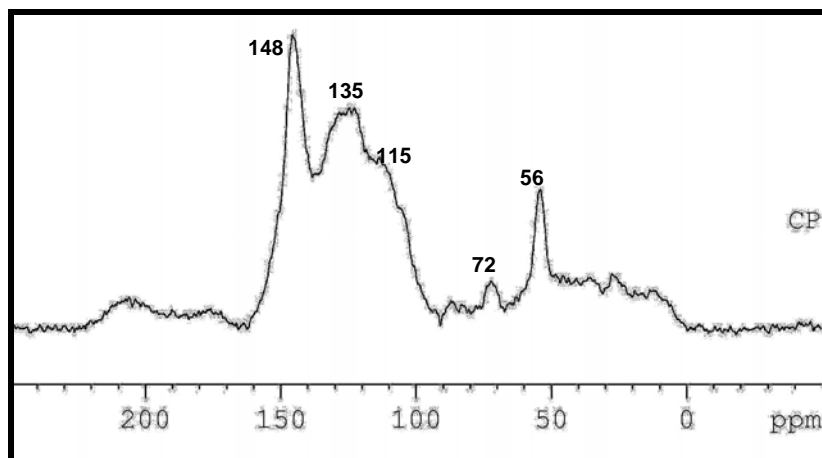


**Figure E.4** CP-TOSS MAS  $^{13}\text{C}$  NMR spectra of residue from biomass APR

Figure E.4 shows the CP-TOSS<sup>r</sup> MAS  $^{13}\text{C}$  NMR of the residue after treatment of biomass with 5% acid in the presence of 10% Pt/Al<sub>2</sub>O<sub>3</sub>. As can be seen, similarities with the natural softwood lignin still exist even after undergoing APR.

As mentioned previously, the peak at around 148 ppm corresponds to the C<sub>3</sub>/C<sub>4</sub> positions in the guaiacyl structure. From Figure E.2, the peaks at 115 and 135 ppm are attributed to the other carbons in the phenolic ring. The peak at 115 ppm corresponds to aromatic carbons that are *ortho*- or *para*- to O-substituted aromatic carbons. C-substituted carbons or unsubstituted ones that are not *ortho*- or *para*- to O-substituted aromatic carbons are represented by the peak at 135 ppm. These are still present in Figure E.4 though the peak at 115 ppm is much fainter than expected. A possible explanation for this is the formation of C-C crosslinks at C<sub>2</sub>, C<sub>5</sub> or C<sub>6</sub> due to condensation reactions in the presence of acid [71].

The presence of carbohydrates is monitored through the peak at 72 ppm. As seen in Figure E.4, this is very minimal in the residue. The presence of a small amount of carbohydrates fits well with the proximate analysis of the residue given in Table 5.5.

---

<sup>r</sup> Total Suppression of Spinning Sidebands.

Here, glucan was shown to comprise only 1.08% of the residue mass. Lastly, the peak at about 56 ppm is considered to be one of the characteristic peaks for lignin in  $^{13}\text{C}$  NMR. It represents the methoxyl carbons in the macropolymer.[197]

In conclusion, the NMR spectrum of the biomass APR residue contains key peaks representative of lignin structures in softwoods. As such, it supports the claim that the acidic APR process do not degrade lignin except for the possibility of condensation reactions due to low pH conditions.

## APPENDIX F

### Aqueous-phase Reforming of Formic Acid (Single Run Experiments)

Formic acid is evolved from the degradation of carbohydrates in acidic media [71, 72]. It is derived from the decarboxylation of 5-hydroxymethyl-2-furaldehyde to give off levulinic acids (see Scheme 1). Sinag et al. [115, 116] suggested that degradation of formic acid is a probable source of  $H_2$ . Several studies have shown that  $H_2$  is indeed a product of one of the degradation possible routes available to formic acid, i.e. decarboxylation [159-164].

In order to gauge  $H_2$  production from formic acid, three experiments were performed. First was processing of formic acid in the presence of water, acid as well as reforming catalyst (i.e. APR) at the reaction temperature of 225°C. This was followed by reaction with acid only and lastly, with Pt/ $Al_2O_3$  only. The amount of formic acid used was 5.08g in 43.30 mL of water. The volume of added acid was 1.295 mL while 0.523g of Pt/ $Al_2O_3$  was charged to the reactor.

The typical 3-hour batch run time was not reached for any of the three experiments because of rapid gas evolution. The Parr reactor has a working pressure of 1400 psig. Once the 1300 psig marked was reached, the reaction was stopped for safety considerations. Among the three runs, the one with just the reforming catalyst had the fastest rate. The reaction was stopped after 56 minutes. The “least” reactive system, containing only acid, was stopped after 72 minutes. The results of these experiments are shown in Figure F.1.



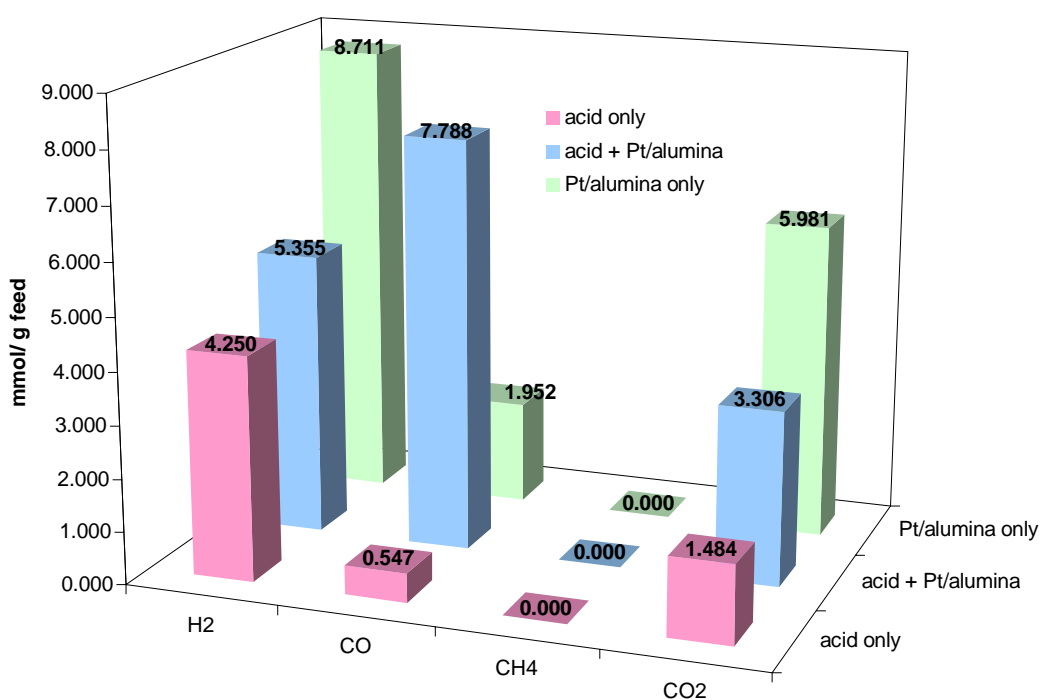


**Figure F.1** Gas composition of different formic acid experiments

As can be seen from the figure, aside from being the most reactive, Pt/Al<sub>2</sub>O<sub>3</sub> catalyzed the highest production of H<sub>2</sub>. Carbon monoxide was the least formed. From this, decarboxylation reaction seemed to be the preferred route. For the acid-only catalyzed reaction, H<sub>2</sub> production was the lowest. In this run, decarboxylation was also in effect. On the other hand, addition of both acid and Pt catalyst produced H<sub>2</sub> that is in the middle between the values of the previous two. Also, carbon monoxide was the major product, pointing to dehydration as the preferred degradation route. Since the reaction conditions are the same for both runs, the only explanation that could be given is that H<sub>2</sub>SO<sub>4</sub> (more specifically the sulfates) reacted with the Pt/Al<sub>2</sub>O<sub>3</sub> thus forming a “catalyst”, in the process conditions for this run, which favors dehydration over decarboxylation.

No repetition the runs were done. It was later found that formic acid is very corrosive to stainless steel at 10% concentration at high temperatures (2<sup>nd</sup> only to sulfuric at same concentration and conditions among acetic acid, ferric chloride, hydrobromic, hydrofluoric and phosphoric acids) [199]. This has implication on further use of formic acid as a direct feed for hydrothermal processing. Though it is a very robust source of hydrogen, reactor construction must be considered critically.

## REFERENCES:

1. *Homo erectus: tool use and adaptation to the environment*. [cited 2006 June]; Available from: [http://www.wsu.edu/gened/learn-modules/top\\_longfor/timeline/erectus/erectus-b.html](http://www.wsu.edu/gened/learn-modules/top_longfor/timeline/erectus/erectus-b.html).
2. Walsh, M.E., et al., *Biomass Feedstock Availability in the United States: 1999 State Level Analysis*. 2000, Oak Ridge National Laboratory.
3. *Petroleum Overview, 1949-2004*. 2005 [cited 2006 June]; Available from: <http://www.eia.doe.gov/emeu/aer/txt/stb0501.xls>.
4. Nath, K. and D. Das, *Hydrogen from biomass*. Current Science, 2003. **85**(3): p. 265-271.
5. Milciuviene, S., D. Milcius, and B. Praneviciene, *Towards hydrogen economy in Lithuania*. International Journal of Hydrogen Energy, 2006. **31**(7): p. 861-866.
6. Deffeyes, K.S., *Beyond Oil*. 2005, New York: Hill and Wang.
7. Rioche, C., et al., *Steam Reforming of model compounds and fast pyrolysis bio-oil on supported noble metal catalysts*. Appl. Catal. B, 2005. **61**(1-2): p. 130-139.
8. Yaman, S., *Pyrolysis of biomass to produce fuels and chemical feedstocks*. Energy Conversion and Management, 2004. **45**(5): p. 651-671.
9. Mohan, D., C.U. Pittman, and P.H. Steele, *Pyrolysis of wood/biomass for bio-oil: A critical review*. Energy & Fuels, 2006. **20**(3): p. 848-889.
10. Dalai, A.K., et al., *Catalytic gasification of sawdust derived from various biomass*. Energy & Fuels, 2003. **17**(6): p. 1456-1463.
11. Fushimi, C., et al., *Effect of heating rate on steam gasification of biomass. 2. Thermogravimetric-mass spectrometric (TG-MS) analysis of gas evolution*. Industrial & Engineering Chemistry Research, 2003. **42**(17): p. 3929-3936.
12. Xu, X.D., et al., *Carbon-catalyzed gasification of organic feedstocks in supercritical water*. Industrial & Engineering Chemistry Research, 1996. **35**(8): p. 2522-2530.

13. Cortright, R.D., R.R. Davda, and J.A. Dumesic, *Hydrogen from catalytic reforming of biomass-derived hydrocarbons in liquid water*. Nature, 2002. **418**(6901): p. 964-967.
14. Davda, R.R., et al., *Aqueous-phase reforming of ethylene glycol on silica-supported metal catalysts*. Appl. Catal., B, 2003. **43**(1): p. 13-26.
15. Shabaker, J.W. and J.A. Dumesic, *Kinetics of aqueous-phase reforming of oxygenated hydrocarbons: Pt/Al(2)O(3) and Sn-modified Ni catalysts*. Ind. Eng. Chem. Res., 2004. **43**(12): p. 3105-3112.
16. Shabaker, J.W., et al., *Aqueous-phase reforming of ethylene glycol over supported platinum catalysts*. Catal. Lett., 2003. **88**(1-2): p. 1-8.
17. Davda, R.R. and J.A. Dumesic, *Renewable hydrogen by aqueous-phase reforming of glucose*. Chemical Communications, 2004. **1**: p. 36-37.
18. Huber, G.W., R.D. Cortright, and J.A. Dumesic, *Renewable alkanes by aqueous-phase reforming of biomass-derived oxygenates*. Angew. Chem. Int. Ed., 2004. **43**(12): p. 1549-1551.
19. *Key World Energy Statistics*. 2005, International Energy Association: Paris, France.
20. *Annual Energy Review 2004*, Energy Information Administration: Washington D.C.
21. [www.doe.gov/energysources/fossilfuels.htm](http://www.doe.gov/energysources/fossilfuels.htm). [cited 2006 May].
22. Ahlbrandt, T.S., *Fossil Fuels*, in *Macmillan Encyclopedia of Energy*. 2001, Macmillan Reference USA: New York.
23. Hubbert, M.K., *Nuclear Energy and the Fossil Fuels*. 1956, Shell Development Company - Exploration and Production Research Division.
24. Hubbert, M.K., *Energy from Fossil Fuels*. Science, 1949. **109**: p. 103-109.
25. Fainberg, A.F., *Consumption of Coal*, in *Macmillan Encyclopedia of Energy*. 2001, Macmillan Reference USA: New York.
26. Dunkerley, J., *Lessons from the past thirty years*. Energ. Policy, 2006. **34**: p. 503-507.

27. Kamm, B., et al., *Biorefinery Systems - An Overview*, in *Biorefineries - Industrial Processes and Products*, B. Kamm, P.R. Gruber, and M. Kamm, Editors. 2006, Wiley-VCH Verlag GmbH & Co. KGaA.
28. Kenney, J.F., et al., *The evolution of multicomponent systems at high pressures: VI. The thermodynamic stability of the hydrogen-carbon system: The genesis of hydrocarbons and the origin of petroleum*. Proc. Natl. Acad. Sci. U.S.A, 2002. **99** (17): p. 10976-10981
29. Simoneit, B.R.T., *Prebiotic organic synthesis under hydrothermal conditions: an overview*. Adv. Space Res., 2004. **33**(1): p. 88-94.
30. Scott, H.P., et al., *Generation of methane in the Earth's mantle: In situ high pressure-temperature measurements of carbonate reduction* Proc. Natl. Acad. Sci. U.S.A, 2004. **101**(39): p. 14023-14026.
31. *International Energy Annual 2003*. 2003, Energy Information Administration: Washington D.C.
32. *World Petroleum Assessment 2000-Description and Results*. 2000, US Geological Survey: Reston, Virginia.
33. Campbell, C.J. 2003, Association for the Study of Peak Oil and Gas: Cork, Ireland.
34. Greene, D.L., J.L. Hopson, and J. Li, *Have we run out of oil yet? Oil peaking analysis from an optimist's point of view*. Energ. Policy, 2006. **34**: p. 515-531.
35. Greene, D.L., J.L. Hopson, and J. Li, *Running out of and into oil: Analyzing global oil depletion and transition through 2050*. 2003, Oak Ridge National Laboratory: Knoxville, Tennessee.
36. *Short-Term Energy Outlook 2006*, Energy Information Administration: Washington D.C.
37. *International Energy Outlook 2005*. 2005, Energy Information Administration: Washington D.C.
38. *April 2006 International Petroleum Monthly*. 2006, Energy Information Administration: Washington D.C.
39. *Alternative Fuels*. 3/2006 [cited 2006 May]; Available from: <http://www.eere.energy.gov/afdc/altfuel/altfuels.html>.

40. *Advanced Energy Initiative*, O.o.t. President, Editor. 2006.
41. *The Role of Coal as an Energy Resource*. 2003 [cited 2006 May]; Available from: [http://www.netl.doe.gov/technologies/coalpower/refshelf/role\\_of\\_coal.pdf](http://www.netl.doe.gov/technologies/coalpower/refshelf/role_of_coal.pdf).
42. *Annual Coal Report*. 2004, Energy Information Administration: Washington D.C.
43. Tien, J.C., *Production of Coal*, in *Macmillan Encyclopedia of Energy*. 2001, Macmillan Reference USA: New York.
44. Shepherd, W. and D.W. Shepherd, *Energy Studies*. 2nd ed. 2003, London: Imperial College Press.
45. *Coal Facts 2005*. [cited 2006 May]; Available from: <http://www.worldcoal.org/pages/content/index.asp?PageID=188>.
46. *Electric Power Annual with Data for 2004*. 2005, Energy Information Administration: Washington D.C.
47. Hodgson, P.E., *Nuclear Power, Energy and the Environment*. 1999, London: Imperial College Press.
48. Halbouty, M.T., *Natural Gas*, in *McGraw-Hill Encyclopedia of Energy*, S.P. Parker, Editor. 1981, McGraw-Hill Book Company: New York.
49. Tussing, A.R., *Consumption of Natural Gas*, in *Macmillan Encyclopedia of Energy*. 2001, Macmillan Reference USA: New York.
50. *Geopolitical Energy Context and World Resources and Accessibility*, in *Oil Gas European Magazine*. 2003. p. 10-12.
51. *Natural Gas*. [cited 2006 May ]; Available from: <http://www.doe.gov/energysources/naturalgas.htm>.
52. *Natural Gas Fuel Market*. [cited 2006 May]; Available from: [http://www.eere.energy.gov/afdc/altfuel/gas\\_market.html](http://www.eere.energy.gov/afdc/altfuel/gas_market.html).
53. *World Nuclear Reactors*. [cited 2006 May]; Available from: [http://www.eia.doe.gov/cneaf/nuclear/page/nuc\\_reactors/reactsum2.html](http://www.eia.doe.gov/cneaf/nuclear/page/nuc_reactors/reactsum2.html).

54. *World Uranium Production*. [cited 2006 May]; Available from:  
<http://www.uxc.com/fuelcycle/uranium/production-uranium.html>.
55. Ozdamar, A., et al., *Investigation of the potential of wind-waves as a renewable energy resource: by the example of Cesme-Turkey*. *Renewable & Sustainable Energy Reviews*, 2004. **8**(6): p. 581-592.
56. *Uranium quick facts*. [cited 2006 June]; Available from:  
<http://web.ead.anl.gov/uranium/guide/facts/>.
57. Smith, B. *Insurmountable Risks: The Dangers of Nuclear Power to Combat Global Climate Change*. 2006 [cited 2006 May]; Available from:  
<http://www.ieer.org/reports/insurmountablerisks/summary.pdf>.
58. Omoto, A., *Nuclear Power for Sustainable Growth and Relevant IAEA Activities for the Future*. *Prog. Nucl. Energ.*, 2005. **47**(1-4): p. 16-26.
59. *US Energy Consumption by Energy Source*. [cited 2006 June]; Available from:  
<http://www.eia.doe.gov/cneaf/solar.renewables/page/trends/table1.html>.
60. *NASA's Solar System Exploration*. 2006 May 2006 [cited 2006 June]; Available from:  
<http://solarsystem.nasa.gov/planets/profile.cfm?Object=Sun&Display=Facts>.
61. Sheahan, R.T., *Alternative Energy Sources: A Strategy Planning Guide*. 1981, Maryland: Aspen Systems Corporation.
62. Da Rosa, A.V., *Fundamentals of Renewable Energy Processes*. 2005, Massachusetts: Elsevier Inc.
63. *BP Statistical Review of World Energy 2005*. 2005 [cited June 2006]; Available from:  
[www.bp.com](http://www.bp.com).
64. Ragauskas, A.J., et al., *From wood to fuels: Integrating biofuels and pulp production*. *Industrial Biotechnology*, 2006. **2**(1): p. 55-65.
65. Kuga, S., S. Takagi, and R.M. Brown, *Native Folded-Chain Cellulose-II*. *Polymer*, 1993. **34**(15): p. 3293-3297.
66. Brown, R.M., *"Brave new world" of microbial cellulose: Novel applications*. Abstracts of Papers of the American Chemical Society, 2005. **229**: p. U297-U297.

67. Czaja, W., et al., *Microbial cellulose - the natural power to heal wounds*. Biomaterials, 2006. **27**(2): p. 145-151.
68. Legge, R.L., *Microbial Cellulose as a Speciality Chemical*. Biotechnology Advances, 1990. **8**(2): p. 303-319.
69. Brown, R.M., Jr. *Microbial Cellulose: A New Resource for Wood, Paper, Textiles, Food and Specialty Products*. [cited 2006 June]; Available from: <http://www.botany.utexas.edu/facstaff/facpages/mbrown/position1.htm>.
70. Smook, G.A., *Handbook for Pulp & Paper Technologists*. 1992, Vancouver: Angus Wilde Publications.
71. Sjöström, E., *Wood Chemistry*. 2nd ed. 1999, New York: Academic Press.
72. Robyt, J.F., *Essentials of Carbohydrate Chemistry*. 1998, New York: Springer.
73. Maloney, M.T., T.W. Chapman, and A.J. Baker, *Dilute Acid-Hydrolysis of Paper Birch - Kinetics Studies of Xylan and Acetyl-Group Hydrolysis*. Biotechnol. Bioeng., 1985. **27**(3): p. 355-361.
74. Ebringerova, A., *Structural Diversity and Application Potential of Hemicelluloses*. Macromol. Symp., 2006. **232**: p. 1-12.
75. Garrote, G., H. Dominguez, and J.C. Parajo, *Hydrothermal processing of lignocellulosic materials*. Holz Als Roh-Und. Werkstoff., 1999. **57**(3): p. 191-202.
76. Harris, J.F., et al., *Two-Stage, Dilute Sulfuric Acid Hydrolysis of Wood: An Investigation of Fundamentals*. 1985, US Forest Products Laboratory.
77. Parajo, J.C., et al., *Prehydrolysis of Eucalyptus Wood with Dilute Sulfuric-Acid - Operation in Autoclave*. Holz Als Roh-Und. Werkstoff, 1994. **52**(2): p. 102-108.
78. Tran, A.V. and R.P. Chambers, *Behaviors of Southern Red Oak Hemicelluloses and Lignin in a Mild Sulfuric Acid Hydrolysis*. Biotechnol. Bioeng., 1986. **28**: p. 811-817.
79. Reale, S., et al., *Mass spectrometry in the biosynthetic and structural investigation of lignins*. Mass Spectrometry Reviews, 2004. **23**(2): p. 87-126.



80. Yasuda, S. and K. Asano, *Preparation of strongly acidic cation-exchange resins from gymnosperm acid hydrolysis lignin*. Journal of Wood Science, 2000. **46**(6): p. 477-479.
81. Matsushita, Y. and S. Yasuda, *Preparation of anion-exchange resins from pine sulfuric acid lignin, one of the acid hydrolysis lignins*. Journal of Wood Science, 2003. **49**(5): p. 423-429.
82. Matsushita, Y. and S. Yasuda, *Reactivity of a condensed-type lignin model compound in the Mannich reaction and preparation of cationic surfactant from sulfuric acid lignin*. Journal of Wood Science, 2003. **49**(2): p. 166-171.
83. Matsushita, Y., A. Iwatsuki, and S. Yasuda, *Application of cationic polymer prepared from sulfuric acid lignin as a retention aid for usual rosin sizes to neutral papermaking*. Journal of Wood Science, 2004. **50**(6): p. 540-544.
84. Matsushita, Y., et al., *Preparation and evaluation of a dispersant for gypsum paste from acid hydrolysis lignin*. Journal of Applied Polymer Science, 2005. **98**(6): p. 2508-2513.
85. Matsushita, Y. and S. Yasuda, *Preparation and evaluation of lignosulfonates as a dispersant for gypsum paste from acid hydrolysis lignin*. Bioresource Technology, 2005. **96**(4): p. 465-470.
86. Gokarn, A.N. and H.J. Muhlen, *Catalysis of char gasification by mixed lignosulfonates: Quantification of role of each component*. Fuel, 1996. **75**(1): p. 96-98.
87. Gokarn, A.N. and H.J. Muhlen, *Catalysis of Coal-Gasification by Na Lignosulfonate*. Fuel, 1995. **74**(1): p. 124-127.
88. Hasegawa, I., et al., *Lignin-silica hybrids as precursors for silicon carbide*. Journal of Applied Polymer Science, 1999. **73**(7): p. 1321-1328.
89. Hasegawa, I., et al., *Lignin-silica-titania hybrids as precursors for Si-Ti-C-O fibers*. Journal of Sol-Gel Science and Technology, 1998. **13**(1-3): p. 485-488.
90. Pye, E.K., *Industrial Lignin Production and Applications*, in *Biorefineries - Industrial Processes and Products*, B. Kamm, P.R. Gruber, and M. Kamm, Editors. 2006, Wiley-VCH Verlag GmbH & Co. KGaA: Weinheim.
91. Kamm, B., et al., *Lignocellulose-based Chemical Products and Product Family Trees*, in *Biorefineries - Industrial Processes and Products*, B. Kamm, P.R. Gruber, and M. Kamm, Editors. 2006, Wiley-VCH Verlag GmbH & Co. KGaA: Weinheim.

92. Sharma, D.K., *Bioprospecting for drug, research and functional foods for the prevention of diseases - Role of flavonoids in drug development*. Journal of Scientific & Industrial Research, 2006. **65**(5): p. 391-401.
93. Balasundram, N., K. Sundram, and S. Samman, *Phenolic compounds in plants and agri-industrial by-products: Antioxidant activity, occurrence, and potential uses*. Food Chemistry, 2006. **99**(1): p. 191-203.
94. Brahmachari, G. and D. Gorai, *Progress in the research on naturally occurring flavones and flavonols: An overview*. Current Organic Chemistry, 2006. **10**(8): p. 873-898.
95. Willke, T. and K.D. Vorlop, *Industrial bioconversion of renewable resources as an alternative to conventional chemistry*. Applied Microbiology and Biotechnology, 2004. **66**(2): p. 131-142.
96. Mok, W.S.L. and M.J. Antal, *Uncatalyzed Solvolysis of Whole Biomass Hemicellulose by Hot Compressed Liquid Water*. Industrial & Engineering Chemistry Research, 1992. **31**(4): p. 1157-1161.
97. *Top Value Added Chemicals from Biomass: Volume I - Results of Screening for Potential Candidates from Sugars and Synthesis Gas*, T. Werpy and G. Petersen, Editors. 2004, Pacific Northwest National Laboratory (PNNL) and National Renewable Energy Laboratory (NREL).
98. *What is a biorefinery?* [cited 2006 June]; Available from: <http://www.nrel.gov/biomass/biorefinery.html>.
99. *EIA- 819 Monthly Oxygenate Report*. 2006 [cited 2006 June]; Available from: [http://www.eia.doe.gov/pub/oil\\_gas/petroleum/data\\_publications/monthly\\_oxygenate\\_report/current/pdf/819mhilt.pdf](http://www.eia.doe.gov/pub/oil_gas/petroleum/data_publications/monthly_oxygenate_report/current/pdf/819mhilt.pdf).
100. *Energy Policy Act (EPAAct) of 2005*. [cited 2006 June]; Available from: <http://www.ferc.gov/legal/maj-ord-reg/fed-sta/ene-pol-act.asp?new=sc2#skipnavsub>.
101. *Biomass FAQs*. 2/8/2006 [cited 2006 June]; Available from: [http://www1.eere.energy.gov/biomass/biomass\\_basics\\_faqs.html#ethanol](http://www1.eere.energy.gov/biomass/biomass_basics_faqs.html#ethanol).
102. Gray, K.A., L.S. Zhao, and M. Emptage, *Bioethanol*. Current Opinion in Chemical Biology, 2006. **10**(2): p. 141-146.

103. Oliva, J.M., et al., *Effects of acetic acid, furfural and catechol combinations on ethanol fermentation of Kluyveromyces marxianus*. Process Biochemistry, 2006. **41**(5): p. 1223-1228.
104. Bobleter, O., R. Niesner, and M. Rohr, *Hydrothermal Degradation of Cellulosic Matter to Sugars and Their Fermentative Conversion to Protein*. Journal of Applied Polymer Science, 1976. **20**(8): p. 2083-2093.
105. Juanbaro, J. and L. Puigjaner, *Saccharification of Concentrated Brewing Bagasse Slurries with Dilute Sulfuric-Acid for Producing Acetone Butanol by Clostridium-Acetobutylicum*. Biotechnology and Bioengineering, 1986. **28**(10): p. 1544-1554.
106. Klinke, H.B., A.B. Thomsen, and B.K. Ahring, *Inhibition of ethanol-producing yeast and bacteria by degradation products produced during pre-treatment of biomass*. Applied Microbiology and Biotechnology, 2004. **66**(1): p. 10-26.
107. Clements, L.D. and D.L. Van Dyne, *The Lignocellulosic Biorefinery - A Strategy for Returning to a Sustainable Source of Fuels and Industrial Organic Chemicals*, in *Biorefineries - Industrial Processes and Products*, B. Kamm, P.R. Gruber, and M. Kamm, Editors. 2006, Wiley-VCH Verlag GmbH & Co. KGaA: Weinheim.
108. Meier, D., A. Oasmaa, and G.V.C. Peacocke, *Properties of Fast Pyrolysis Liquids: Status of Test Methods*, in *Developments in Thermochemical Biomass Conversion*, A.V. Bridgwater and D.G.B. Boocock, Editors. 1997, Blackie Academic & Professional: London.
109. Brown, R.M., *Biomass Refineries Based on Hybrid Thermochemical-Biological Processing - An overview*, in *Biorefineries-Industrial Processes and Products*, B. Kamm, P.R. Gruber, and M. Kamm, Editors. 2006, Wiley-VCH Verlag GmbH & Co. KGaA: Weinheim.
110. Beaumont, O., *Flash Pyrolysis Products from Beech Wood*. Wood and Fiber Science, 1985. **17**(2): p. 228-239.
111. Milne, T.A., et al., *A Review of the Chemical Composition of Fas-Pyrolysis Oils from Biomass*, in *Developments in Thermochemical Biomass Conversion*, A.V. Bridgwater and D.G.B. Boocock, Editors. 1997, Blackie Academic & Professional: London.
112. *Hydrogen Production - Biomass Gasification*. 2/08/2006 [cited 2006 June]; Available from: [http://www.eere.energy.gov/hydrogenandfuelcells/production/biomass\\_gasification.html](http://www.eere.energy.gov/hydrogenandfuelcells/production/biomass_gasification.html).

113. Modell, M., *Gasification and Liquefaction of Forest Products in Supercritical Water*, in *Fundamentals of Thermochemical Biomass*, R.P. Overend, T.A. Milne, and L.K. Mudge, Editors. 1985, Elsevier Applied Science Publishers Ltd.: London.
114. Antal, M.J., et al., *Biomass gasification in supercritical water*. Industrial & Engineering Chemistry Research, 2000. **39**(11): p. 4040-4053.
115. Sinag, A., A. Kruse, and J. Rathert, *Influence of the heating rate and the type of catalyst on the formation of key intermediates and on the generation of gases during hydrolysis of glucose in supercritical water in a batch reactor*. Industrial & Engineering Chemistry Research, 2004. **43**(2): p. 502-508.
116. Sinag, A., A. Kruse, and V. Schwarzkopf, *Key compounds of the hydrolysis of glucose in supercritical water in the presence of K<sub>2</sub>CO<sub>3</sub>*. Ind. Eng. Chem. Res., 2003. **42**(15): p. 3516-3521.
117. Matsumura, Y., et al., *Biomass gasification in near- and super-critical water: Status and prospects*. Biomass & Bioenergy, 2005. **29**(4): p. 269-292.
118. Matsumura, Y., X. Xu, and M.J. Antal, *Gasification characteristics of an activated carbon in supercritical water*. Carbon, 1997. **35**(6): p. 819-824.
119. Karagoz, S., et al., *Hydrothermal upgrading of biomass: Effect of K<sub>2</sub>CO<sub>3</sub> concentration and biomass/water ratio on products distribution*. Bioresource Technology, 2006. **97**(1): p. 90-98.
120. Hao, X.H., et al., *Hydrogen production from catalytic gasification of cellulose in supercritical water*. Chemical Engineering Journal, 2005. **110**(1-3): p. 57-65.
121. Kabyemela, B.M., et al., *Mechanism and kinetics of cellobiose decomposition in sub- and supercritical water*. Industrial & Engineering Chemistry Research, 1998. **37**(2): p. 357-361.
122. Kruse, A. and A. Gawlik, *Biomass conversion in water at 330-410 degrees C and 30-50 MPa. Identification of key compounds for indicating different chemical reaction pathways*. Industrial & Engineering Chemistry Research, 2003. **42**(2): p. 267-279.
123. Davda, R.R., et al., *A review of catalytic issues and process conditions for renewable hydrogen and alkanes by aqueous-phase reforming of oxygenated hydrocarbons over supported metal catalysts*. Appl. Catal., B, 2005. **56**(1-2): p. 171-186.

124. Shabaker, J.W., et al., *Aqueous-phase reforming of methanol and ethylene glycol over alumina-supported platinum catalysts*. J. Catal., 2003. **215**(2): p. 344-352.
125. Huber, G.W., J.W. Shabaker, and J.A. Dumesic, *Raney Ni-Sn catalyst for H<sub>2</sub> production from biomass-derived hydrocarbons*. Science, 2003. **300**(5628): p. 2075-2077.
126. Shabaker, J.W., G.W. Huber, and J.A. Dumesic, *Aqueous-phase reforming of oxygenated hydrocarbons over Sn-modified Ni catalysts*. Journal of Catalysis, 2004. **222**(1): p. 180-191.
127. Shabaker, J.W., et al., *Sn-modified Ni catalysts for aqueous-phase reforming: Characterization and deactivation studies*. Journal of Catalysis, 2005. **231**(1): p. 67-76.
128. Huber, G.W., et al., *Aqueous-phase reforming of ethylene glycol over supported Pt and Pd bimetallic catalysts*. Appl. Catal., B, 2006. **62**(3-4): p. 226-235.
129. Huber, G.W., et al., *Production of liquid alkanes by aqueous-phase processing of biomass-derived carbohydrates*. Science, 2005. **308**(5727): p. 1446-1450.
130. Ying, B., et al., *Hydrogen Production by Aqueous-Phase Reforming of Ethylene Glycol over Pt Catalysts Supported on gamma-Alumina Modified with Ce and Mg*. Chinese Journal of Catalysis, 2006. **27**: p. 275-280.
131. Ragauskas, A.J., et al., *The Path Forward for Biofuels and Biomaterials*. Science, 2006. **311**: p. 484-489.
132. Haq, E., *Biomass for Electricity Generation*. 2002, Energy Information Administration: Washington D.C.
133. *What is southern pine?* [cited 2006 May]; Available from: <http://www.southernpine.com/whatis.shtml>.
134. *What is Southern pine? - The Southern Pines*. [cited 2006 May]; Available from: <http://www.southernpine.com/expert/index.pl?leafcode=23>.
135. Davda, R.R. and J.A. Dumesic, *Catalytic reforming of oxygenated hydrocarbons for hydrogen with low levels of carbon monoxide*. Angew. Chem. Int. Ed., 2003. **42**(34): p. 4068-4071.

136. Huber, G.W. and J.A. Dumesic, *An overview of aqueous-phase catalytic processes for production of hydrogen and alkanes in a biorefinery*. Catal. Today, 2006. **111**(1-2): p. 119-132.
137. Bai, Y., et al., *Hydrogen production by aqueous-phase reforming of ethylene glycol over Pt catalysts supported on gamma-Al<sub>2</sub>O<sub>3</sub> modified with ce and mg*. Chinese Journal of Catalysis, 2006. **27**(3): p. 275-280.
138. Barbe, N. 2004, Georgia Institute of Technology.
139. Barth, T., *Optimising reaction conditions relative to product slates in aqueous presurized pyrolysis of biomass and waste samples*, in *Pyrolysis and Gasification of Biomass and Waste, Proceedings of an Expert Meeting*, A.V. Bridgewater, Editor. 2003, CPL Press: Newbury, UK.
140. Lucchessi, A., et al., *A pilot plant for the study of the production of hydrogen-rich syngas by gasification of biomass*, in *Thermochemical Biomass Conversion*, A.V. Bridgewater and J.L. Kuester, Editors. 1988, Elsevier London, UK.
141. *Thermal Conductivity Detectors (TCDs)*. [cited 2006 May]; Available from: [http://www.gow-mac.com/products/product.cfm?prod\\_id=29&cat\\_id=10](http://www.gow-mac.com/products/product.cfm?prod_id=29&cat_id=10).
142. McNair, H.M. and J.M. Miller, *Basic Gas Chromatography*. Techniques in Analytical Chemistry. 1998, New York: John Wiley & Sons, Inc.
143. Miller, J.M., *Chromatography: Concepts and Contrasts*. 2nd ed. 2005, New Jersey: John Wiley & Sons, Inc.
144. Publishing, P.E. 1987 [cited 2006 May]; Available from: <http://www.tak2000.com/data2.htm>.
145. *Feedstock Composition Glossary*. 2005 [cited 2006 May]; Available from: [http://www1.eere.energy.gov/biomass/feedstock\\_glossary.html](http://www1.eere.energy.gov/biomass/feedstock_glossary.html).
146. Fengel, D. and G. Wegener, *Wood: Chemistry, Ultrastructure, Reactions*. 1983, Berlin: Walter de Gruyter & Co.
147. Toivanen, T.J. and R. Alen, *Variations in the chemical composition within pine (Pinus sylvestris) trunks determined by diffuse reflectance infrared spectroscopy and chemometrics*. Cellulose, 2006. **13**(1): p. 53-61.

148. Wise, L.E., *Wood Chemistry*. 1952, New York: Reinhold.
149. d'A Clark, J., *Pulp Technology and Treatment for Paper*. 1985, San Francisco: Miller Freeman Publications Inc.
150. *Concentrated Acid Hydrolysis*. 1/2006 [cited 2006 May]; Available from: [http://www1.eere.energy.gov/biomass/concentrated\\_acid.html](http://www1.eere.energy.gov/biomass/concentrated_acid.html).
151. Saeman, J.F., *Kinetics of Wood Saccharification - Hydrolysis of Cellulose and Decomposition of Sugars in Dilute Acid at High Temperature*. Industrial and Engineering Chemistry, 1945. **37**(1): p. 43-52.
152. Glasser, W.G., *Fundamentals of Thermochemical Biomass Conversion*, ed. R.P. Overend, T.A. Milne, and L.K. Mudge. 1985, London: Elsevier Applied Science Publishers Ltd.
153. Feather, M.S., D.W. Harris, and S.B. Nichols, *Routes of Conversion of D-Xylose, Hexuronic Acids, and L-Ascorbic-Acid to 2-Furaldehyde*. J. Org. Chem., 1972. **37**(10): p. 1606-&.
154. Feather, M.S. and J.F. Harris, *Absence of Proton Exchange During Conversion of Hexose to 5-(Hydroxymethyl)-2-Furaldehyde*. Tetrahedron Lett., 1968(55): p. 5807-&.
155. Harris, D.W. and M.S. Feather, *Evidence for a C-2-JC-1 Intramolecular Hydrogen Transfer During Acid-Catalyzed Isomerization of D-Glucose to D-Fructose*. Carbohydr. Res., 1973. **30**(2): p. 359-365.
156. Antal, M.J., et al., *Kinetic-Studies of the Reactions of Ketoses and Aldoses in Water at High-Temperature .3. Mechanism of Formation of 2-Furaldehyde from D-Xylose*. Carbohydr. Res., 1991. **217**: p. 71-85.
157. Antal, M.J., W.S.L. Mok, and G.N. Richards, *Kinetic-Studies of the Reactions of Ketoses and Aldoses in Water at High-Temperature .1. Mechanism of Formation of 5-(Hydroxymethyl)-2-Furaldehyde from D-Fructose and Sucrose*. Carbohydr. Res., 1990. **199**(1): p. 91-109.
158. Antal, M.J., T. Leesomboon, and W.S. Mok, *Mechanism of formation of 2-furaldehyde from D-xylose*. Carbohydr. Res., 1991. **217**: p. 71-85.
159. Blake, P.G., H.H. Davies, and G.E. Jackson, *Dehydration Mechanisms in Thermal Decomposition of Gaseous Formic Acid*. J Chem. Soc. B, 1971(10): p. 1923-&.

160. Saito, K., et al., *Thermal Unimolecular Decomposition of Formic-Acid*. J Chem. Phys., 1984. **80**(10): p. 4989-4996.
161. Saito, K., et al., *Unimolecular decomposition of formic acid in the gas phase - On the ratio of the competing reaction channels*. J Phys. Chem. A, 2005. **109**(24): p. 5352-5357.
162. Akiya, N., Savage, P. , *Role of Water in Formic Acid Decomposition*. AIChE J, 1998. **44**(2): p. 405-415.
163. Bjerre, A.B. and E. Sorensen, *Thermal-Decomposition of Dilute Aqueous Formic-Acid Solutions*. Industrial & Engineering Chemistry Research, 1992. **31**(6): p. 1574-1577.
164. Yu, J.L. and P.E. Savage, *Decomposition of formic acid under hydrothermal conditions*. Industrial & Engineering Chemistry Research, 1998. **37**(1): p. 2-10.
165. Tokmakov, I.V., et al., *Thermal decomposition of formic acid in the gas phase: bimolecular and H<sub>2</sub>O catalysed reactions*. Mol. Phys., 1997. **92**(3): p. 581-586.
166. Yagasaki, T., S. Saito, and I. Ohmine, *A theoretical study on decomposition of formic acid in sub- and supercritical water*. J Chem. Phys., 2002. **117**(16): p. 7631-7639.
167. Watanabe, M., et al., *Glucose reactions with acid and base catalysts in hot compressed water at 473 K*. Carbohydrate Research, 2005. **340**(12): p. 1925-1930.
168. Ehrman, T., *Determination of acid-soluble lignin in biomass*. 1996, National Renewable Energy Laboratory.
169. Wallis, A.F.A., *Solvolysis by acids and bases*, in *Lignins: occurrence, formation, structure and reactions*, K.V. Sarkanen and C.H. Ludwig, Editors. 1971, Wiley Interscience: New York. p. 345-372.
170. Matsushita, Y. and S. Yasuda, *Preparation and evaluation of lignosulfonates as a dispersant for gypsum paste from acid hydrolysis lignin*. Bioresour. Technol., 2005. **96**(4): p. 465-470.
171. Barbier, J., *Deactivation of Reforming Catalysts by Coking - a Review*. Applied Catalysis, 1986. **23**(2): p. 225-243.



172. Chen, P., et al., *Carbon deposition on meso-porous Al<sub>2</sub>O<sub>3</sub> supported Ni catalysts in methane reforming with CO<sub>2</sub>*. Reaction Kinetics and Catalysis Letters, 2005. **86**(1): p. 51-58.
173. Parera, J.M. and J.N. Beltramini, *Stability of Bimetallic Reforming Catalysts*. Journal of Catalysis, 1988. **112**(2): p. 357-365.
174. Biswas, J., P.G. Gray, and D.D. Do, *The Reformer Lineout Phenomenon and Its Fundamental Importance to Catalyst Deactivation*. Applied Catalysis, 1987. **32**(1-2): p. 249-274.
175. Figoli, N.S., et al., *Operational Conditions and Coke Formation on Pt-Al<sub>2</sub>O<sub>3</sub> Reforming Catalyst*. Applied Catalysis, 1983. **5**(1): p. 19-32.
176. Basso, T.C., Z. Zhang, and W.M.H. Sachtler, *Characterization by pulsed oxidation of coke on platinum/alumina*. Applied Catalysis A: General, 1991. **79**(2): p. 227-240.
177. Shakhshi, B.Z., *Chemical Demonstrations: A Handbook for Teachers of Chemistry*. 1983. 77-78.
178. Watts, J.F. and J. Wolstenholme, *An Introduction to Surface Analysis by XPS and AES*. 2003, England: John Wiley and Sons Ltd.
179. Moulder, J.F., et al., *Handbook of X-ray Photoelectron Spectroscopy*, ed. J. Chastain and R.C.J. King. 1995, Minnesota: Physical Electronics, Inc.
180. [cited 2006 June]; Available from: <http://www.organic-chemistry.org/frames.htm?http://www.organic-chemistry.org/synthesis/O2S/sulfones.shtm>.
181. Deng, Y.Q. and L.D. An, *Sulfate Accumulation in Commercial Pd-Pt/Al<sub>2</sub>O<sub>3</sub> and Pt/Al<sub>2</sub>O<sub>3</sub> Catalysts Used for Removal of Hydrogen from Carbon-Dioxide*. Applied Catalysis a-General, 1994. **119**(1): p. 13-22.
182. Saur, O., et al., *The Structure and Stability of Sulfated Alumina and Titania*. Journal of Catalysis, 1986. **99**(1): p. 104-110.
183. Pieplu, A., et al., *A kinetic model for alumina sulfation*. Journal of Catalysis, 1996. **159**(2): p. 394-400.

184. Waqif, M., et al., *Acidic Properties and Stability of Sulfate-Promoted Metal-Oxides*. Journal of Molecular Catalysis, 1992. **72**(1): p. 127-138.
185. Shabaker, J.W., G.W. Huber, and J.A. Dumesic, *Aqueous-phase reforming of oxygenated hydrocarbons over Sn-modified Ni catalysts*. J. Catal., 2004. **222**(1): p. 180-191.
186. <http://www.ima-eu.org/en/ccawhat.html>. [cited.
187. Loerting, T., et al., *On the surprising kinetic stability of carbonic acid (H<sub>2</sub>CO<sub>3</sub>)*. Angew. Chem. Int. Ed., 2000. **39**(5): p. 892-+.
188. Watanabe, M., et al., *Glucose reactions within the heating period and the effect of heating rate on the reactions in hot compressed water*. Carbohydrate Research, 2005. **340**(12): p. 1931-1939.
189. Carey, F.A., *Organic Chemistry*. 1996, New York: McGraw-Hill Companies Inc.
190. Aghalayam, P., et al., *A CI mechanism for methane oxidation on platinum*. Journal of Catalysis, 2003. **213**(1): p. 23-38.
191. Mhadeshwar, A.B. and D.G. Vlachos, *Microkinetic modeling for water-promoted CO oxidation, water-gas shift, and preferential oxidation of CO on pt*. J. Phys. Chem. B, 2004. **108**(39): p. 15246-15258.
192. Gratzel, M., *Artificial Photosynthesis - Water Cleavage into Hydrogen and Oxygen by Visible-Light*. Acc. Chem. Res., 1981. **14**(12): p. 376-384.
193. Karagoz, S., et al., *Low-temperature catalytic hydrothermal treatment of wood biomass: analysis of liquid products*. Chemical Engineering Journal, 2005. **108**(1-2): p. 127-137.
194. Kabyemela, B.M., et al., *Degradation kinetics of dihydroxyacetone and glyceraldehyde in subcritical and supercritical water*. Industrial & Engineering Chemistry Research, 1997. **36**(6): p. 2025-2030.
195. Kabyemela, B.M., et al., *Glucose and fructose decomposition in subcritical and supercritical water: Detailed reaction pathway, mechanisms, and kinetics*. Industrial & Engineering Chemistry Research, 1999. **38**(8): p. 2888-2895.
196. Sasaki, M., et al., *Cellulose hydrolysis in subcritical and supercritical water*. J Supercrit. Fluids, 1998. **13**(1-3): p. 261-268.

197. Hatcher, P.G., *Chemical Structural Studies of Natural Lignin by Dipolar Dephasing Solid-State C-13 Nuclear-Magnetic-Resonance*. Organic Geochemistry, 1987. **11**(1): p. 31-39.
198. Oliveira, L., et al., *Structural characterization of lignin from leaf sheaths of "dwarf cavendish" banana plant*. Journal of Agricultural and Food Chemistry, 2006. **54**(7): p. 2598-2605.
199. Kelly, J., *Stainless Steels*, in *Handbook of Materials Selection*, M. Kutz, Editor. 2002, John Wiley & Sons, Inc.: New York.